



Development and characterisation of haemophilic arthropathy in a rat model of haemophilia A



PhD thesis 2017
Kristine Rothaus Christensen

UNIVERSITY OF COPENHAGEN
FACULTY OF HEALTH AND MEDICAL SCIENCES
PHD THESIS 2017
ISBN 978-87-93476-86-8

KRISTINE ROTH AUS CHRISTENSEN

Development and characterisation of haemophilic arthropathy in a rat model of haemophilia A



LIFE PHARM

NOVO NORDISK & LIFE IN VIVO PHARMACOLOGY CENTRE

Development and characterisation of haemophilic arthropathy in a rat model of haemophilia A

This thesis has been submitted to the Graduate School of Health and Medical Sciences, University of Copenhagen, Denmark.

Faculty: Faculty of Health and Medical Sciences

Department: Department of Veterinary Disease Biology

Industry: Haemophilia Pharmacology, Novo Nordisk A/S

Author: Kristine Rothaus Christensen

Title: Development and characterisation of haemophilic arthropathy in a rat model of haemophilia A

Principal supervisor: Axel Kornerup Hansen, Prof., Section of Experimental Animal Models, Dept. of Veterinary Disease Biology, University of Copenhagen

Co-supervisors: Mads Kjelgaard-Hansen, DVM, PhD, Haemophilia Biology, Novo Nordisk A/S
Lise Nikolic Nielsen DVM, CertSAM, PhD, Associate Professor in Veterinary Clinical Pathology, Department of Veterinary Clinical and Animal Sciences, University of Copenhagen
Kirstine Roepstorff, PhD, Histology and Bioimaging, Novo Nordisk A/S
Søren Skov, Prof., Section of Experimental Animal Models, Dept. of Veterinary Disease Biology, University of Copenhagen

Assessment committee: Associate Prof. Johannes Jakobsen Sidelmann, Thrombosis Research, University of Southern Denmark, Denmark
Dr. Eva Zetterberg, MD, PhD. Clinical Coagulation Research Unit, Lund University, Sweden
Prof. Fintan McEvoy, Dept. of Veterinary Clinical and Animal Sciences, University of Copenhagen, Denmark

Submitted: December 18th 2016

Cover pictures: Image of rat kindly permitted for reprint by Gubra. Photo by Muusfoto ©.
The μ CT and histology image are photos obtained from the studies included in the thesis

Table of content

Table of content	iii
Preface and acknowledgements	vii
Abbreviations	ix
Abstract	xi
Dansk resumé	xiii
List of papers and manuscripts included in the thesis	xv
1. Introduction	17
1.1. Haemophilia A	17
1.2. Haemophilic arthropathy	19
1.2.1. Pathogenesis	20
1.2.2. Synovitis	20
1.2.3. Cartilage damage	22
1.2.4. Pathological bone remodelling	24
1.2.5. Angiogenesis	25
1.2.6. Vicious cycle	26
1.3. Diagnosis of haemophilic arthropathy	28
1.3.1. Clinical evaluation of haemophilic arthropathy	28
1.3.2. Radiographic imaging and evaluation of haemophilic arthropathy	29
1.3.3. Magnetic resonance imaging and evaluation of haemophilic arthropathy	30
1.3.4. Ultrasonographic assessment of haemophilic arthropathy	32
1.4. Animal models of haemophilia and haemophilic arthropathy	33
1.4.1. The haemophilic dog	34
1.4.2. The F8 knock-out mouse models	35
1.4.3. The F8 knock-out rat model	35
1.4.4. Models of haemophilic arthropathy	36
1.5. Remaining questions in the pathobiology of haemophilic arthropathy	39
2. Objectives	41
2.1. Aims and hypotheses	41
3. Experimental Work	43
3.1.1. Validation of the F8 KO rat as a model of HA	43
3.1.2. Evaluation of ultrasonography and micro-computed tomography as techniques for assessing joint pathology following haemarthrosis in F8 KO rats	44
3.1.3. Characterisation of the early onset of haemophilic arthropathy	45
3.2. Additional immunohistochemical stains and results	47
3.2.1. Characterisation of joint vascularity following haemarthrosis	47
4. Discussion	49
4.1.1. Development and validation of the F8 KO rat as a model of haemophilic arthropathy	49

4.1.2. Development and validation of imaging modalities and scoring systems for assessment of haemophilic arthropathy	50
4.1.3. The early development of haemophilic arthropathy.....	51
5. Conclusion	55
6. Perspectives.....	57
7. References	59
8. Appendix: Papers and manuscript.....	67

Preface and acknowledgements

This thesis constitutes the work and results obtained during my time as a PhD-student. The project is funded by the Novo Nordisk-LIFE *in vivo* pharmacology centre (LIFEPHARM), and is a collaboration between the department of Haemophilia Pharmacology at Novo Nordisk A/S and the department of Veterinary Disease Biology, Section of Experimental Animal Models at the Faculty of Health and Medical Sciences, University of Copenhagen.

The main part of the project and results presented in this thesis were obtained at Novo Nordisk A/S, Måløv, Denmark from November 2013 to December 2016.

Several people have been involved in the project of which I owe thanks, in particular my whole family of supervisors, who have been a great team of support and knowledge. First of all, I would like to thank Lise Nikolic Nielsen and Axel Kornerup Hansen for believing in an “outsider”, and for giving me the opportunity to conduct a PhD with an *in vivo* focus, despite my lack of veterinarian insights. I would like to thank you, Lise, for always encouraging me and cheering me on with your eternal positive spirit and energy, giving me good advice, and provide me with many interesting scientific ideas, discussions and reflections regarding my project. Thank you, Axel, for being a dedicated supervisor, being up to date with my experiments and progress, despite my often long periods of radio silence. Your extensive knowledge and experience have over the past three years provided me with a lot of scientific discussions and ideas about my project and future work.

I would also like to extend my sincere gratitude to Mads Kjelgaard-Hansen, who took on the role as external supervisor halfway through the project. You have encouraged me on a daily basis to evolve and improve my skills as a scientist. I highly appreciate our daily interaction and discussions, where you always challenge me that extra little bit, both when discussing study designs, results, and interpretations. You have taught me a lot about the academic mind-set over the last three years, and I continue to include your guidance in my everyday work. I would also like to express my gratitude to Kirstine Roepstorff, who I have enjoyed discussing in particular tomography and histological results with; I have had many fun and enlightening conversations with you. I have learned a lot from your scientific approach and guidance, and thank you also for always finding my missing s’. Lastly, thank you to Søren Skov for always being ready with scientific input and ideas regarding the immunological part of the thesis.

Besides my supervisors, I would also like to thank Helle Friis Kierkegaard for teaching me how to take care of our haemophilic rat, and for always being on “team Kristine”, and rooting for the success of my experiments.

Jeanette Juul also deserves a sincere thank you for teaching me the wonderful work of histology and immunohistochemistry, and for always being in the loop, and willing to lend an ear to a sometimes frustrated PhD student. I also wish to extend a special thank you to Maj Petersen for teaching me how to

interpret the micro-computed tomography images, and for all the fun remarks and observations regarding the life as a PhD student. Kåre and Anders who helped with the many many rats and joint scans also deserve a special thanks.

I wish to thank all my colleagues at Novo Nordisk, in particular the departments 2783, 2784 and 903 for all the help in the lab, and for ensuring an educational, warm and fun work place throughout the past three years, as well as my colleagues at the university for always being inclusive and interested in my somewhat distant project.

Additionally, I would like to extend my gratitude to Floris Lafeber and his group at the University Medical Center, Utrecht for allowing me to visit and learn from his lab. Thank you Astrid and Jan for having me, and taking such good care of me, and thank you Katja for all the work you did in the lab for us.

Finally, a big thank you to my friends and family, who have been standing on the side-line, cheering me on and helping me in whatever way they could. Thank you Rikke for being my eternal study-buddy always listening and helping me, and encouraging me with your positive mind and spirit. Thank you for being my own personal editor in addition to my proof readers Molly and Adrian. Thank you Karin for all our, more or less, scientific discussions and for making the long afternoons at the office so much more fun. Thank you Laura for being the voice of reason and sanity and for being supportive even while struggling with the future of your own project. The last three years would not have been the same without our little PhD team.

A special thank you to my parents and sister for always being supportive of and interested in my nerdy work life.

Lastly, thank you to my husband, Jens. Thank you for always taking care of me, supporting me and encouraging me. Thank you for being the best person in the world, and for making me laugh every day, even on the longest of PhD days.

Abbreviations

α SMA	Alfa-smooth muscle actin
FVIII	Coagulation factor VIII
CD	Cluster of differentiation
CD3	Cluster of differentiation 3
CD31	Cluster of differentiation 31
CD68	Cluster of differentiation 68
DAB	3,3'-Diaminobenzidine
F8	Factor VIII coding gene
GAG	Glycosaminoglycan's
HA	Haemophilic arthropathy
HIF1 α	Hypoxia inducible factor-1 α
HJHS	Hemophilia Joint Health Score
H ₂ O ₂	Hydrogen Peroxide
IL	Interleukin
KC	Keratinocyte-derived chemokine
KO	Knock-out
MCP-1	Monocyte chemotactic protein-1
MPO	Myeloperoxidase
MRI	Magnetic resonance imaging
Pax5	Paired box protein 5
RANK	Receptor activator of nuclear factor-kappa B
RANKL	Receptor activator of nuclear factor-kappa B ligand
rhFVIII	Recombinant human factor VIII
ROI	Region of interest
ROS	Reactive oxygen species
TF	Tissue factor
TNF α	Tumor Necrosis Factor-alpha
TRAP	Tartrate resistant acid phosphatase
US	Ultrasonography
VEGF	Vascular endothelial growth factor
VAS	Visual analogue scale
V/v	Volume/volume
WFH	World Federation of Hemophilia
X-ray	Radiography
μ CT	Micro-computed tomography

Abstract

Haemophilic arthropathy (HA) is a debilitating complication of the bleeding disorder haemophilia A, and is characterised by progressive joint deterioration. HA develops as a result of multiple joint bleeds (haemarthrosis). Once early arthropathic changes are diagnosed, the joint deterioration will likely continue to progress towards a completely degraded joint resulting in chronic pain and discomfort for the patient.

The pathobiology of HA is difficult to investigate in human patients, as the bleeding phenotype prevents joint tissue biopsy sampling. Consequently, the mechanisms driving the progression from haemarthrosis to chronic arthropathy have only partially been resolved. Understanding disease development is, however, important as it can reveal new possible treatment targets, which in the future can help prevent joint destruction and improve quality of life for haemophilia patients.

This thesis is aimed at characterising the early onset and development of HA following a single haemarthrosis. Since this is not possible to study in human haemophilia patients, an animal model of haemophilia, the factor VIII gene (F8) knock-out (KO) rat, was employed and the possibility of using it as a model of human HA investigated.

The first study in the thesis hypothesised that induction of a joint-bleed in the knee-joint of F8 knock-out rats will cause arthropathic changes of the joint that resemble human HA and can be verified by histological assessment. Furthermore, the hypothesis that treatment with recombinant human factor VIII (rhFVIII) prior to the induction of haemarthrosis would reduce or abolish joint changes was tested. Both hypotheses were confirmed.

The second study explored and successfully proved that in addition to the previously established histological assessment, ultrasonography (US) and micro-computed tomography (μ CT) can be utilised to assess arthropathic joint deterioration.

The third study aimed at a detailed mapping of the progression from haemarthrosis to HA. To this end, 100 F8 KO rats were subjected to a sham or joint-bleed procedure and a group of each euthanised from day one to seven after the procedure.

The combined studies in this thesis show that the F8 KO rat can be used as a model of HA with a high face and construct validity. Furthermore, the imaging modalities, US and μ CT can be utilised to show pathology in the soft and bone tissue of the joint, respectively.

Finally, the application of the F8 KO HA model and the assessment tools revealed a rapid development of HA following haemarthrosis with considerable joint damage developing within one week. Synovitis developed within 24 hours followed by both cartilage loss and bone pathology developing concurrently

and already from day two to three. This is in contrast to the general belief that the pathology develops sequentially with synovitis as the instigating mechanism, followed by gradual cartilage loss eventually resulting in bone deterioration.

Future animal studies of HA onset and development should therefore consider implementing this short study timeline for disease assessment. Furthermore, the concurrent pathology in all joint structures warrants new intervention strategies, not only attempting to prevent synovitis as a means to prevent HA development.

Dansk resumé

Hæmofil arthropathi (HA) er en følgesygdom, der udvikler sig i leddene hos patienter med blødersygdommen hæmofili A. Arthropathien er karakteriseret ved progressiv nedbrydning af leddet, som følge af ledblødninger (hæmarthroses). Når først der er tidlige tegn på ledforandringer vil tilstanden med stor sandsynlighed forværres, og slutresultatet er patienter med fuldstændig nedbrudte led. Et led, der er helt ødelagt af HA er både smertefuldt og invaliderende og kræver kirurgiske indgreb for at forbedre livskvaliteten for patienten.

Den underliggende sygdomsbiologi, der forårsager udviklingen af HA er vanskelig at undersøge i patienter med hæmofili, da deres blødende fænotype forhindrer, at man kan udtage biopsier fra de påvirkede led. Derfor er mekanismerne, der medfører udviklingen fra ledblødningen til kronisk HA kun delvist belyst. Kendskab til sygdomsudviklingen er vigtig idet mekanismerne bag kan afsløre nye mulige behandlingsstrategier, som i fremtiden kan forhindre nedbrydningen af leddet og dermed forbedre livskvaliteten for hæmofili patienter.

I denne afhandling var målet at karakterisere den tidlige sygdomsudvikling fra begyndelsen af leddets nedbrydning til tilstedeværelsen af kronisk HA efter en enkelt induceret ledblødning. Da dette ikke er muligt i hæmofili patienter, blev det først undersøgt om F8 KO rotten kunne bruges som model for HA.

Det første studie i afhandlingen testede hypotesen, at en induceret ledblødning i knæleddet på F8 KO rotten vil føre til patologiske forandringer i leddet, der minder om human HA. Derudover blev det også testet hvorvidt behandling med rekombinant faktor VIII inden ledblødningen kan reducere eller forhindre forandringerne i leddet. Begge hypoteser blev bekræftet.

Studie to undersøgte muligheden for at bruge ultralyd (US) og micro-computed tomography (μ CT) som redskaber til at undersøge nedbrydningen af leddet. Ligeledes blev korrelationen mellem de semi-kvantitative billedanalyser og de histologiske undersøgelser af leddet evalueret.

Efter at have påvist at F8 KO rotten kan bruges som model for HA, og at US og μ CT kan benyttes til visualisering af ledforandringerne blev studie tre designet med det formål at lave en detaljeret kortlægning af progressionen fra hæmarthrose til HA.

Til dette formål blev 100 F8 KO rotter udsat for en ledblødning eller en sham procedure, og en gruppe af hver blev aflivet dag et til syv efter proceduren.

Sammenlagt viser studierne i denne afhandling, at F8 KO rotten kan bruges som model for HA med en høj face og construct validity. Ydermere blev US og μ CT bekræftet som modaliteter, der kan visualisere patologien i henholdsvis leddets bløddele og knoglevæv.

Endelig blev modellen og visualiseringsmetoderne benyttet til at vise, at der sker en meget hurtig udvikling af HA i F8 KO rotten med betragtelig skade i leddet allerede indenfor de første syv dage efter en induceret ledblødning.

Synovitis var til stede allerede indenfor 24 timer hvorefter tab af brusk samt knoglepatologi blev påvist. Brusk og knogleforandringerne skete samtidig og udviklede sig allerede fra dag to til tre. Dette er i uoverensstemmelse med tidligere teorier om en sekventiel nedbrydning af leddet, der starter med synovitis, efterfulgt af gradvise bruskforandringer, der på sigt vil føre til knogle nedbrydning.

Fremtidige studier af HA udvikling i dyremodeller bør derfor overveje at implementere det korte studie set-up for karakterisering af sygdommen. Ydermere, bør man, set i lyset af den samtidige udvikling af sygdom i brusk, knogle og synovial membranen, genoverveje fremtidige behandlingsstrategier, som indtil nu har fokuseret primært på forhindring af synovitis og tidlig bruskskade.

List of papers and manuscripts included in the thesis

- I. **The F8^{-/-} rat as a model of haemophilic arthropathy**
Sørensen, KR.; Roepstorff, K.; Wiinberg, B.; Hansen, AK.; Tranholm, M.; Nielsen, LN.; Kjelgaard-Hansen, M.
J. Thromb. Haemost. 2016;14:1216-25
PMID: 27060449

- II. **Visualization of haemophilic arthropathy in F8^{-/-} rats by ultrasonography and micro-computed tomography**
Christensen, KR.; Roepstorff, K.; Petersen, M.; Wiinberg, B.; Hansen, AK.; Kjelgaard-Hansen, M.; Nielsen, LN.
Haemophilia. 2017 Jan;23(1):152-162
PMID: 27611596

- III. **Rapid inflammation and early degeneration of bone and cartilage revealed in a time-course study of induced hemarthrosis in hemophilic rats**
Christensen, KR.; Kjelgaard-Hansen, M.; Nielsen, LN.; Wiinberg, B.; Althoehn, FA.; Poulsen, NB.; Vøls, KK.; Thyme, A.; Lövgren, KM.; Hansen, AK.; Roepstorff, K.
Manuscript

1. Introduction

1.1. Haemophilia A

The disease haemophilia A is caused by the lack of coagulation factor VIII (FVIII), with patients suffering from prolonged bleeding or in severe cases also episodes of spontaneous bleeds. The disease is the most common bleeding disorder of the two haemophilia's (haemophilia A and B), representing 80-85% of the haemophilic population [1-3]. Approximately 1 in 10.000 new-borns are affected, and an additional 0.2-1.0 per million are believed to annually acquire the disease [1].

The gene coding for FVIII is located on the q arm of the X-chromosome, which explains why the recessive disease primarily affects males whereas females most often present as carriers [4-6].

Despite the knowledge of a hereditary pattern, it is now recognised that approximately 30% of the diagnosed cases of haemophilia A are due to a spontaneous mutation of the FVIII coding (F8) gene, with an inversion of intron 22 as the most common mutation in the F8 gene [4-6]. Depending on the mutation of the F8 gene, different levels of FVIII activity can be measured in plasma. The severity of haemophilia A is determined by the amounts of circulating functionally active FVIII in plasma, and the disease is, therefore, divided into three phenotypes: mild (6-40% FVIII activity), moderate (1-5%), and severe (less than 1%). Patients with severe haemophilia A represent the majority as they constitute approximately half of the haemophilia A population [7-9].

In a healthy subject, damage to the vessel wall will initiate the coagulation cascade and lead to activation of FVIII, which in turn will bind and form the tenase complex with activated coagulation factor IX (see Figure 1). This complex activates coagulation factor X, enabling the activated factor X to bind activated coagulation factor V [10, 11]. This complex, known as the pro-thrombinase complex then cleaves large amounts of pro-thrombin into thrombin (also known as FII and FIIa, respectively) in a process known as the thrombin burst. Finally, the activated thrombin is capable of cleaving fibrinogen into fibrin, a key component of a blood clot [10, 11].

In haemophilia, the lack of FVIII prevents formation of the tenase complex, and thereby also the subsequent pro-thrombinase complex. Without these complexes there is no formation of large amounts of thrombin and thereby also fibrin, resulting in an inability to form a stable blood clot upon vascular injury.

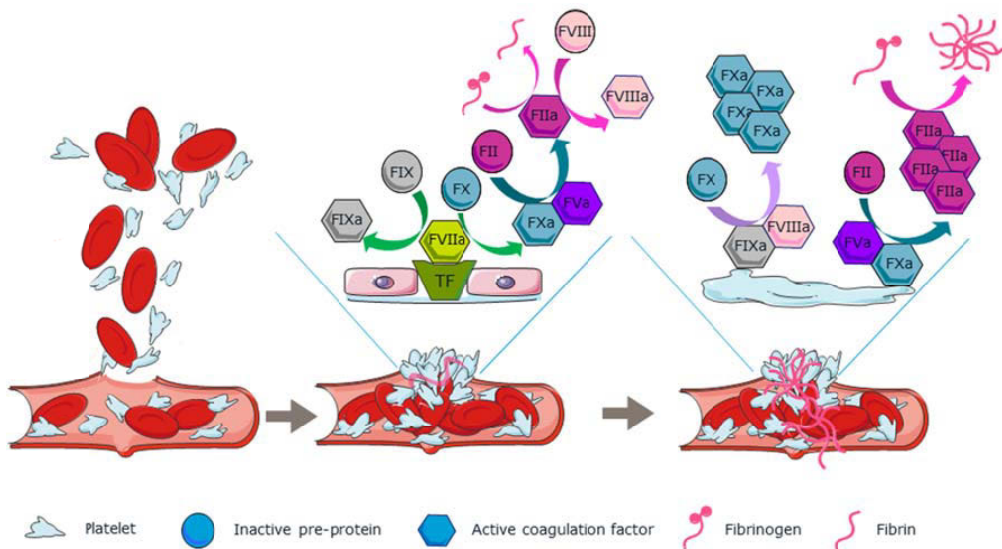


Figure 1: The coagulation cascade

Upon rupture of a vessel, blood cells and platelets will spill into the hole and the surrounding tissue. The damaged endothelium at the ruptured site exposes sub endothelial cells that express the extravascular tissue factor (TF), the principal initiator of coagulation which instigates the initiation phase of coagulation. Circulating FVII binds to the exposed TF, which is then activated to FVIIa.

The FVIIa then activates FX to FXa and FIX to FIXa. FXa forms the pro-thrombin complex with FVa, and cleaves FII (pro-thrombin) into FIIa (thrombin). The small amounts of FIIa formed, cleaves fibrinogen into fibrin, which stabilise the initial platelet plug formed at the rupture site. Finally, the cleaved FIIa is also capable of cleaving FVIII into FVIIIa.

In the next phase, known as the amplification phase, FVIIIa forms the tenase complex with FIXa on the surface of activated platelets that are adhered to the site of rupture.

The tenase complex is capable of cleaving large amounts of FX to FXa, which remain on the platelet surface and form the pro-thrombin complex with FVa. The numerous pro-thrombin complexes are then capable of generating large amounts of FIIa (known as the thrombin burst), which then cleaves multiple fibrinogen molecules into fibrin and ensures a stable clot is formed.

Source and permission: Modified from Servier Medical Art, <http://servier.com/Powerpoint-image-bank>.

Severe haemophilia, has a serious diathesis with patients suffering multiple spontaneous bleeding episodes, usually appearing first during the toddler years as the child learns to crawl and walk [12]. The bleeding episodes continue to occur throughout the patients' lifetime with as many as 20-35 episodes per year [2, 13, 14]. The most serious bleeds arise intracranially [4], and without treatment, the life expectancy for patients with severe haemophilia is short, with many dying before reaching adulthood [15, 16].

Today, the treatment of haemophilia is focused on preventing spontaneous or pro-longed bleeds and maintaining a normal coagulative potential by treating the patients with factor replacement therapy. The treatment is either given as regular infusions (prophylaxis) or on-demand when a spontaneous bleed

occurs. Prophylactic treatment reduces the severe bleeding phenotype; however, despite an extensive and thorough prophylactic treatment regimen, spontaneous bleeds are not completely prevented [13, 17].

The majority (>90%) [18] of the spontaneous bleeds occur in the large synovial joints with the ankle joint being the most affected, followed by the knee and elbow [13, 19]. Why these joints are more vulnerable to spontaneous bleeds are uncertain. Repetitive intra-articular bleeding, also known as haemarthrosis, can cause development of a degenerative disorder of the joint known as haemophilic arthropathy (HA) [7, 13, 20].

1.2. Haemophilic arthropathy

Extravasation of blood into the joint leads to the progressive and painful disorder HA (see Figure 2). This complication is characterised by a loss of function and limited range of motion of the joint as it stiffens due to degenerative joint changes. The deteriorated and painful joint diminishes the patients' mobility and reduces their quality of life [13, 21-23]. Thus, 49% percent of severe haemophilia A patients report that the most common comorbidity is bone or skeletal problems such as arthritis, with 38% suffering chronic pain [13, 21, 22].

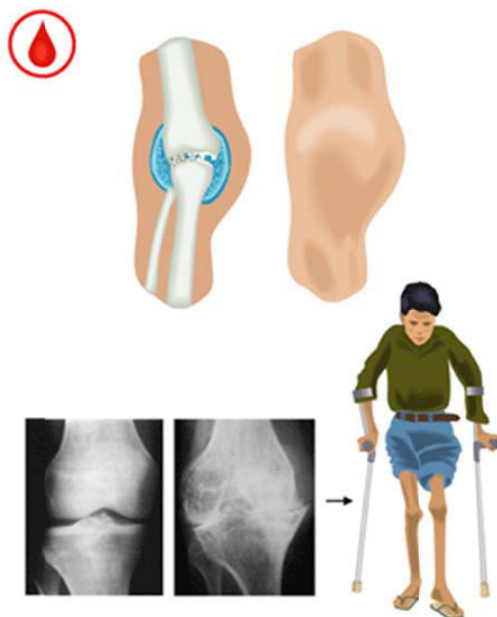


Figure 2: The consequences of haemophilic arthropathy

The long-term consequence of HA is destruction of the joint. This results in joint narrowing (as seen on the X-ray image) and pathology in joint cartilage and bone. This causes loss of joint function, limited range of motion and joint stiffness. Combined the joint deterioration is painful and debilitating for the patient.

With permission from: Hemophilia in Pictures, 2005, World Federation of Hemophilia.

<http://www1.wfh.org/en/index.html>

Although HA remains a complication for haemophilia patients prophylactic treatment regimens have greatly reduced the risk and slowed the process of arthropathic development. However, prophylactic

treatment is expensive and many patients, in particular in developing countries, do not have access to prophylaxis [24], which is why HA remains a problem for many haemophilia patients.

The disorder usually becomes evident already during childhood and adolescence [7, 25] and studies have shown that by the age of 30-40 years, 90% of patients with severe haemophilia on prophylaxis already have degenerative joint disease [19, 26]. Many patients will eventually undergo orthopaedic surgery in an attempt to reduce the pain, allow for increased usage of the joint and thereby also increase the quality of life for the patient.

Studies attempting to clarify the pathobiology of HA are therefore important, as the results can help improve treatment and joint outcome and thereby also the quality of life of the patients. However, studies of HA onset and development have been complicated by the bleeding phenotype of patients making biopsy sampling difficult. Therefore, studies of human HA pathogenesis have mostly been conducted on late-stage tissue samples obtained during intervention surgery. However, together with *in vitro* analysis and animal studies, some insights to the pathogenesis of HA have been obtained, although many aspects of the biology behind disease progression remain unresolved.

1.2.1. Pathogenesis

Upon haemarthrosis, blood will enter the otherwise enclosed and encapsulated joint, causing swelling, warmth, and distention of the joint area [12]. If the bleed is minor, the blood will be resorbed by the thin synovial membrane covering the joint (see Figure 3) [20]. However, if repetitive bleeds or extensive haemarthrosis overwhelms the capacity of the synovial cells to remove the blood, then haemarthrosis can lead to chronic synovitis and possibly further joint damage, i.e. HA.

1.2.2. Synovitis

The healthy synovial joint is encapsulated by ligaments, lined on the inside with a thin membrane (two to three cell layer thick) composed of synovial cells (see Figure 3) [12]; the macrophage-like A-type cells and the fibroblast-like B-type cells. The role of the B-type cells of the synovial membrane is to produce and secrete the synovial fluid composed of nutrients and lubricant for the intra-articular cartilage, while also producing the extracellular matrix scaffold of the synovial membrane [27, 28]. The role of the A-type cells is to resorb and remove debris and extracellular fluid in the joint cavity [28].

Bleeding into the joint causes marked changes to the synovial membrane such as enlargement and inflammatory infiltration [29]. This can be seen macroscopically, as an overall joint swelling develops [7, 15, 30]. This enlargement and swelling can be reversible if the bleed only has had a minor impact on the joint. If, however, the condition persists for more than six months, then early degenerative arthropathic changes are considered to be present [30, 31].

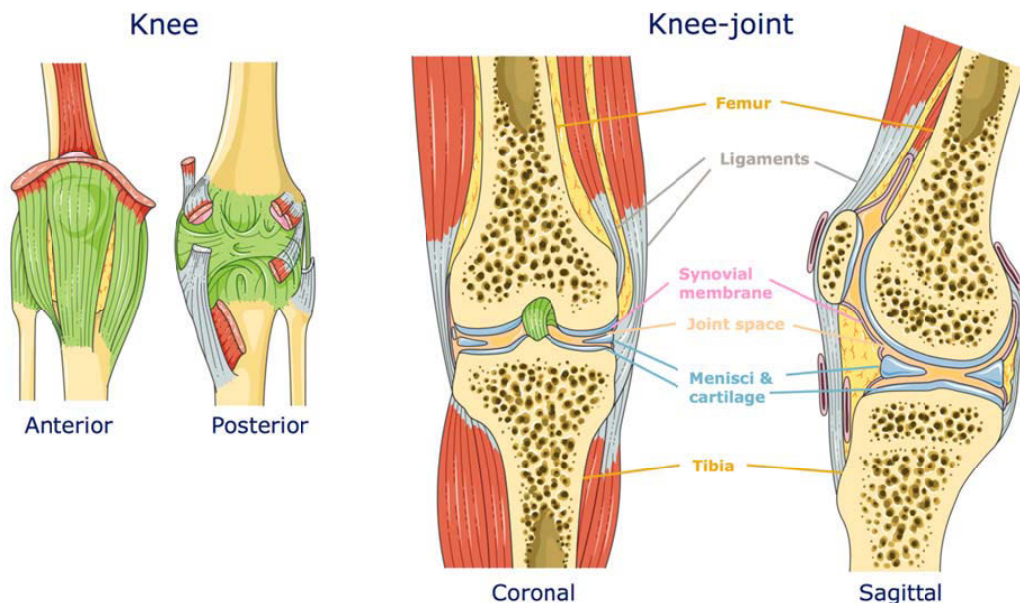


Figure 3: Overview of the knee joint

To the left is the anterior and posterior view of the encapsulated knee shown. To the right the coronal and sagittal view of the knee-joint is shown. Articular cartilage covers the femur and tibia bone ends in the joint where the two bones meet. The joint is lined with the synovial membrane, and filled with synovial fluid.

Source and permission: Modified from Servier Medical Art, <http://servier.com/Powerpoint-image-bank>.

Human tissue samples from patients with synovitis have shown a hyper vascularised, hypertrophic, and hyperplastic synovium [27, 32, 33], a pathology that is aggravated as the synovitis progresses and becomes chronic. The inflamed membranes also contain infiltrations of inflammatory cells, and develop synovial villi¹ and in advanced synovitis, an invasive pannus² is often present [29, 34-37]. As the condition progresses, the synovial membrane also gradually undergoes fibrosis becoming fragile and brittle, offering little support to the joint [27, 32-34].

In detail, the extravasation of blood into the joint causes the A-type synovial cells to resorb and remove the blood from the joint. As a result of the resorption, the A-type cells become activated and an acute inflammatory response arises [38]. This has been demonstrated by *in vitro* culturing of synovial tissue from HA patients, where increased expression of pro-inflammatory cytokines such as Tumour Necrosis Factor-alpha (TNF α), Interleukin (IL)-1 β , and IL-6 [33, 38, 39] was detected compared to healthy synovium. Likewise, increased amounts of IL-1 β , IL-6, keratinocyte-derived chemokine (KC) and monocyte chemotactic protein-1 (MCP-1) were found in the synovial fluid of haemophilic mice subjected to an

¹ Small projections from the surface of the synovial membrane stretching into the cavity of the joint

² A destructive inflammatory fibrovascular front composed of synovial and infiltrated immune cells

induced haemarthrosis when compared to synovial fluid of non-haemophilic mice subjected to the same procedure [40].

Upon acute haemarthrosis, the released cytokines and chemokines from the synovium lead to recruitment and infiltration of inflammatory cells such as neutrophils and macrophages that expands the capacity of the joint to resorb the extravasated blood [41-43]. The released cytokines cause activation of inflammatory cells and propagation of the inflammatory response, aggravating the developing synovitis [42-44]. Studies using IL-6 antagonists in combination with rhFVIII support the theory of an inflammatory driven response and degeneration of the synovial membrane as mice subjected to haemarthrosis receiving this treatment had reduced synovitis and cartilage damage compared to mice treated solely with rhFVIII [45].

The inflammatory response also leads to proliferation of the synovial membrane and the infiltrating cells, which explains why the synovial membrane becomes thickened and enlarged [46-48].

In the process of erythrophagocytosis, the activated macrophages and the A-type cells of the synovial membrane also degrade haem-incorporated iron. During this process, reactive oxygen species (ROS) are released, which are also capable of inducing an inflammatory signal, further exacerbating the condition [49-52].

The end-product of iron degradation is haemosiderin, which is seen intracellularly in the phagocytic cells of the synovial membrane and sometimes also in chondrocytes, and is considered a hallmark of HA [29, 34].

The changes to the synovial membrane are suspected to have wide-ranging consequences causing damage to other parts of the joint, both as a result of the proliferative state of the synovial cells with increasing nutritious demands, but also as a result of the continuous inflammatory condition.

1.2.3. Cartilage damage

Articular cartilage provides a low friction surface of the bone and a biomechanical function allowing for load transmission and distribution in the joint. The articular hyaline cartilage is composed of an extracellular matrix primarily constituted of collagen type II, proteoglycans and glycosaminoglycans (GAG) embedded with chondrocytes [53]. The chondrocytes are responsible for maintaining cartilage homeostasis by production of cartilage extracellular matrix components such as collagen type II and aggrecan, as well as secretion of enzymes degrading the extracellular matrix e.g. matrix metalloproteinases [53, 54].

The chondrocytes are cells of mesenchymal origin and in the adult they very rarely divide or proliferate [53], why the delicate homeostasis maintaining the articular cartilage is vulnerable to chondrocyte damage. Haemarthrosis not only influences the cells of the synovial membrane, but also affects the chondrocytes and cartilage of the joint.

HA patients present with damage to the cartilage in the form of apoptotic or lacking chondrocytes and a disappearance of extracellular cartilage matrix [34, 35, 55].

The apoptosis of chondrocytes leads to a gradual loss of the extracellular matrix particularly in the weight-bearing areas, which gradually leads to fibrillations and clefts in the cartilage [34, 35, 55]. Eventually a complete disappearance of the intra-articular cartilage can be seen, with exposure of the underlying bone [34, 35, 56, 57].

The pathobiology behind the cartilage damage is incompletely understood, but is suggested to arise from an indirect and a direct mechanism [14, 39]. The direct mechanism is believed to be caused by the blood itself. This is supported by *in vitro* studies of human cartilage explants, where only two days of culturing with 50% whole blood (v/v) led to decreased proteoglycan synthesis, a major extracellular component of cartilage [54]. Furthermore, the damage from this short-lived exposure was enough to cause persistent reduction in proteoglycan synthesis even after a 20 days recovery period of the cultures [54, 58-60]. Short-term blood exposure *in vivo* has also been shown to reduce proteoglycan synthesis, supporting the theory of a direct effect of blood on cartilage [41].

The mechanism behind the direct effect of blood-induced cartilage damage is believed to be caused by the phagocytosis of erythrocytes by macrophages and the concurrent breakdown of iron. This hypothesis is supported by studies that have shown erythrocytes and monocytes alone cause damage to the proteoglycan synthesis of human cartilage explants comparable to the damage caused by whole blood exposure [58, 60].

The process of iron degradation in the joint occurs according to the Fenton reaction where free iron obtained from degradation of haem in the form of Fe^{2+} reacts with hydrogen peroxide (H_2O_2) resulting in formation of hydroxyl radicals [50].

The hydroxyl radicals induce expression of matrix-degrading enzymes from the chondrocytes such as collagenase, but perhaps more harmful is the apoptotic effect of these radicals on chondrocytes [49, 51, 52, 61, 62]. Thereby, the degradation of iron has a dual effect on the cartilage, afflicting both the matrix and the cells, which combined lead to a detrimental loss of cartilage in the joint. In addition, iron has been shown to induce proliferation of synovial cells, propagating the synovitis of the joint [46, 48, 63, 64].

Besides the direct effect of blood, an indirect inflammatory mechanism causing progressive cartilage loss has been suggested. The initial synovitis developed in response to haemarthrosis leads to a pro-inflammatory environment in the joint, as described. In particular, the cytokine IL-1 β has been shown to have a pivotal role in cartilage degradation [61]. Firstly, IL-1 β induces hydrogen peroxide production from chondrocytes themselves as well as infiltrated monocytes, aggravating the production of hydroxyl radicals and the loss of cartilage in the joint [49, 61]. Secondly, studies of cartilage explants have shown that inhibition of IL-1 β signalling, by anti-IL-1 β neutralising antibodies or IL-1 β receptor antagonists, prevents chondrocytes apoptosis and can rescue the proteoglycan synthesis otherwise compromised following

blood exposure [61]. Likewise, studies have shown a protective effect of the anti-inflammatory cytokines IL-4 and IL-10 on the proteoglycan synthesis following blood exposure [39, 59, 65].

It remains uncertain whether the direct or indirect path to cartilage damage is equally responsible for cartilage degradation or if they have a synergistic effect, but combined they are responsible for the gradual destruction of intra-articular cartilage.

1.2.4. Pathological bone remodelling

Where a joint is formed, two bone ends meet and extend into the joint space, with the epiphyseal bone-ends positioned beneath the articular cartilage (see Figure 3). The capsule surrounding the joint stretches across the joint space, cartilage and the subchondral bone and attaches caudal and distal to the epiphyseal bone-ends [12].

Examinations using imaging or *post-mortem* dissection have revealed the severity of HA related bone pathology in human patients, including joint space narrowing, widening of the intercondylar notch of the femur, bone erosions, subchondral cyst formation and osteophytosis [32, 35, 66]. Additionally, studies have shown a general osteoporotic tendency in patients with HA [67-70].

Despite the very active tissue of the bone, the damage to the bone observed in HA patients following haemarthrosis are generally accepted to develop secondary to synovitis and cartilage degeneration [7, 31, 71].

Both inflammatory responses and mechanistic damage due to imbalanced load-bearing following cartilage loss have been suggested to be the underlying cause of the bone degeneration seen in HA patients, which is considered an end-stage characteristic of chronic HA [66, 68].

The theory of mechanically induced bone pathology poses that progressive loss of articular cartilage, leads to a reduced capacity of the cartilage to distribute and withstand weight-loading [66, 68]. The absence of cartilage means the load is gradually displaced directly onto the bone surfaces. In osteoarthritis, this has been proposed to result in increased pressure on the marrow space, causing subchondral haemorrhages and development of subchondral cysts. The same mechanism has been suggested to occur in HA, perhaps even aggravated by the concomitant increase in intra-articular pressure arising during acute haemarthrosis increasing the stress put on the bone marrow [31, 71].

Compelling evidence also suggests that an inflammatory process mediates the change in bone turnover, resulting in the observed bone pathology. The regulation of bone formation and resorption is controlled through complex intra- and inter-cellular communication that has yet to be completely elucidated. Several of the mechanisms responsible do, however, involve the inflammatory cytokines found upregulated in synovia following haemarthrosis.

Both IL-1 β and TNF α have been shown to induce receptor activator of nuclear factor-kappa B ligand (RANKL) production, a potent stimulator of osteoclast³ activation [72]. Concurrent to their induction of bone resorption by activating osteoclasts, IL-1 β and TNF α have also been shown to regulate bone formation by inhibiting the bone producing osteoblasts, further pushing the balance of bone homeostasis towards excessive resorption [73, 74].

Histological examination of synovia from HA patients' support these studies, as RANKL expression is increased in HA patients compared to osteoarthritic patients [75]. Moreover, osteoprotegerin, a decoy receptor for RANKL and an important regulator that reduces bone resorption, is significantly reduced in HA synovial tissue [75].

In addition to the effects of IL-1 β and TNF α , IL-6 which is also found in synovial fluid of HA patients is known to regulate osteoclast progenitor cells by inducing differentiation into mature osteoclasts, thereby increasing the pool of bone resorption cells [72, 74, 76].

These findings are in line with the positive correlation found between HA and osteopenia and osteoporosis [68-70]. Furthermore, the increased magnitude of bone loss in HA patients are believed to arise from excessive bone resorption as a consequence of the disuse and immobilisation of the joint because of joint deformity, pain and restricted use following haemarthrosis [67, 68].

Despite detailed descriptions of HA related bone pathology, the pathobiology of the bone changes is not fully elucidated. The early mechanisms behind HA related pathobiology of the bone remains largely uncharacterised, due to the difficulty in studying the earliest changes to the bone in haemophilia patients. Studies of haemophilic animal models have only recently focused on the early response of the bone to haemarthrosis.

Only three animal studies of HA development following blood-induced joint-damage have shed light on the earlier development of bone changes, and only one of these focused on disease characterisation [77-79]. Lau *et al.* studied HA development in F8 KO mice following an induced haemarthrosis in the knee-joint and found that a single joint bleed led to an acute loss of trabecular bone and an overall loss of bone mineral density [78]. The loss of bone appeared concurrent to changes in the periosteum which developed a rough appearance. This study provided an insight to the initial events of haemarthrosis-induced bone pathology; however, the molecular mechanisms remain unknown. It is likely due to a combination of both the mechanistically and inflammation induced deregulation of bone homeostasis.

1.2.5. Angiogenesis

A final process in HA that has received much attention in the recent years is the process of new vessel formation or angiogenesis [80]. The hypothesis of a potential angiogenic influence on HA development has been supported by both human and animal studies pointing to an increased angiogenic activity in synovitis and HA [47, 81-83].

³ The cells responsible for bone resorption

Patients with HA have been shown to have hyper vascular synovial tissue [47, 81]. Furthermore, plasma from HA patients contains increased angiogenic factors such as the vascular endothelial growth factor (VEGF), and the VEGF receptor-1 and -2, and is capable of inducing tube formation of endothelial cells *in vitro* [81]. Also, VEGF has been shown upregulated in the joint within the first 24 hours after haemarthrosis in an induced joint-bleed mouse model of HA [84].

Similar studies using mouse models of HA have also shown an increased vascularity of the synovial tissue following a single induced haemarthrosis [47]. This vascularity was superior to the vascularity of synovial tissue from mouse models of induced osteoarthritis and rheumatoid arthritis. This indicates that angiogenesis is specifically related to HA and not other arthritic joint disorders [47, 85].

The path from extravasation of blood to increased angiogenesis is suggested to be instigated both by an inflammatory signal and by the joint tissues' demand for oxygen.

With larger haemarthroses, the pressure in the joint increases, and eventually can surpass the intra-capillary pressure, causing these to collapse, and the joint tissue to become oxygen deprived, i.e. hypoxic [18]. Hypoxia leads to expression and stabilisation of the transcription factor hypoxia inducible factor-1 α (HIF-1 α), which in turn leads to expression of growth factors and mitogens, of which VEGF is perhaps the most important in relation to angiogenesis [86-88]. The expression of VEGF leads to the process of sprouting and formation of new vessels, which provides new routes of oxygen supply to the joint tissue [86-88].

In addition to the hypoxic environment developing as a direct effect of haemarthrosis, synovitis is also believed to activate angiogenic pathways, as the tissue has an increased oxygen demand due to the proliferative and inflamed condition of the cells [55]. Thus, inflammatory signals such as the cytokines IL-1 β and IL-6 have been shown to increase angiogenesis in other disorders such as cancer [89, 90].

1.2.6. Vicious cycle

The individual tissue responses and the overall inflammatory condition initiated by the haemarthrosis have been suggested to increase the risk of re-bleeding, and thereby instigating a vicious cycle of progressive joint deterioration with a continuously increased risk of haemarthrosis (see Figure 4) [91].

The theory is based on the inflamed synovial tissue requiring more oxygen alongside the already hypoxic environment following haemarthrosis inducing angiogenesis.

The angiogenic response causes formation of new immature vessels that could be prone to rupture, thereby increasing the risk of joint-bleeds. This theory has, however, been challenged in a study by Zetterberg *et al.* who showed that vessels in the synovium of HA patients were covered in pericytes [92], considered a sign of vessel maturity and indicate the vessels are not at increased risk of rupture [93].

In addition to the theory of an angiogenic driven risk of re-bleeds, the continued loss of cartilage extracellular matrix and erosions of cartilage and bone cause misuse of the joint, and can lead to additional stress on other structures of the joint, such as ligaments and subchondral structures. The wear and tear of the misused joint are also believed to increase the risk of haemarthrosis or subchondral bleeds, adding further to the elevated risk of haemarthrosis [32, 69].

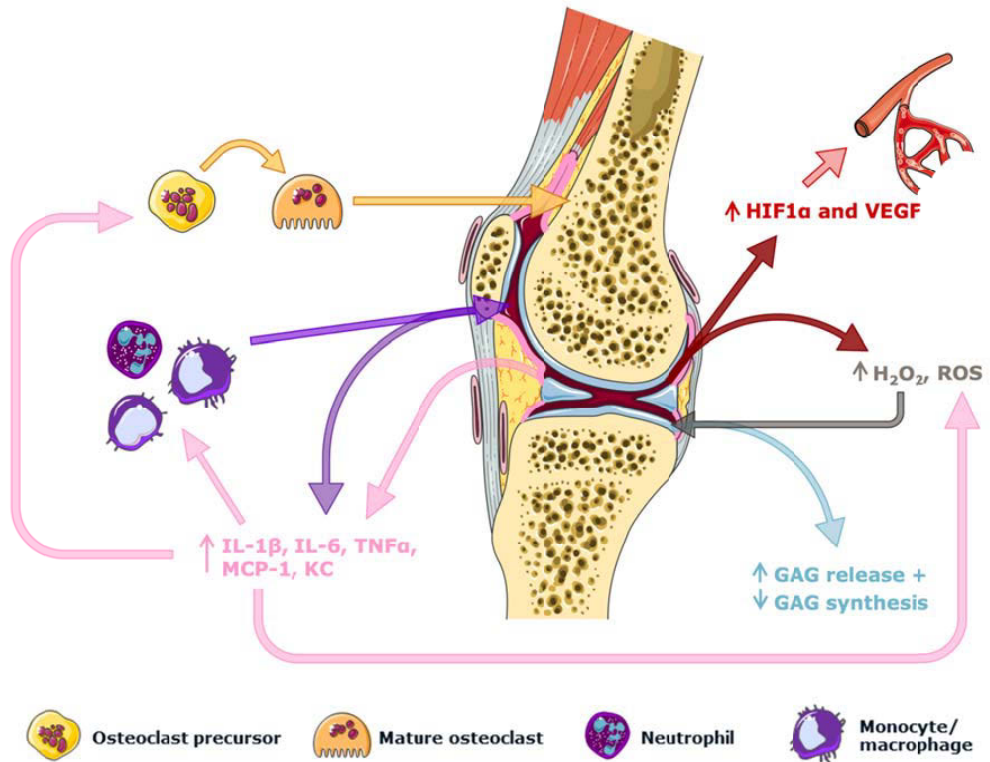


Figure 4: Initiated processes in response to haemarthrosis in haemophilic patients

When blood fills up the joint cavity, the synovial cells secrete inflammatory cytokines such as IL-1 β , IL-6, TNF α and MCP-1. These cytokines can recruit and activate immune cells such as monocytes/macrophages and neutrophils. In the joint these cells together with the A-type cells of the synovial membrane will attempt to resolve the blood. This causes further release of cytokines and propagation of the inflammation. The cytokines also increases osteoclastogenesis (differentiation of premature osteoclasts into mature osteoclasts) pushing the bone homeostasis towards resorption. In addition, the cytokines, the resorption of blood, and iron degradation cause production of hydrogen peroxide (H₂O₂) and reactive oxygen species (ROS). These in turn cause chondrocyte damage and apoptosis leading to reduced glycosaminoglycan (GAG) synthesis and release from the chondrocytes. The net result is a loss of cartilage. Finally, the blood in the joint increases the pressure, causing capillary collapse. This together with an increased oxygen demand due to the inflammation leads to HIF1 α and VEGF expression and an angiogenic response. The newly formed vessels and the wear and tear of the joint are believed to increase the risk of re-bleeding, instigating a vicious cycle of progressive joint deterioration.

Source and permission: Modified from Servier Medical Art, <http://servier.com/Powerpoint-image-bank>.

The continuous haemarthroses and degeneration of the joint will eventually cause complete destruction of the intra-articular structures, resulting in a joint with an enlarged fibrotic synovial membrane, without

supporting cartilage, and with bone erosions and possibly subchondral cysts (see Figure 5). Such a joint is painful and debilitating and requires surgical intervention, such as replacement or fusion of the joint [31].



Figure 5: Progressive joint deterioration as a result of haemarthrosis

The blood in the joint fills up the joint cavity and causes synovial thickening and inflammation. This will gradually lead to cartilage thinning and disappearance. The bone is also affected likely due to an increased resorption, leading to erosions and osteopenia as the condition progresses. Eventually the patient walks on a joint devoid of cartilage with a chronically thickening and inflamed synovial membrane with serious bone abnormalities. The final stage of arthropathy requires surgical intervention to relief pain and increase quality of life for the patient.

Source and permission: Journal of Applied Hematology, <http://jahjournal.org/> [94].

The vicious cycle initiated by haemarthrosis with subsequent joint degeneration and increased risk of re-bleeding underscores the importance of an early diagnosis of synovitis and HA, as the early diagnosis can help aid the correct factor supplementation and use of the joint, leading hopefully to the prevention or halting of the development of late-stage HA.

1.3. Diagnosis of haemophilic arthropathy

The tools for diagnosis of HA are continuously being evaluated and improved in a desire to obtain an early precise diagnosis of joint changes, allowing for individual treatment adjustment and thereby hopefully preventing further joint deterioration.

When evaluating the joints of a haemophilic patient with possible joint disease, both a clinical investigation and imaging assessment are utilised to determine the degree of arthropathy.

Radiographic imaging (X-ray) is the most described and widespread imaging technique to determine arthropathic changes, however, within the recent decades magnetic resonance imaging (MRI) and ultrasonography (US) have become increasingly recognised for their ability to show earlier changes to the joint.

1.3.1. Clinical evaluation of haemophilic arthropathy

Different clinical evaluation systems assessing acute haemarthrosis and joint status in relation to HA have been developed within the last century. The World Federation of Hemophilia (WFH) today recommends

either the Gilbert score (also known as the WFH Physical Examination Score) or the Hemophilia Joint Health Score (HJHS) [15].

Both scores are additive scores including parameters such as swelling, muscle atrophy, deformity, and range of motion to determine the presence of haemarthrosis, chronic synovitis, or more severe arthropathy [15, 95]. Studies have shown a high correlation between clinical evaluation and plain X-ray imaging of affected joints [96-98]; however, clinical examinations are unable to determine the extent of HA and osteochondral damage, which is why imaging remains an essential part of determining HA in haemophilia patients.

1.3.2. Radiographic imaging and evaluation of haemophilic arthropathy

The first imaging technique deployed for diagnosing and grading HA was X-ray and the technique is still used today [15, 99]. The drawback of this imaging modality however, is the fact that X-ray imaging of joints can only visualise more severe often irreversible disease complications. Thus, the technique does not allow for assessment of the earlier soft tissue changes following haemarthrosis, such as synovitis and damage to the cartilage [100]. Some of the earliest HA related changes identifiable by X-ray are squaring of the patella and widening of the intercondylar notch [101-103]. Later-stage HA changes visible in X-ray images include joint space narrowing, erosions, subchondral cysts, and bone deformity [101, 103].

Other radiographic techniques with higher resolution such as computed tomography (CT) provide cross-sectional images with a high level of detail [99], however, the level of radiation prevents the repetitive use of this technique as is required for continuous monitoring of joint health.

To assess the degree of arthropathy in X-ray images different scoring systems have been suggested [31, 103], and today the most applied grading system is the Pettersson score (see Table 1), recommended by the World Federation of Hemophilia [15, 26, 98, 102, 103].

Soft-tissue changes such as synovial thickening and initial cartilage disappearance are, however, difficult to assess using X-ray, which is why MRI and US are increasingly employed [96, 99, 102, 103].

Table 1: Overview of the Pettersson score applied to radiological images [103]

Parameter	Assessment	Score
Osteoporosis	Absent	0
	Present	1
Enlargement of epiphysis	Absent	0
	Present	1
Irregularity of subchondral surface	Absent	0
	Slightly	1
	Pronounced	2
Narrowing of joint space	Absent	0
	<50%	1
	>50%	2
Subchondral cyst formation	Absent	0
	1 cyst	1
	>1 cyst	2
Erosions at joint margins	Absent	0
	Present	1
Incongruence between joint surfaces	Absent	0
	Slight	1
	Pronounced	2
Deformity (angulation and/or displacement of articulating bones)	Absent	0
	Slight	1
	Pronounced	2

1.3.3. Magnetic resonance imaging and evaluation of haemophilic arthropathy

The sensitivity of MRI to reveal soft tissue and osteochondral lesions are superior to both X-ray and the clinical examination [99, 100, 104]. Studies have thus shown that patients who have suffered haemarthrosis with a normal appearance on X-ray most often have considerable damage to the joint in the form of cartilage loss and minor erosion of bone visible on MRI. Likewise, clinically normal joints have on MRI been shown to suffer early signs of synovitis and HA [56, 97, 105, 106].

The findings of early HA pathology on MRI include joint effusions and thickening of the synovial membrane sometimes with an inflamed appearance [56, 97, 105]. Cartilage thinning or loss has also been demonstrated in MRI, as have bone deformations such as erosions and cystic lesions [105, 106]. In addition to the structural changes and pathology of the joint, MRI can also show deposition of haemosiderin, as an indication of previous haemarthrosis and the condition of the synovium [98, 105].

MRI is now considered the best imaging modality for assessing joint deterioration and evaluating progression of HA because it allows for visualisation of both soft tissue and bone structures [101, 107, 108].

Several scoring systems for assessing HA using MRI have been developed in order to grade the severity of arthropathic changes and aid in decision making of future treatment [99, 107, 109]. Recently, a new scale has been suggested, which is based on a combination of the previous X-ray and MRI scores, and divided into sub scores, allowing for individual assessment of soft tissue and bone (see Table 2) [109].

Table 2: Overview of the IPSG scale for assessment of arthropathic changes on MRI [109]

Score type	Parameter	Assessment	Score	
Soft tissue changes	Effusion/haemarthrosis	Small	1	
		Moderate	2	
		Large	3	
	Synovial hypertrophy	Small	1	
		Moderate	2	
		Large	3	
	Haemosiderin	Small	1	
		Moderate	2	
		Large	3	
	Soft tissue sub score		<i>Maximum</i>	9
	Osteochondral changes	Surface erosions (involving subchondral cortex or joint margins)	Any surface erosion	1
			≥50% of the articular surface eroded in at least one bone	1
Subchondral cysts		At least one	1	
		Cysts in at least two bones, or cystic changes involving ≥1/3 of the articular surface in at least one bone	1	
		Any loss of cartilage-height	1	
Cartilage degradation		Loss of ≥50% of the total cartilage volume in at least one bone	1	
		Full-thickness loss of joint cartilage in at least some area in at least one bone	1	
		Full-thickness loss of joint cartilage including ≥50% of joint surface in at least one bone	1	
Osteochondral sub score			<i>Maximum</i>	8

Despite the high level of sensitivity of MRI, the technique is both expensive and time consuming and many younger patients require sedation during the procedure [110]. Perhaps, therefore, studies of HA

visualisation and evaluation need to continue and other modalities such as US are also suggested as an alternative for evaluating soft tissue pathology of HA.

1.3.4. *Ultrasonographic assessment of haemophilic arthropathy*

The use of US in assessment of haemarthrosis and HA has been refined throughout the last four decades and is now routinely employed in some haemophilia clinics for regular evaluation of joint status [108, 111]. The technique has received increasing attention and has become widely embraced due to the relatively easy and rapid procedure, requiring no sedation and with no radiation exposure [110, 112].

US can readily show the presence of intra-articular fluid and thereby help verify an acute haemarthrosis and determine factor replacement treatment. Ceponis and colleagues recently highlighted the relevance of this capacity in a study, where they used US to examine patients with painful joints causing them to suspect a joint bleed [113]. The study showed that the majority of the assumed bleeds were in fact caused by arthritic degeneration of the joint and vice versa. Like MRI, the technique can, therefore, aid in treatment decision making in early stages of haemarthrosis and HA, as additional factor replacement therapy would not affect the patients who suffered due to arthritic changes and not haemarthrosis.

US is user-dependent, however, and evaluation of cartilage loss, erosions and subchondral cysts is more difficult to assess with US. The presence of such damage seems to be underestimated with US compared to MRI [110, 111, 114]. Likewise, haemosiderin has proven difficult to estimate, and is often not reported [110, 111, 113, 115, 116].

As in X-ray and MRI, scores have been applied and developed in an attempt to stratify patients according to severity of joint damage. Protocols for US scanning procedures have also been designed in order to minimise operator-dependent variance between scans [114, 117-120]. These protocols provide information on joint positioning during US procedures and correct placement of the US transducer according to defined landmarks within the joints.

Recently Martinoli and colleagues developed the Haemophilic Early Arthropathy Detection with Ultrasound (HEAD-US) score (see Table 3), an additive score specifically designed for US of the most haemarthrosis affected joints [119].

So far no single score is recommended by the World Federation of Hemophilia for US images [15]. Likely, once sufficient evidence exists for validity and reliability of one or more scores, these will be employed more widely in US assessment of HA.

Table 3: Overview of the HEAD-US score for assessment of arthropathy on US [119]

Score type	Parameter	Assessment	Score
Disease activity (synovitis)	Hypertrophic synovium	Absent/minimal	0
		Mild/moderate	1
		Severe	2
Disease damage (articular surfaces)	Cartilage	Normal	0
		Echo-texture abnormalities, focal partial/full-thickness loss involving <25% of the target surface	1
		Partial/full-thickness loss of articular cartilage involving at least ≤50% of the target surface	2
		Partial/full-thickness loss of articular cartilage involving >50% of the target surface	3
	Complete cartilage destruction or absent visualisation of the articular cartilage on target bony surface	4	
	Bone	Normal	0
		Mild irregularities of the subchondral bone with/without initial osteophytes around the joint	1
Deranged subchondral bone with/without erosions and presence of prominent osteophytes around the joint		2	

Note: Target surface: Elbow: anterior aspect of the distal humerus epiphysis; Knee: femoral trochlea; Ankle: anterior aspect of the talar dome.

Despite the improvements in imaging and diagnosis of the early phases of HA, the pathobiology of disease development in the progress of haemarthrosis to synovitis and onwards towards HA is still complicated by the inability to study very early joint changes in patients. To this end, studies employing animal models of haemophilia and HA have been employed.

1.4. Animal models of haemophilia and haemophilic arthropathy

Animal models have to date proven indispensable in pathobiological and pharmacological studies, and have been used to study haemophilia and HA throughout the last century, aiding in drug testing and disease understanding.

Some of the earliest studies of haemophilia and HA in animals emerged after a haemophilic dog was discovered and from it a colony of haemophilic dogs was established [16, 57, 121, 122]. Since then, other animals with spontaneous haemophilia have been described, such as the sheep and pig [123, 124]. With the development of techniques allowing for gene editing, rodent models of haemophilia and HA have also

been developed [125, 126]. To date, the most widely used animal models of haemophilia are the early established dog model and the genetically modified mouse models.

1.4.1. The haemophilic dog

The first described dog with haemophilia was an Irish setter, and from the kennel of this dog, heterozygous females were brought to the University of North Carolina, Chapel Hill, where a colony of haemophilic dogs was bred and characterised [121, 122].

The disease in dogs is X-linked and recessive thereby resembling the human inheritance pattern. The mutation underlying the haemophilic disease of the Chapel Hill colony was recently shown to be due to an inversion in the F8 gene analogous to the common intron 22 inversion of human haemophilia A patients [121, 127]. Furthermore, the manifestations of the disease are similar to the human clinical phenotype, with variation in bleeding severity, although most dogs appear to have a severe phenotype [121].

The dogs also experience spontaneous and trauma-related haemorrhages first appearing early in life, and the majority of these are situated in the joints [16, 121]. The result of multiple haemarthroses is development of a condition that clinically and physiologically resembles HA. Upon a haemarthrosis, the joint of the dog swells, appears painful and is flexed in an immobile position [121]. When examining the joints of haemophilic dogs *post mortem*, they are shown to contain an enlarged, fibrotic synovium discoloured due to haemosiderin depositions. The cartilage of the joint is sometimes eroded, resulting in joint space narrowing, which can be accompanied by bone changes such as osteophytes or subchondral cysts [57].

Due to the similarities between dog and human haemophilia and HA, the dog is considered a valuable model, and has been utilised in both pharmacological and pathophysiological research [16, 121]. The large size of the animal allows for repetitive blood sampling for pharmacokinetic studies, and the spontaneous bleeds have made it possible to study HA in an *in vivo* setting. However, despite the clear advantages of the dog, some difficulties also exist. First, compared to rodent animal models, the dog has a longer oestrous cycle, which is why a large colony of haemophilic dogs is difficult to maintain. Additionally, the price of maintaining such a colony is considerable, which to some extent can limit the dissemination of the model.

In contrast, rodent animal models are often inexpensive compared to larger animal models, and have a very short oestrous cycle. The F8 knock-out (KO) mouse models, therefore, have received much attention since they were developed, and have been quickly employed in haemophilia research.

1.4.2. The F8 knock-out mouse models

Two haemophilia A mouse models exist, however, unlike the dog model, the haemophilia A mouse models were genetically modified. The genetic disruption of the F8 gene has resulted in no measurable FVIII activity in both strains.

Upon incision, the KO mice have prolonged bleeding, and studies of tail vein transection have shown the lethality of the F8 mutation in these mouse strains [125]. However, unlike the haemophilic dog and human patients, the F8 KO mouse models of haemophilia A do not suffer spontaneous bleeds [125, 128].

The lack of spontaneous bleeds have both been considered a flaw in the translational potential of the mouse models, but also an advantage as treatment is not necessary during breeding and housing. This ensures that animals involved in pre-clinical drug testing have not previously been treated with plasma or recombinant human FVIII (rhFVIII) products, which otherwise could have resulted in anti-FVIII antibodies already present at initiation of testing. Additionally, the joints of these mice are not naturally destroyed by spontaneous haemarthrosis. Therefore, the natural progression of HA has not been possible to study *in vivo* in this mouse model. However, the pristine joints of the mice have allowed for studies of the effect the first haemarthrosis have on the joint, as models of induced haemarthrosis have been developed (see the section entitled Models of haemophilic arthropathy).

Another aspect of the mouse physiology considered an advantage, is the small blood volume of the mouse. Mouse studies require smaller dosages in drug testing, due to the smaller blood volume, which reduce study costs. Unfortunately, the smaller blood volume at the same time also limits the frequency and volume of blood sampling, which consequently can require the enrolment of more animals in the studies to cover several sampling time points [129].

In addition to the physiological aspects of the mouse models, practical advantages include lower space and cost requirements necessary to house and breed a colony. Finally, well-established methods of genetic modifications also exist in the mouse, enabling insertion of human genes into the mouse genome, allowing for humanisation of the F8 KO mouse model for future pre-clinical testing of drug immunogenicity.

Although the mouse models present with relevant advantages for studies in HA development, the limitation due to the size of the mouse have recently lead to development of a new animal model of haemophilia, namely the F8 KO rat [126].

1.4.3. The F8 knock-out rat model

The rat as a laboratory animal has already been widely used and characterised, and it provides the same gestational frequency and relatively easy handling and housing as the mouse. The rat is also approximately 10 times larger than the mouse, allowing for considerably larger and more frequent blood sampling [129]. Finally, like the mouse, genetic engineering is also possible in the rat. This allowed for development of a F8

KO rat, in the hope of creating a phenotypically translational rat model of haemophilia with spontaneous bleeds, but retaining the advantages of a minor laboratory animal such as the mouse [126].

The genetically modified F8 KO rat has no measurable FVIII activity, and overall the clinical manifestations are in accordance with the bleeding phenotype of the dog and also human haemophilia A patients. The F8 KO rats suffer prolonged bleeding [126], but the rat also presents with spontaneous bleeds. The majority of the spontaneous bleeds are in the fore-limbs, with the paws and hocks being the most affected places. Upon histological examination, evidence of both intra- and extra-articular bleeds was found. Interestingly, the knee-joint of the rat seem spared from spontaneous bleeding events [126]. The majority of the spontaneous bleeds in the rat occurred mostly between six to ten weeks of age, i.e. in immature rats [126, 130], consistent with human haemophilia A patients.

In addition to the genetically modified F8 KO rat model, another spontaneous haemophilic rat has been reported. This strain (WAG-F8^{m1 Ycb}) suffers a single point mutation causing disruption of the FVIII protein structure and below 1% FVIII activity. The result is prolonged bleeding and spontaneous bleeding events consistent with severe haemophilia in rats homozygous for the mutation [131, 132].

Both the F8 KO and the WAG-F8^{m1 Ycb} rat have potential translational value in haemophilia and HA. Additional beneficial properties of the larger rat versus the mouse model are the possibility of using the rat as its own historic control when blood sampling longitudinally and the relatively easier visualisation of joint structures. Combined, the properties of the rat make development of the haemophilic rat as a model of HA desirable.

1.4.4. Models of haemophilic arthropathy

The dog model of haemophilia allowed for studies in HA manifestations subsequent to spontaneous bleeding episodes, but studying specific time points following haemarthrosis is difficult in a spontaneous bleeding model. Furthermore, as the mouse model of haemophilia A does not suffer spontaneous bleeds, studies of HA onset and progressive pathology required development of a method for generating haemarthrosis.

Traditionally, the knee-joint has been the joint utilised for these models of HA, as this previously was the most affected joint in human haemophilic patients, and the large size of the joint is also favourable.

Different approaches have been utilised to simulate or induce a joint bleed, with some developed specifically for haemophilic animal models and one allowing for studies of haemarthrosis in wild type animals.

Injection of autologous blood from the same animal into the knee-joint has been employed as a method for simulating joint bleeds (see **Fejl! Henvisningskilde ikke fundet.**). The advantage of this method is that

it can be applied in both haemophilic and wild type animals, which have enabled studies in other species than the original haemophilic models, e.g. rabbits [29].

The translational value of this method is, however, debatable, as the injected blood constitutes a fixed volume and does not resemble a haemarthrosis with prolonged bleeding.

To study HA development in response to a haemarthrosis with continuous bleeding into the joint, haemophilic animal models are used. Two well-established models of induced haemarthrosis in the F8 KO mouse have been described.

The first model developed is the so-called blunt trauma model, where a haemarthrosis is induced in the knee-joint of the mouse, by placing the mouse in dorsal recumbence, with a spring-loaded device above the knee (see **Fejl! Henvisningskilde ikke fundet.**B). When triggered, the device will impose a trauma to the knee and induce haemarthrosis which have been shown to cause synovitis and HA [133, 134].

The advantage of this model is that it resembles the trauma-induced haemarthrosis of human haemophilia patients. The disadvantage of this method is that the trauma can cause damage to the joint structures, making interpretation of the pathological effect of haemarthrosis in the joint difficult upon histological assessment.

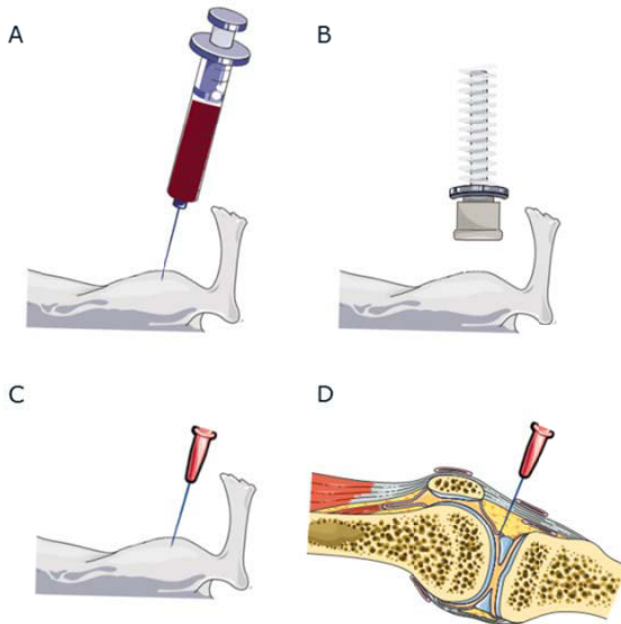


Figure 6: Overview of induced HA models

A) Injection of autologous blood into the joint of a haemophilic or wild type animal

B) Blunt force trauma model where a spring load device is placed above the knee joint and when released imposes a trauma to the joint

C) Needle-induced model, where a 30 gauge needle is inserted into the knee joint through the patella ligament

D) The knee joint shown in the sagittal view with the needle placed through the patella ligament as it is performed in the needle-induced joint bleed model

Source and permission: Modified from Servier Medical Art, <http://servier.com/Powerpoint-image-bank>.

In an attempt to refine the blunt trauma model of induced haemarthrosis and develop a method resembling more spontaneous bleeds, Hakobyan *et al.* developed the needle-induced model [79]. In this model, a haemarthrosis is induced in the knee-joint by shortly inserting a 30 gauge needle into the joint space through the patella ligament (see **Fejl! Henvisningskilde ikke fundet.**C and D).

The advantage of this model is that the joint-puncture can be performed without damage to the cartilage and bone structures of the joint, allowing for pathophysiological evaluation of these structures. The disadvantage of this model is the penetration of the joint capsule and the often relatively large bleeds induced, which can require euthanasia of the affected animal premature to study finalisation.

To complete the characterisation of the needle-induced arthropathy model, Valentino and Hakobyan also developed a histological assessment score. Histology remains the gold standard for evaluation of HA, and a score can help grade severity of joint damage in a similar manner as the employed imaging scores for human haemophilia patients. The score is developed as a method for assessing synovitis and is an additive score including parameters such as synovial hyperplasia and haemosiderin depositions (see Table 4) [135].

Table 4: The synovitis grading scheme developed by Valentino and Hakobyan [135]

Parameter	Assessment	Score
Synovial hyperplasia	Normal, less than four cell layers	0
	Four to five layers	1
	Six to seven layers	2
	More than seven layers	3
Vascularity (400x zoom)	None	0
	$< \frac{1}{3}$ of the field of view	1
	$\frac{1}{3} - \frac{2}{3}$ of the field of view	2
	$> \frac{2}{3}$ of the field of view	3
Discoloration by haemosiderin	Absent	0
	Present	1
Blood (erythrocytes)	Absent	0
	Present	1
Villus formation	Absent	0
	Present	1
Cartilage erosion	Absent	0
	Present	1

The animal models of induced haemarthrosis continue to be a valuable tool for studying HA pathobiology and for pharmacological drug testing. However, despite the improved knowledge of tissue response and

joint deterioration derived from animal studies, much remains unknown about the progression from a joint bleed to chronic HA.

1.5. Remaining questions in the pathobiology of haemophilic arthropathy

Although much attention and effort have been put into resolving the pathobiology of HA, several questions remain. In particular the early onset and progression from synovitis to HA have not been determined, and the exact sequence of events driving the continuous deterioration of the joint has still not been established.

Studies of human HA progression have been limited by the inability to obtain tissue samples due to the bleeding phenotype of the patients. Therefore, studies on human HA tissue samples have been performed on chronic end-stage HA samples collected during surgical intervention. Recently, the improvement of imaging techniques has allowed for earlier diagnosis of arthropathic joint changes and some new insight into the onset of disease. However, the imaging is often first applied when changes are suspected or during annual evaluation of joint status. Thereby, the joint is not necessarily assessed in relation to an acute haemarthrosis, and the imaging is too infrequent to study details of HA development.

Animal studies have been valuable in clarifying inflammatory responses and HA pathology. However, animal studies of HA have also often investigated late-stage HA and focused on time points many days apart [79, 84, 133, 134, 136].

Contrary to these studies are the studies of the acute haemarthrosis, but these either focus mostly on the first 24 hours or a few mostly scattered time points in the days after haemarthrosis [40, 84, 137]. Additionally, many studies have focused on describing the degeneration of a single tissue, such as the synovial membrane or intra-articular cartilage, and as mentioned, only one study has focused on the early response of the bone to haemarthrosis [78].

Therefore, despite the detailed knowledge of the processes initiated by blood exposure in individual tissue structures such as cartilage, the continuous progression from haemarthrosis to HA has not been fully characterised *in vivo*.

Thorough characterisation and understanding of the tissues responses in the natural setting of the joint and the progressive deterioration from haemarthrosis to established HA could help determine future treatment targets or strategies in addition to the current clotting factor replacement.

The newly characterised haemophilia A F8 KO rat would be an excellent animal to use for such studies. First of all, the rat has great face validity of haemophilia, as it suffers spontaneous bleeds, but it can also be used in studies with induced haemarthrosis, as the knee-joint in the rat is not affected by spontaneous bleeds. The larger blood volume of the rat will also allow for multiple blood sampling, which consequently means that the systemic effect of haemarthrosis can be assessed over time. Finally, the size of the rat knee-joint would also make it easier to assess joint damage using clinically relevant imaging techniques,

which means a temporal *in vivo* assessment of the joint damage in HA could be obtained. The clinically relevant imaging techniques have only sparsely been employed in animal studies of HA, but hold great potential as they can be used to investigate arthropathic progression, allowing for continuous evaluation and not just end-point assessment.

2. Objectives

The primary objective of this thesis was to substantiate the knowledge of early onset and progression from haemarthrosis to haemophilic arthropathy, by investigating the process in the F8 KO rat model of haemophilia A. The thesis aimed to test the hypothesis that an induced haemarthrosis will cause a temporal development of HA alongside inflammatory infiltrations in the knee-joint of F8 KO rats.

To this end, the hypothesis that the F8 KO rat can function as a translational model of HA first needed to be validated, as well as the hypothesis that the joint degeneration can be assessed using relevant imaging techniques.

In accordance, the project was divided into three sub-aims.

2.1. Aims and hypotheses

- I) Establish the F8 KO rat as a model of HA using the needle-induced joint bleed model

Hypothesis: Induction of haemarthrosis in the F8 KO rat will lead to development of chronic degenerative joint changes, comparable to human HA, characterised by synovitis and haemosiderin deposition, along with damage to cartilage and bone

- II) Evaluate the feasibility of using clinically relevant imaging modalities such as ultrasonography and micro-computed tomography for assessment of arthropathic joint deterioration

Hypothesis: Bleeding into the joint of F8 KO rats causes changes to the individual joint components (e.g. ligaments, fat pad, bone) which can be visualised using clinically relevant imaging modalities (i.e. US and μ CT)

- III) Characterise the early pathological changes of the tissues within the knee-joint following haemarthrosis using the established methods of imaging, and histology

Hypothesis: Haemarthrosis leads to temporal degeneration of joint structures alongside inflammatory infiltrations

3. Experimental Work

The majority of the experimental work conducted in this thesis has been described in the two papers and the manuscript included in the thesis and will here be summarised.

All animal experiments described and presented were performed in accordance with guidelines from, and approved by the Danish Animal Experiments Council, the Danish Ministry of Food, Agriculture and Fisheries, as well as the Novo Nordisk Ethical Research Committee.

3.1.1. Validation of the F8 KO rat as a model of HA

To study the pathogenesis of HA in the F8 KO rat model, the rat first needed to be validated as a model of HA; this was the focus of paper I.

Paper I: *“The F8^{-/-} rat as a model of haemophilic arthropathy”* (Sørensen, KR. J. Thromb. Haemost. 2016;14:1216-25)

The objective of this study was to establish whether the F8 KO rat develops HA with a pathology resembling human HA following an induced joint bleed and whether treatment with rhFVIII prior to induction can prevent arthropathic changes.

The study was designed as a case-control study, using the needle-induced joint bleed model in F8 KO or wild type rats. The rats received either one (on day zero) or two (on day zero and fourteen) induced haemarthroses, respectively and were euthanised 14 days after the final haemarthrosis. Furthermore, to study the potential of the rat as a pharmacological model, two different treatment groups were included, one group where the F8 KO rats received rhFVIII prior to the induced haemarthrosis and the other receiving a vehicle solution.

Histological evaluation of the joints revealed marked joint deterioration in vehicle treated F8 KO rats following one or two haemarthroses. The pathological findings included extensive synovial hyperplasia and inflammation, along with chondrocyte apoptosis with concurrent loss of proteoglycans. Haemosiderin depositions were evident both after one and two joint bleeds as were pathological bone changes in the form of osteophytosis and excessive periosteal bone formation. Wild type rats showed no sign of arthropathic changes in the joint. Treatment with rhFVIII prior to induction reduced or completely abolished the pathological conversion of the joint, returning the rats to a wild type phenotype.

The histological sections were scored according to a new score, entitled the arthropathy score, including assessment of synovitis, chondrocyte and/or proteoglycan loss, haemosiderin depositions and bone pathology. When comparing mean arthropathy scores, both of the F8 KO vehicle treated groups had a significantly higher mean than the corresponding wild type groups. Additionally, the vehicle treated F8 KO group subjected to a single haemarthrosis also had a significantly higher mean compared to the rhFVIII treated F8 KO rats. For the two joint-bleed groups, when excluding rats positive for anti-rhFVIII antibodies

from the rhFVIII treated F8 KO group, a significant difference was found between vehicle and rhFVIII treated F8 KO groups. No difference was found between rhFVIII treated and wild type groups.

Overall, the study confirmed the F8 KO rat as a translational model of HA with a concurrent potential as a pharmacological model for intervention therapy studies.

3.1.2. Evaluation of ultrasonography and micro-computed tomography as techniques for assessing joint pathology following haemarthrosis in F8 KO rats

In addition to developing the F8 KO rat as a model of HA, *in vivo* methods for studying the HA progression were also desired. The capacity of US and μ CT and individually optimised scores to visualise and stratify joint pathology following induction of haemarthrosis in the F8 KO rat were investigated.

Paper II: “**Visualization of haemophilic arthropathy in F8^{-/-} rats by ultrasonography and micro-computed tomography**” (Christensen, KR. Haemophilia 2016, 1–11.)

The aim of this study was to verify the application of ultrasonography and μ CT for joint assessment in rats following induced joint bleeds, characterise the changes in the joint and to determine if the imaging modalities could discriminate between treatment groups.

The imaging modalities were applied to the animals included in the study described in paper I. Thus 60 F8 KO and 20 wild type rats subjected to one or two knee-joint bleeds and treated with vehicle or rhFVIII were scanned using US and μ CT.

Baseline US scans showed joints without any signs of pathology in both F8 KO and wild type animals. Pathology in the joint of F8 KO vehicle treated rats was readily identified in US scans both after one and two joint bleeds. The major findings included subcutaneous oedema, swelling of the patella ligament, heterogeneous echogenicity and displacement of the fat pad, and in a few cases ruffling of the bone.

To stratify severity, a US scoring system was developed. This was based on the Visual Analogue Scale (VAS). F8 KO vehicle treated rats had a significantly higher mean US score compared to wild type rats following both one and two joint bleeds. The same were true for vehicle treated compared to rhFVIII treated rats following one joint bleed. When excluding rats with anti-rhFVIII antibodies from the rhFVIII treated group subjected to two joint bleeds, the F8 KO vehicle treated rats also had a significantly higher mean US score compared to rhFVIII treated F8 KO rats. Similarly, only when including anti-rhFVIII positive animals, a difference between rhFVIII treated F8 KO and wild type rats were seen after two joint bleeds.

The high-resolution images obtained using μ CT revealed extensive pathology of the bone in the majority of vehicle treated F8 KO rats. Osteophytosis of femur, tibia, and patella was evident, as was excessive periosteal bone formation on both femur and tibia. In addition to these findings, subchondral cysts were also identified in several rats in μ CT images. The cysts were confirmed using histology, where a fibro-vascular structure was readily identified beneath the articular cartilage.

Similar to the US assessment, an additive score was developed in order to quantify the extent of pathology identified using μ CT. Vehicle treated F8 KO rats had a significantly higher mean total μ CT score compared to wild type rats after one or two joint bleeds. When comparing vehicle F8 KO rats to rhFVIII treated rats, after two haemarthroses significance was reached when excluding animals' positive for anti-rhFVIII antibodies.

To determine the feasibility of US and μ CT imaging for visualising arthropathic joint changes a correlation analysis was conducted between the total arthropathy score (assigned to the groups in paper I) and the individual total imaging scores (US and μ CT, respectively). A significant, and good correlation between the US and arthropathy score was found, but only after two haemarthroses. μ CT had a significant and strong correlation with the arthropathy score, both after a single or two haemarthroses.

Overall, the study verified the applicability of US and μ CT to show soft- and bone tissue changes in the knee-joint of F8 KO rats following induced haemarthrosis. Additionally, the study confirmed the applicability of the two imaging scoring systems for stratification of treatment groups.

3.1.3. Characterisation of the early onset of haemophilic arthropathy

Having established the rat as a translational model of HA and the feasibility of employing US and μ CT for *in vivo* soft tissue and *ex vivo* bone tissue assessment of joint pathology, characterisation of the progression from haemarthrosis to HA in the F8 KO rat was possible.

Paper III: **“Rapid inflammation and early degeneration of bone and cartilage revealed in a time-course study of induced hemarthrosis in hemophilic rats”** (Manuscript)

To describe the progression from haemarthrosis to HA in detail, a study was designed including 100 F8 KO rats randomly assigned to groups subjected to a needle-induced joint bleed or sham procedure and a group euthanised each day from day one to seven (with nine baseline rats euthanised directly).

US confirmed haemarthrosis in 41 out of 51 rats subjected to needle puncture, as they had a positive VAS score. No sham rats scored positive for pathology in the US images, and there was an even distribution of severity between the haemarthrosis-affected groups.

Histological assessment revealed joint pathology consistent with haemarthrosis and synovitis which progressed to HA along the time-course of the study. Scoring of histological stains using the semi-quantitative arthropathy score showed a fast and progressive synovitis apparent from day one and onwards. Cartilage and bone pathology appeared almost simultaneously on day two to three and rapidly progressed to severe joint damage within the seven days of the study. Finally, haemosiderin deposition was identified from day four and onwards in increasing amounts.

Immunohistochemical staining revealed marked inflammatory infiltrations present 24 hours after haemarthrosis. Quantification of the stains using digital image analysis revealed a sequential pattern of infiltrations, with neutrophils appearing first, closely followed by macrophages, and subsequently and to a much smaller degree, T- and B-lymphocytes.

Finally, to assess synovial hyperplasia, sections were stained for proliferation. Quantification of the stain showed a marked short-lived proliferative response.

The cartilage degradation was studied in detail and revealed an almost complete loss of proteoglycans and chondrocytes in the outer layer of the cartilage on day seven.

Bone pathology was visualised using μ CT, which revealed excessive periosteal bone formation stretching along the shaft of the femur and tibia, and progressing rapidly, as shown by the total μ CT score. Histology confirmed the pathologic periosteal bone formation. In addition, a Tartrate-Resistant-Acid-Phosphatase (TRAP) stain was performed to show osteoclast activity. Increasing amounts of active osteoclasts were found, however not significantly different to baseline until severe bone pathology was already evident.

Interestingly, subchondral cysts had intense osteoclast activity. In addition to the subchondral cystic TRAP activity, also synovial cells were stained positive for TRAP. These appeared to co-localise with macrophages and were only found in areas with high concentrations of erythrocytes or haemosiderin depositions.

On the basis of the results, a model of the early onset of HA was suggested. First a rapidly progressive synovitis develops, which is closely followed by both cartilage and bone pathology. The chondrocytes of the cartilage seem to undergo apoptosis, with progressive proteoglycan loss. The result is a gradual disappearance of proteoglycans and chondrocytes. Excessive periosteal bone formation is the first apparent bone pathology readily identified as calcifications on the surface of the cortical bone, extending from the bone ends along the shaft of the bones away from the joint. This is followed by subchondral cyst formation, possibly as a result of increasing osteoclast activity.

When pathology in all three tissues of the joint is evident, haemosiderin depositions appear.

Overall, the detailed mapping of HA onset and development in the F8 KO rat model of HA revealed that the pathology develops rapidly after haemarthrosis. Furthermore, the pathology of cartilage and bone develops simultaneously and appears shortly after synovitis onset with a rapid progression towards severe HA pathology.

3.2. Additional immunohistochemical stains and results

In addition to the results presented in the three manuscripts, immunohistochemical stains were conducted in the study described in paper III, which were not included in the manuscript.

3.2.1. *Characterisation of joint vascularity following haemarthrosis*

The study characterising the early onset of HA described in paper III included additional immunohistochemical stains performed to assess vascularity of the joint.

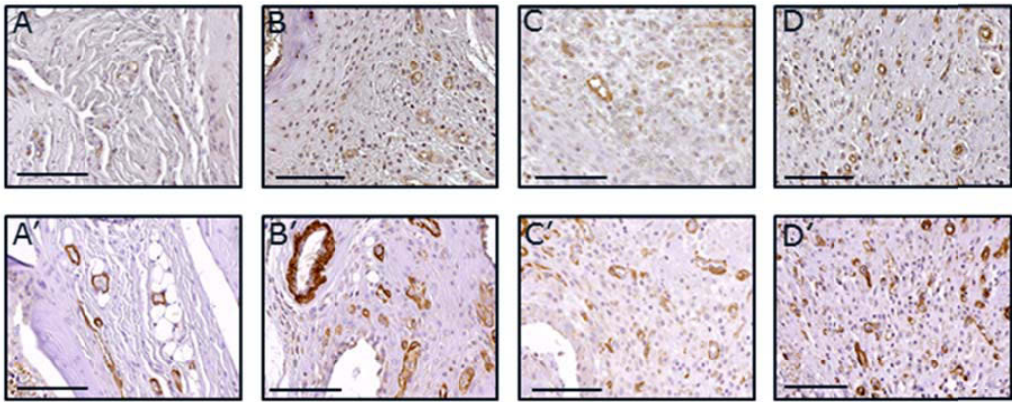
To evaluate joint vascularity in response to haemarthrosis, sections from the 100 rats included in the characterisation, euthanised day zero to seven, were stained for the vascular markers alpha-smooth muscle actin (α SMA) and cluster of differentiation 31 (CD31).

Heat-induced antigen retrieval was performed at 59° C overnight, followed by washing, avidin-biotin (004303, Vector laboratories, Burlingame, California, USA) incubation and blocking with 0.5% skimmed milk, 3% bovine serum albumin (Sigma-Aldrich, St. Louis, Missouri, USA), 3% rat serum and 7% donkey serum (Jackson Immuno Research Labs, Suffolk, Great Britain) for one hour at room temperature. This was followed by incubation with primary antibodies in concentrations of 1 and 3 μ g/mL for α SMA (Ab5694, Abcam, Cambridge, Great Britain) and CD31 (Lifespan Biosciences, Seattle, Washington, USA), respectively. Sections incubated at 4° C overnight. Hereafter, the sections were washed, and incubated for one hour at room temperature with biotinylated secondary donkey-anti-rabbit antibodies (705-065-147, Jackson Immuno Research Labs), before development with 3,3'-Diaminobenzidine (DAB, Sigma-Aldrich).

The stains were scanned using the Nanozoomer slide scanner 2.0 (Hamamatsu Photosonics K.K., Hamamatsu City, Japan) using a 20 times magnification whole slide scan and staining quantified using the Visiopharm Integrator System software (Visiopharm, Hoersholm, Denmark). The stains were quantified both in accordance with the percentage of stained area and the number of vessels in the stain. Quantification of stained area was performed by conducting an unsupervised K-means clustering algorithm generating a region of interest (ROI) consisting of the entire section. Hereafter, ROIs excluding cortical bone and bone marrow were drawn, blinded towards the origin of the section. Finally, a threshold analysis in the DAB channel was performed with the threshold set to 160 for CD31 and 110 for α SMA. Number of vessels were analysed by performing a threshold analysis only accepting stained pixels with a minimum size of 2.8×10^{-6} mm² capturing coherent pixels of vessels.

The stains revealed a rapid increase in both percentage stained area and number of vessels for both the CD31 and α SMA stain (see

Figure 7), although the quantification of the number of vessels for the α SMA stain was first significantly different between sham and haemarthrosis rats on day seven. The increase in the stains persisted throughout the seven days, indicating a vascular response in the joint following haemarthrosis.



E

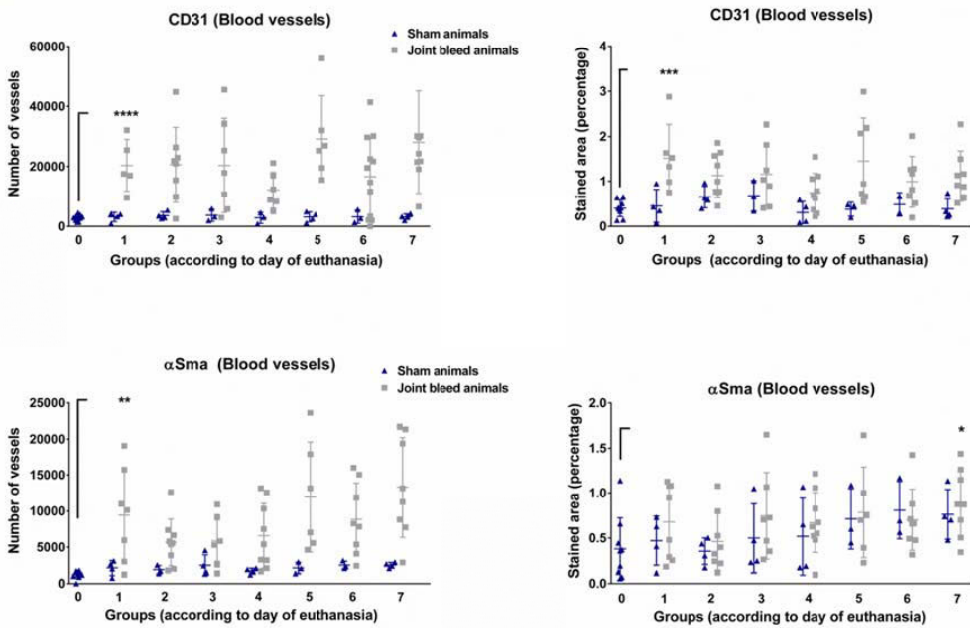


Figure 7: The vascular response in F8 KO rat knee-joints following induced haemarthrosis

Panel A-D) show CD31 stained sections from day 0, 1, 4 and 7 following haemarthrosis. A'-D') show alphaSMA stained sections from day 0, 1, 4 and 7. E) shows the quantification of the number of blood vessels and percentage stained area for CD31 and alphaSMA, respectively. The digital image analysis revealed an early consistent increase in both vessel number and percentage stained area for CD31, and for alphaSMA particularly the number of blood vessels was increased followed haemarthrosis.

The first time of significant difference to baseline was established using sequential Students *t*-test and the first significant difference is thus the only significance reported for all scores.

* P<0.05 ** P<0.01 *** P<0.001 **** P<0.0001

4. Discussion

This thesis aimed to test the hypothesis that haemarthrosis leads to a temporal degeneration of joint structures and infiltrations of immune cells. Prior to this work, the validity of using a needle-induced knee-joint bleed to study development of HA in the F8 KO rat and produce an outcome resembling that of patients with HA was studied. The utility of histology, US and μ CT for visualisation and assessment of disease severity was also explored.

4.1.1. Development and validation of the F8 KO rat as a model of haemophilic arthropathy

Employing the needle-induced joint bleed model to the F8 KO rat led to development of severe arthropathic changes consistent with chronic HA in human patients. The rat exhibited a promising face validity of HA, as the vehicle treated F8 KO rats developed a pathology that resembles human HA (paper I). Severe synovitis, cartilage loss, and bone pathology developed in these rats within two weeks. The synovitis was characterised by hyperplasia, inflammatory infiltrations, and fibrosis along with haemosiderin depositions in the synovium. Cartilage damage was identified as chondrocyte apoptosis and proteoglycan loss, while bone pathology was composed of osteophytosis, periosteal bone formation and subchondral cysts.

Although the cartilage damage was minor compared to late-stage HA in human patients, it was similar to what is observed in the mouse models of HA [79, 133]. Furthermore, a pannus did not develop. Whether the pannus and severe cartilage damage, such as clefts and aberrations, did not develop due to the length of the study or the number of joint bleeds remains uncertain. Cartilage composition differs between humans and mice, and rats, with rodents having a higher density of chondrocytes in the cartilage [138]. The higher density of chondrocytes might to some extent rescue the cartilage from degradation, as the higher density of cells might counteract the damaging effect of haemarthrosis by an increased proteoglycan production compared to human intra-articular cartilage. Consequently, it could be hypothesised that additional time or joint bleeds are necessary for HA development with complete cartilage loss in the F8 KO rats. This theory is in part supported by a recent study that employed the developed F8 KO rat model of HA in a longitudinal study of joint deterioration biomarkers [139]. Here it was shown that markers of cartilage degradation and formation are significantly elevated in serum of rats subjected to knee-joint bleeds. However, the rise in serum concentrations did not become significant before the second injury, indicating that more joint bleeds are necessary to reach a level of cartilage damage severe enough for detection of biomarkers in serum.

Despite the lack of pannus formation and only minor cartilage damage compared to the extensive synovial and bone pathology, the rat represents a promising future translational model of HA and was, consequently, applied in the present thesis work. Studies of HA pathology are focused on preventing joint

deterioration in the early stages of HA development, which is why late stage cartilage and synovial pathology development perhaps is less important.

The HA pathology in the rat model overall resembles that of mouse, dog, and human HA, and in addition to the already described pathology, the F8 KO rats also developed subchondral cysts. Subchondral cysts have not been reported in the mouse model of HA, which is another reason that the rat appears to have a superior face validity that is comparable to the spontaneous dog model of HA. In addition, treatment with clinically relevant replacement therapy reduces or abolishes the joint deterioration, confirming the predictive value of the model.

4.1.2. Development and validation of imaging modalities and scoring systems for assessment of haemophilic arthropathy

The verification of the F8 KO rat as a model of HA, also included establishment of the imaging modalities μ CT and US as tools for HA visualisation as well as, individual scoring systems for histological, US and μ CT HA severity assessment.

Previously, the score of synovitis, developed by Hakobyan and Valentino has been the most widely used score for histological assessment in animal studies of HA [65, 140, 141]. However, this score is developed as a grading system of synovitis, and does not include or stratify several aspects of arthropathic joint changes. Thus, cartilage damage is reduced to absent or present, and bone pathology is not included (see Table 4). Considering the severe arthropathy the models of HA develop within two weeks, it seemed reasonable to develop a score encompassing both synovial, cartilage, and bone pathology. To this end, the arthropathy score was developed, and was shown capable of dividing animals according to treatment and genotype (paper I).

When characterising the development of HA onset, the score was further validated (paper III). The sum score revealed a clear progression of pathology, and in addition, the detailed sub-scores clearly described the individual disease parameters' onset and progression. The synovitis sub-score could appear to reach a ceiling effect since the majority of the rats reached the maximum score within few days. However, the sum score stratification of severity in a study with such narrow time-points of assessment shows the capacity of the score for detailed disease stratification.

Besides the histological assessment with the new arthropathy score, US and μ CT were evaluated as tools for HA investigation in order to obtain additional methods of disease characterisation.

Neither of the two imaging modalities has been widely applied in animal studies of HA [47, 77-79]. Likewise, scales specific for US or μ CT grading HA severity in a similar manner as human HA patients, have not been developed.

Although US in rodent models is complicated by the small size of the joints, the study described in paper II showed that several joint structures were readily assessed in the rats knee-joint, and that arthropathic pathology, similar to US findings of human HA, was detectable in the US images (paper II). Furthermore,

the US VAS score was capable of separating the rats into groups according to genotype and treatment, although only a moderate to good correlation was found between the US score and the histological arthropathy score. The US score includes both extra- and intra-articular structures, whereas the arthropathy score only includes intra-articular pathology. Furthermore, at the time of US and histological assessment, severe arthropathic changes were evident, which included severe bone and cartilage pathology. Such changes are not visualised using US, which is likely why the correlation between the US VAS score and arthropathy score was only moderate to good.

Finally, utilising the strength of the US to show soft tissue changes, haemarthrosis was successfully verified in animals subjected to the needle-induced joint bleed model (paper III).

μ CT revealed extensive bone pathology two weeks after haemarthrosis, beyond what was identified by histology (paper II), emphasising the efficacy of this imaging modality for evaluation of HA related bone pathology in rodent models. In addition, the developed μ CT score successfully, and with high correlation to the histological score, separated groups according to treatment and genotype.

Likewise, the μ CT score proved capable of stratifying F8 KO rats across time-points within the first seven days after haemarthrosis with a continuous increase in pathology (paper III). The many end-points investigated in such a short time period provide a high resolution of disease progression, but also challenge stratification tools. However, the strength of the μ CT images and score were verified with the ability of the score to show detailed HA progression.

The validation of US and μ CT substantiate the methods for assessing HA, as well as disease stratifications, using the corresponding scoring systems.

4.1.3. *The early development of haemophilic arthropathy*

Applying the three modalities (histology, US and μ CT) and their individual scoring methods revealed that severe joint damage develops much faster than previously shown in animal models of HA (paper III). Thus, severe cartilage damage, a manifestation of arthropathy, developed within seven days, concurrent with development of bone pathology.

Previous studies in mouse models of HA have generally evaluated HA two or four weeks after haemarthrosis following one or two joint bleeds, respectively (as in paper I). Histological evaluation at these time-points reveals a severe chronic HA, similar to the findings in the rat (paper I). Animal models of HA must in general be considered to have an accelerated disease development compared to human patients, as they develop such severe arthropathy much more rapidly than human HA patients. However, chronic arthropathy is well characterised in human patients, and the purpose of animal studies is generally to establish the pathobiology of progression from haemarthrosis to HA and prevention thereof.

Looking at the early pathology in detail using histology, immunohistochemistry, and μ CT revealed that both cartilage and bone pathology develop shortly after synovitis is evident. This is in contrast to the general belief that synovitis develops first, followed by cartilage damage, and subsequent to this bone

pathology. Considering these findings, the focus of treating HA by preventing synovitis and cartilage damage seems insufficient, as bone damage possibly develops independent of cartilage damage.

As mentioned, cartilage damage is believed to arise as a combination of inflammatory- and blood-driven degradation. The very early cartilage damage suggests that a direct effect of blood is involved (paper III). However, the damage was present prior to any haemosiderin depositions in the joint, the formation of which is believed to drive the direct damage caused by blood. Whether the damaging effects from haem-degradation occurs prior to the end-product haemosiderin, or if the damage seen in the study is due to inflammation that causes the chondrocytes to produce damaging reactive oxygen species is unresolved.

The response of bone cells to blood in the joint has not been thoroughly investigated, although mechanisms of hypoxia and individual cytokines have shown an increase in osteoclast formation and activity *in vitro* [72, 74, 76, 142]. Contrary to this, the first pathology of the bone characterised was excessive periosteal bone formation stretching along the shafts of both femur and tibia (paper III). This pathology has recently also been described in the mouse model of HA two weeks after needle-puncture with concurrent loss of trabecular bone structure [78]. Lau *et al.* hypothesised that the changes are due to calcification of adjacent ligament and attachment sites. However, considering the extent of the pathology, stretching far away from the joint (paper III), and the clear presence of developing bone on histological sections, it seems unlikely that the pathology is merely ligament calcifications. Rather, it seems that the initial response to haemarthrosis of the bone is augmented bone formation. This activity may subside for a later increased bone resorption response, eventually resulting in reduced bone mineral density and osteopenia or osteoporosis as seen in late-stage HA patients [68, 69].

The rapid formation of bone following haemarthrosis indicates that the pathology is not just driven by the continuous synovitis with progressive cartilage loss, but perhaps blood also has a direct effect on bone, similar to the direct and indirect mechanisms of cartilage damage.

In addition to the periosteal bone formation, subchondral cysts also developed rapidly after haemarthrosis. Again, the pathobiology of cyst formation is largely undescribed, but they have been suggested to develop secondary to subchondral haematomas. However, no sign of subchondral haematomas was evident in any of the cysts examined by histology. The late-stage HA and subchondral cysts characterised on day 14 (paper II) is potentially too late in the progression to determine the presence of blood. However, the cysts identified within the first seven days (paper III) showed no signs of haematomas or residual erythrocytes, nor were there haemosiderin depositions in the cysts. Rather the cysts appeared to be of a fibrous nature with an excessive osteoclast activity, eating away the bone beneath the cartilage. The formation of subchondral cysts has also been suggested to be caused by an increased load put on the bone due to cartilage loss, possibly causing subchondral haematomas. However, in the study of the first seven days after haemarthrosis subchondral cysts developed in rats with residual cartilage and within such short time, that load-bearing as the instigating mechanism seems unlikely. The results warrant new theories of subchondral cyst formation in HA and highlight the importance of

conducting further studies that examine the pathobiology behind the development of HA-related bone pathology.

The characterisation also included evaluation of the vascularity in the joint following haemarthrosis. Immunohistochemistry revealed a marked increase in the number of vessels in the joint already 24 hours after the joint bleed, which persisted throughout the study. Due to the fast response, the initial increase is likely also due to recruitment of dormant capillaries (without red blood cell flow). Whether the continuously increased number of vessels is due to persistent recruitment of these vessels or due to increased angiogenesis requires further investigation, such as staining for angiogenic markers.

Finally, the characterisation of HA onset also revealed cells positive for osteoclastic markers in the synovium, co-localised with macrophages (TRAP-CD68 co-localisation, paper III). The presence of these cells appeared to be dependent on the proximity to high concentrations of erythrocytes or, in later time-points, haemosiderin. Studies have previously shown the ability of macrophages to obtain an osteoclastic phenotype with the capacity of bone resorption [143]. Whether erythrophagocytosis can lead to such a transformation is unknown, as is the function of these intra-articular TRAP-positive macrophages in HA. The intriguing possibility of these cells' involvement in the pathobiology of HA warrants further studies.

Overall, the study in the early characterisation of HA also challenges the generally applied protocol for studying HA in animal models, i.e. one or two joint bleeds induced two weeks apart, with euthanasia two weeks after the final joint bleed. The rapid progression of HA suggests earlier time-points should at least be included, if not be the general standard end-points for studies of HA development in rodent models. Not only will reduction of study length align HA characterisation with actual disease onset as seen in paper III, it will also be an ethical improvement as the time the animals are in distress will be greatly reduced.

5. Conclusion

The studies in this thesis demonstrate new knowledge of HA development through the careful mapping and characterisation of the progression from haemarthrosis to established HA. Furthermore, the initial studies and results provide not only a new animal model of HA, but also various new tools for assessing disease onset and severity in rodent models.

In relation to the outlined hypotheses, the first part of the thesis was focused on validating the F8 KO rat as a model of HA using the needle-induced joint bleed model.

The data presented in this thesis confirm the usability of the F8 KO rat as a translational model of HA with high face validity, as haemarthrosis causes synovitis, cartilage loss, and bone pathology, including subchondral cysts, resembling HA in human patients. Likewise, replacement therapy in the form of rhFVIII can prevent joint deterioration in the F8 KO rat, indicating construct validity of the model, and evidence supporting use of the rat as a pharmacological model.

The aim of establishing additional tools for HA assessment, specifically in the form of US and μ CT was addressed in the second part of the thesis, where the imaging modalities were tested *in vivo* and *ex vivo* respectively. The data presented show that both US and μ CT can visualise joint deterioration in the form of soft and bone tissue, respectively. In addition, by applying specifically designed imaging HA scores, disease severity can be stratified and treatment groups and genotypes distinguished.

The final part of the thesis provides characterisation of the early development of HA, and shows the temporal degeneration of individual tissue types of the joint. The investigation of the joint using both imaging modalities, and histological methods revealed a rapid deterioration of the joint with development of HA within seven days after the induced haemarthrosis. The temporal characterisation showed the recruitment of inflammatory cells, i.e. neutrophils and macrophages, within hours after haemarthrosis, which combined with the blood in the joint, caused severe synovitis already at 24 hours. The data also showed that the subsequent destruction of cartilage and pathological bone turnover, in contrast to previous suggestions, develop concurrently. Furthermore, the application of μ CT and histology showed the initial response of bone tissue to haemarthrosis is increased periosteal bone formation. Finally, the histological assessment also revealed macrophages co-localising with cells positive for the osteoclastic marker TRAP in the inflamed synovium in areas with high density of erythrocytes or haemosiderin. Additional studies are, however, required to determine the potential capacity of bone resorption in these cells and their role in HA development.

In addition to the characterisation of HA development, the application of the arthropathy and μ CT scores in assessment of severity in the short study protocol also substantiated the validation of these scores, as they were capable of stratifying groups with such narrow time points.

In summary, the sub-aims and hypotheses of this thesis were successfully addressed in the three studies. Thus, the hypothesis that induction of haemarthrosis in the F8 KO rat leads to development of degenerative joint changes resembling human HA was tested in paper I and validated. The second hypothesis stating that induced joint-bleeds in F8 KO rats causes changes to the individual joint components, which can be visualised using US and μ CT was tested and accepted, as shown in paper II. The final hypothesis that haemarthrosis leads to temporal degeneration of joint structures alongside inflammatory infiltrations was tested and confirmed in paper III. The degeneration did, however, develop almost simultaneously, in contrast to the previously suggested sequential joint deterioration.

6. Perspectives

The validation of the F8 KO rat as a pharmacological model of HA provides a new animal model for preclinical drug-testing within the field of HA intervention therapy. For such studies, the rat has the optimal smaller rodent size with a favourable blood volume for drug testing, while retaining the possibility of longitudinal blood sampling. In future studies, this can be utilised for multiple blood samples, using the rat as its own historic control, and thereby reduce animal numbers in the pharmacological studies.

Furthermore, the assessment tools and corresponding scores developed provide the possibility of stratifying disease severity making it possible to distinguish treatment efficacy in future studies, rather than just confirm absence or presence of arthropathy. Although μ CT was only utilised *ex vivo* in the two studies (paper II and III), implementation of *in vivo* μ CT is possible, which is why it in future studies hopefully can be added to the available tools for *in vivo* investigation of HA development.

Additionally, the ability of US to show intra-articular bleeding *in vivo* can in future studies be utilised to study correlation between degree of haemarthrosis and severity of the subsequent arthropathy. This can allow for a deeper understanding of the influence that the volume of blood in the joint and duration of bleeding have on joint outcome.

In addition to the tools for assessment of HA, the seven-day protocol employed for characterisation of HA development could be valuable for future studies of HA pathobiology. By implementing the short study design, the ability of intervention therapies to protect joint structures from blood-induced destruction can be viewed directly in the individual joint tissues, as the pathology develops and progresses in parallel during the seven-day protocol.

The results from paper III also warrant additional studies of intervention therapy. Previously, a direct mechanism of blood-induced damage to cartilage caused by breakdown of iron into haemosiderin has been suggested. The difference in cartilage damage onset and haemosiderin appearance shown in paper III highlights that future treatment strategies of cartilage protection should likely include both an anti-inflammatory component and a component protecting against the blood-induced damage. Suggestions of such could be IL-1 β antagonists and the iron-chelator deferasirox. Both have individually been shown to have a protective effect on cartilage following haemarthrosis [61, 140].

Whether the anti-inflammatory treatment or the iron-chelator alone or in combination can affect the increased bone formation following haemarthrosis could also be investigated in the rat model.

The usage of the iron chelator deferasirox may also be helpful in determining the origin of the TRAP-positive macrophages. Treatment with deferasirox prior to haemarthrosis may reveal the absence or presence of these TRAP-positive cells in the synovium, providing the first clues of a potential iron-induced transformation of macrophages. Whether the cells then have capacity for bone resorption, and if they are involved in HA related bone pathology will require additional *in vitro* and *in vivo* studies.

In conclusion, the F8 KO rat allows for intriguing future studies in both HA pathobiology and the treatment hereof. The studies should likely include the short study design, as HA develops much faster than previously described and with a simultaneous pathological onset between joint tissues. In addition, the rapid bone formation and subchondral cyst formation warrant further studies into the biological mechanisms behind these pathologies.

7. References

1. Bolton-Maggs PH, Pasi KJ: **Haemophilias A and B.** *Lancet* 2003, **361**(9371):1801-1809.
2. Mannucci PM, Tuddenham EG: **The hemophilias--from royal genes to gene therapy.** *The New England journal of medicine* 2001, **344**(23):1773-1779.
3. Franchini M, Gandini G, Di Paolantonio T, Mariani G: **Acquired hemophilia A: a concise review.** *American journal of hematology* 2005, **80**(1):55-63.
4. Graw J, Brackmann HH, Oldenburg J, Schneppenheim R, Spannagl M, Schwaab R: **Haemophilia A: from mutation analysis to new therapies.** *Nat Rev Genet* 2005, **6**(6):488-501.
5. Gitschier J, Wood WI, Goralka TM, Wion KL, Chen EY, Eaton DH, Vehar GA, Capon DJ, Lawn RM: **Characterization of the human factor VIII gene. 1984.** *Biotechnology* 1992, **24**:288-292.
6. O'Brien D: **The purification of factor VIII and the characterization of the human factor VIII gene.** *Haemophilia : the official journal of the World Federation of Hemophilia* 1995, **1 Suppl 2**:3.
7. Roosendaal G, Lafeber FP: **Blood-induced joint damage in hemophilia.** *Seminars in thrombosis and hemostasis* 2003, **29**(1):37-42.
8. Soucie JM, Cianfrini C, Janco RL, Kulkarni R, Hambleton J, Evatt B, Forsyth A, Geraghty S, Hoots K, Abshire T *et al*: **Joint range-of-motion limitations among young males with hemophilia: prevalence and risk factors.** *Blood* 2004, **103**(7):2467-2473.
9. Soucie JM, Miller CH, Kelly FM, Payne AB, Creary M, Bockenstedt PL, Kempton CL, Manco-Johnson MJ, Neff AT, Haemophilia Inhibitor Research Study I: **A study of prospective surveillance for inhibitors among persons with haemophilia in the United States.** *Haemophilia : the official journal of the World Federation of Hemophilia* 2014, **20**(2):230-237.
10. Hoffman M: **Remodeling the blood coagulation cascade.** *J Thromb Thrombolysis* 2003, **16**(1-2):17-20.
11. Hoffman M, Monroe DM, 3rd: **A cell-based model of hemostasis.** *Thrombosis and haemostasis* 2001, **85**(6):958-965.
12. Acharya SS: **Exploration of the pathogenesis of haemophilic joint arthropathy: understanding implications for optimal clinical management.** *British journal of haematology* 2012, **156**(1):13-23.
13. Nugent D, Kalnins W, Querol F, Gregory M, Pilgaard T, Cooper DL, Iorio A: **Haemophilia Experiences, Results and Opportunities (HERO) study: treatment-related characteristics of the population.** *Haemophilia : the official journal of the World Federation of Hemophilia* 2015, **21**(1):e26-38.
14. Gringeri A, Ewenstein B, Reininger A: **The burden of bleeding in haemophilia: is one bleed too many?** *Haemophilia : the official journal of the World Federation of Hemophilia* 2014, **20**(4):459-463.
15. <http://www.wfh.org/en/page.aspx?pid=637>
16. Hutt FB, Rickard CG, Field RA: **Sex-linked hemophilia in dogs.** *J Hered* 1948, **39**(1):2-9.
17. Manco-Johnson MJ, Abshire TC, Shapiro AD, Riske B, Hacker MR, Kilcoyne R, Ingram JD, Manco-Johnson ML, Funk S, Jacobson L *et al*: **Prophylaxis versus episodic treatment to prevent joint disease in boys with severe hemophilia.** *The New England journal of medicine* 2007, **357**(6):535-544.
18. Valentino LA: **Blood-induced joint disease: the pathophysiology of hemophilic arthropathy.** *Journal of thrombosis and haemostasis : JTH* 2010, **8**(9):1895-1902.
19. Oldenburg J: **Optimal treatment strategies for hemophilia: achievements and limitations of current prophylactic regimens.** *Blood* 2015, **125**(13):2038-2044.
20. Knobe KB, E.: **Haemophilia and joint disease: pathophysiology, evaluation and management.** *Journal of Comorbidity* 2011, **1**(1).
21. Forsyth AL, Gregory M, Nugent D, Garrido C, Pilgaard T, Cooper DL, Iorio A: **Haemophilia Experiences, Results and Opportunities (HERO) Study: survey methodology and population demographics.** *Haemophilia : the official journal of the World Federation of Hemophilia* 2014, **20**(1):44-51.
22. Cassis FR, Buzzi A, Forsyth A, Gregory M, Nugent D, Garrido C, Pilgaard T, Cooper DL, Iorio A: **Haemophilia Experiences, Results and Opportunities (HERO) Study: influence of haemophilia on interpersonal relationships as reported by adults with haemophilia and parents of children with**

- haemophilia.** *Haemophilia : the official journal of the World Federation of Hemophilia* 2014, **20**(4):e287-295.
23. Cassis FR, Querol F, Forsyth A, Iorio A, Board HIA: **Psychosocial aspects of haemophilia: a systematic review of methodologies and findings.** *Haemophilia : the official journal of the World Federation of Hemophilia* 2012, **18**(3):e101-114.
 24. Bolton-Maggs PH: **Optimal haemophilia care versus the reality.** *British journal of haematology* 2006, **132**(6):671-682.
 25. Altisent C, Martorell M, Crespo A, Casas L, Torrents C, Parra R: **Early prophylaxis in children with severe haemophilia A: clinical and ultrasound imaging outcomes.** *Haemophilia : the official journal of the World Federation of Hemophilia* 2015.
 26. Aledort LM, Haschmeyer RH, Pettersson H: **A longitudinal study of orthopaedic outcomes for severe factor-VIII-deficient haemophiliacs. The Orthopaedic Outcome Study Group.** *Journal of internal medicine* 1994, **236**(4):391-399.
 27. Roosendaal G, Mauser-Bunschoten EP, De Kleijn P, Heijnen L, van den Berg HM, Van Rinsum AC, Lafeber FP, Bijlsma JW: **Synovium in haemophilic arthropathy.** *Haemophilia : the official journal of the World Federation of Hemophilia* 1998, **4**(4):502-505.
 28. Iwanaga T, Shikichi M, Kitamura H, Yanase H, Nozawa-Inoue K: **Morphology and functional roles of synoviocytes in the joint.** *Arch Histol Cytol* 2000, **63**(1):17-31.
 29. Madhok R, Bennett D, Sturrock RD, Forbes CD: **Mechanisms of joint damage in an experimental model of hemophilic arthritis.** *Arthritis Rheum* 1988, **31**(9):1148-1155.
 30. Madhok R, York J, Sturrock RD: **Haemophilic arthritis.** *Annals of the rheumatic diseases* 1991, **50**(8):588-591.
 31. Arnold WD, Hilgartner MW: **Hemophilic arthropathy. Current concepts of pathogenesis and management.** *J Bone Joint Surg Am* 1977, **59**(3):287-305.
 32. Speer DP: **Early pathogenesis of hemophilic arthropathy. Evolution of the subchondral cyst.** *Clinical orthopaedics and related research* 1984(185):250-265.
 33. Roosendaal G, Vianen ME, Wenting MJ, van Rinsum AC, van den Berg HM, Lafeber FP, Bijlsma JW: **Iron deposits and catabolic properties of synovial tissue from patients with haemophilia.** *The Journal of bone and joint surgery British volume* 1998, **80**(3):540-545.
 34. Stein H, Duthie RB: **The pathogenesis of chronic haemophilic arthropathy.** *The Journal of bone and joint surgery British volume* 1981, **63B**(4):601-609.
 35. van Creveld S, Hoedemaeker PJ, Kingma MJ, Wagenvoort CA: **Degeneration of joints in haemophiliacs under treatment by modern methods.** *The Journal of bone and joint surgery British volume* 1971, **53**(2):296-302.
 36. Mejia-Carvajal C, Hakobyan N, Enockson C, Valentino LA: **The impact of joint bleeding and synovitis on physical ability and joint function in a murine model of haemophilic synovitis.** *Haemophilia : the official journal of the World Federation of Hemophilia* 2008, **14**(1):119-126.
 37. Blobel CP, Haxaire C, Kalliolias GD, DiCarlo E, Salmon J, Srivastava A: **Blood-induced arthropathy in hemophilia: mechanisms and heterogeneity.** *Seminars in thrombosis and hemostasis* 2015, **41**(8):832-837.
 38. Sward P, Frobell R, Englund M, Roos H, Struglics A: **Cartilage and bone markers and inflammatory cytokines are increased in synovial fluid in the acute phase of knee injury (hemarthrosis)--a cross-sectional analysis.** *Osteoarthritis and cartilage / OARS, Osteoarthritis Research Society* 2012, **20**(11):1302-1308.
 39. Jansen NW, Roosendaal G, Hooiveld MJ, Bijlsma JW, van Roon JA, Theobald M, Lafeber FP: **Interleukin-10 protects against blood-induced joint damage.** *British journal of haematology* 2008, **142**(6):953-961.
 40. Ovlisen K, Kristensen AT, Jensen AL, Tranholm M: **IL-1 beta, IL-6, KC and MCP-1 are elevated in synovial fluid from haemophilic mice with experimentally induced hemarthrosis.** *Haemophilia : the official journal of the World Federation of Hemophilia* 2009, **15**(3):802-810.
 41. Jansen NW, Roosendaal G, Wenting MJ, Bijlsma JW, Theobald M, Hazewinkel HA, Lafeber FP: **Very rapid clearance after a joint bleed in the canine knee cannot prevent adverse effects on cartilage and synovial tissue.** *Osteoarthritis and cartilage / OARS, Osteoarthritis Research Society* 2009, **17**(4):433-440.
 42. Harigai M, Hara M, Yoshimura T, Leonard EJ, Inoue K, Kashiwazaki S: **Monocyte chemoattractant protein-1 (MCP-1) in inflammatory joint diseases and its involvement in the cytokine network of rheumatoid synovium.** *Clin Immunol Immunopathol* 1993, **69**(1):83-91.

43. Schenk M, Fabri M, Krutzik SR, Lee DJ, Vu DM, Sieling PA, Montoya D, Liu PT, Modlin RL: **Interleukin-1beta triggers the differentiation of macrophages with enhanced capacity to present mycobacterial antigen to T cells.** *Immunology* 2014, **141**(2):174-180.
44. Haxaire C, Blobel CP: **With blood in the joint - what happens next? Could activation of a pro-inflammatory signalling axis leading to iRhom2/TNFalpha-convertase-dependent release of TNFalpha contribute to haemophilic arthropathy?** *Haemophilia : the official journal of the World Federation of Hemophilia* 2014, **20 Suppl 4**:11-14.
45. Narkbunnam N, Sun J, Hu G, Lin FC, Bateman TA, Mihara M, Monahan PE: **IL-6 receptor antagonist as adjunctive therapy with clotting factor replacement to protect against bleeding-induced arthropathy in hemophilia.** *Journal of thrombosis and haemostasis : JTH* 2013, **11**(5):881-893.
46. Nishiya K: **Stimulation of human synovial cell DNA synthesis by iron.** *J Rheumatol* 1994, **21**(10):1802-1807.
47. Bhat V, Olmer M, Joshi S, Durden DL, Cramer TJ, Barnes RF, Ball ST, Hughes TH, Silva M, Luck JV et al: **Vascular remodeling underlies rebleeding in hemophilic arthropathy.** *American journal of hematology* 2015, **90**(11):1027-1035.
48. Hakobyan N, Kazarian T, Jabbar AA, Jabbar KJ, Valentino LA: **Pathobiology of hemophilic synovitis I: overexpression of mdm2 oncogene.** *Blood* 2004, **104**(7):2060-2064.
49. Mendes AF, Caramona MM, Carvalho AP, Lopes MC: **Hydrogen peroxide mediates interleukin-1beta-induced AP-1 activation in articular chondrocytes: implications for the regulation of iNOS expression.** *Cell Biol Toxicol* 2003, **19**(4):203-214.
50. von Drygalski A, Adamson JW: **Iron metabolism in man.** *JPEN J Parenter Enteral Nutr* 2013, **37**(5):599-606.
51. Schneider N, Mouithys-Mickalad AL, Lejeune JP, Deby-Dupont GP, Hoebeke M, Serteyn DA: **Synoviocytes, not chondrocytes, release free radicals after cycles of anoxia/re-oxygenation.** *Biochemical and biophysical research communications* 2005, **334**(2):669-673.
52. Allen RE, Blake DR, Nazhat NB, Jones P: **Superoxide radical generation by inflamed human synovium after hypoxia.** *Lancet* 1989, **2**(8657):282-283.
53. Pearle AD, Warren RF, Rodeo SA: **Basic science of articular cartilage and osteoarthritis.** *Clin Sports Med* 2005, **24**(1):1-12.
54. Jansen NW, Roosendaal G, Bijlsma JW, Degroot J, Lafeber FP: **Exposure of human cartilage tissue to low concentrations of blood for a short period of time leads to prolonged cartilage damage: an in vitro study.** *Arthritis Rheum* 2007, **56**(1):199-207.
55. van Vulpen LF, Roosendaal G, van Asbeck BS, Mastbergen SC, Lafeber FP, Schutgens RE: **The detrimental effects of iron on the joint: a comparison between haemochromatosis and haemophilia.** *Journal of clinical pathology* 2015, **68**(8):592-600.
56. Yulish BS, Lieberman JM, Strandjord SE, Bryan PJ, Mulopulos GP, Modic MT: **Hemophilic arthropathy: assessment with MR imaging.** *Radiology* 1987, **164**(3):759-762.
57. Swanton MC: **Hemophilic arthropathy in dogs.** *Lab Invest* 1959, **8**:1269-1277.
58. Hooiveld M, Roosendaal G, Wenting M, van den Berg M, Bijlsma J, Lafeber F: **Short-term exposure of cartilage to blood results in chondrocyte apoptosis.** *Am J Pathol* 2003, **162**(3):943-951.
59. van Meegeren ME, Roosendaal G, van Veghel K, Mastbergen SC, Lafeber FP: **A short time window to profit from protection of blood-induced cartilage damage by IL-4 plus IL-10.** *Rheumatology (Oxford)* 2013, **52**(9):1563-1571.
60. Roosendaal G, Vianen ME, Marx JJ, van den Berg HM, Lafeber FP, Bijlsma JW: **Blood-induced joint damage: a human in vitro study.** *Arthritis Rheum* 1999, **42**(5):1025-1032.
61. van Vulpen LF, Schutgens RE, Coeleveld K, Alsema EC, Roosendaal G, Mastbergen SC, Lafeber FP: **IL-1beta, in contrast to TNFalpha, is pivotal in blood-induced cartilage damage and as such a potential target for therapy.** *Blood* 2015.
62. Hooiveld MJ, Roosendaal G, van den Berg HM, Bijlsma JW, Lafeber FP: **Haemoglobin-derived iron-dependent hydroxyl radical formation in blood-induced joint damage: an in vitro study.** *Rheumatology (Oxford)* 2003, **42**(6):784-790.
63. Wen FQ, Jabbar AA, Chen YX, Kazarian T, Patel DA, Valentino LA: **c-myc proto-oncogene expression in hemophilic synovitis: in vitro studies of the effects of iron and ceramide.** *Blood* 2002, **100**(3):912-916.

64. de Sousa M, Dynesius-Trentham R, Mota-Garcia F, da Silva MT, Trentham DE: **Activation of rat synovium by iron.** *Arthritis Rheum* 1988, **31**(5):653-661.
65. van Meegeren ME, Roosendaal G, Coeleveld K, Nieuwenhuizen L, Mastbergen SC, Lafeber FP: **A single intra-articular injection with IL-4 plus IL-10 ameliorates blood-induced cartilage degeneration in haemophilic mice.** *British journal of haematology* 2013, **160**(4):515-520.
66. Stoker DJ, Murray RO: **Skeletal changes in hemophilia and other bleeding disorders.** *Semin Roentgenol* 1974, **9**(3):185-193.
67. Wallny TA, Scholz DT, Oldenburg J, Nicolay C, Ezziddin S, Pennekamp PH, Stoffel-Wagner B, Kraft CN: **Osteoporosis in haemophilia - an underestimated comorbidity?** *Haemophilia : the official journal of the World Federation of Hemophilia* 2007, **13**(1):79-84.
68. Gerstner G, Damiano ML, Tom A, Worman C, Schultz W, Recht M, Stopeck AT: **Prevalence and risk factors associated with decreased bone mineral density in patients with haemophilia.** *Haemophilia : the official journal of the World Federation of Hemophilia* 2009, **15**(2):559-565.
69. Kovacs CS: **Hemophilia, low bone mass, and osteopenia/osteoporosis.** *Transfus Apher Sci* 2008, **38**(1):33-40.
70. Katsarou O, Terpos E, Chatzismalis P, Provelengios S, Adraktas T, Hadjidakis D, Kouramba A, Karafoulidou A: **Increased bone resorption is implicated in the pathogenesis of bone loss in hemophiliacs: correlations with hemophilic arthropathy and HIV infection.** *Ann Hematol* 2010, **89**(1):67-74.
71. Sokoloff L: **Biochemical and physiological aspects of degenerative joint diseases with special reference to hemophilic arthropathy.** *Ann N Y Acad Sci* 1975, **240**:285-290.
72. Lorenzo J, Horowitz M, Choi Y: **Osteoimmunology: interactions of the bone and immune system.** *Endocr Rev* 2008, **29**(4):403-440.
73. Weitzmann MN, Ofotokun I: **Physiological and pathophysiological bone turnover - role of the immune system.** *Nat Rev Endocrinol* 2016, **12**(9):518-532.
74. Gilbert L, He X, Farmer P, Boden S, Kozlowski M, Rubin J, Nanes MS: **Inhibition of osteoblast differentiation by tumor necrosis factor-alpha.** *Endocrinology* 2000, **141**(11):3956-3964.
75. Melchiorre D, Milia AF, Linari S, Romano E, Benelli G, Manetti M, Guiducci S, Ceccarelli C, Innocenti M, Carulli C *et al*: **RANK-RANKL-OPG in hemophilic arthropathy: from clinical and imaging diagnosis to histopathology.** *J Rheumatol* 2012, **39**(8):1678-1686.
76. Kim JH, Jin HM, Kim K, Song I, Youn BU, Matsuo K, Kim N: **The mechanism of osteoclast differentiation induced by IL-1.** *J Immunol* 2009, **183**(3):1862-1870.
77. Wang KC, Amirabadi A, Wang KC, Moineddin R, Jong R, Tomlinson C, Doria AS: **Longitudinal assessment of bone loss using quantitative ultrasound in a blood-induced arthritis rabbit model.** *Haemophilia : the official journal of the World Federation of Hemophilia* 2015, **21**(5):e402-410.
78. Lau AG, Sun J, Hannah WB, Livingston EW, Heymann D, Bateman TA, Monahan PE: **Joint bleeding in factor VIII deficient mice causes an acute loss of trabecular bone and calcification of joint soft tissues which is prevented with aggressive factor replacement.** *Haemophilia : the official journal of the World Federation of Hemophilia* 2014, **20**(5):716-722.
79. Hakobyan N, Enockson C, Cole AA, Sumner DR, Valentino LA: **Experimental haemophilic arthropathy in a mouse model of a massive haemarthrosis: gross, radiological and histological changes.** *Haemophilia : the official journal of the World Federation of Hemophilia* 2008, **14**(4):804-809.
80. Rodriguez-Merchan EC: **Pathophysiology of the disturbed angiogenesis in hemophilia.** *Expert review of hematology* 2016, **9**(10):933-938.
81. Acharya SS, Kaplan RN, Macdonald D, Fابيي OT, DiMichele D, Lyden D: **Neoangiogenesis contributes to the development of hemophilic synovitis.** *Blood* 2011, **117**(8):2484-2493.
82. Forbes CD, Greig WR, Prentice CR, McNicol GP: **Radioisotope knee joint scans in haemophilia and Christmas disease.** *The Journal of bone and joint surgery British volume* 1972, **54**(3):468-475.
83. Karapnar TH, Karadas N, Ozek G, Tufekci O, Atabay B, Turker M, Yuksel F, Karapinar DY, Vergin C, Irken G *et al*: **The investigation of relationship between joint findings and serum angiogenic and inflammatory factor levels in severe hemophilia A patients.** *Blood coagulation & fibrinolysis : an international journal in haemostasis and thrombosis* 2014, **25**(7):703-708.
84. Sen D, Chapla A, Walter N, Daniel V, Srivastava A, Jayandharan GR: **Nuclear factor (NF)-kappaB and its associated pathways are major molecular regulators of blood-induced joint damage in a murine model of hemophilia.** *Journal of thrombosis and haemostasis : JTH* 2013, **11**(2):293-306.

85. Nassiri F, Cusimano MD, Scheithauer BW, Rotondo F, Fazio A, Yousef GM, Syro LV, Kovacs K, Lloyd RV: **Endoglin (CD105): a review of its role in angiogenesis and tumor diagnosis, progression and therapy.** *Anticancer Res* 2011, **31**(6):2283-2290.
86. Lee JW, Bae SH, Jeong JW, Kim SH, Kim KW: **Hypoxia-inducible factor (HIF-1)alpha: its protein stability and biological functions.** *Exp Mol Med* 2004, **36**(1):1-12.
87. Holmes DJ, Zachary I: **The vascular endothelial growth factor (VEGF) family: angiogenic factors in health and disease.** *Genome Biol* 2005, **6**(2):209.
88. Neufeld G, Cohen T, Gengrinovitch S, Poltorak Z: **Vascular endothelial growth factor (VEGF) and its receptors.** *FASEB J* 1999, **13**(1):9-22.
89. Lee JM, Song JY, Baek M, Jung HY, Kang H, Han IB, Kwon YD, Shin DE: **Interleukin-1beta induces angiogenesis and innervation in human intervertebral disc degeneration.** *J Orthop Res* 2011, **29**(2):265-269.
90. Huang SP, Wu MS, Shun CT, Wang HP, Lin MT, Kuo ML, Lin JT: **Interleukin-6 increases vascular endothelial growth factor and angiogenesis in gastric carcinoma.** *J Biomed Sci* 2004, **11**(4):517-527.
91. Lobet S, Hermans C, Lambert C: **Optimal management of hemophilic arthropathy and hematomas.** *J Blood Med* 2014, **5**:207-218.
92. Zetterberg E, Palmblad J, Wallensten R, Morfini M, Melchiorre D, Holmstrom M: **Angiogenesis is increased in advanced haemophilic joint disease and characterised by normal pericyte coverage.** *European journal of haematology* 2014, **92**(3):256-262.
93. Bergers G, Song S: **The role of pericytes in blood-vessel formation and maintenance.** *Neuro Oncol* 2005, **7**(4):452-464.
94. Alhaosawi MM: **Guidelines of management of musculoskeletal complications of hemophilia.** *Journal of Applied Hematology* 2014, **5**(3):75-85.
95. <http://www.wfh.org/en/resources/functional-and-physical-examination-tools>
96. Klukowska A, Czzyrny Z, Laguna P, Brzewski M, Serafin-Krol MA, Rokicka-Milewska R: **Correlation between clinical, radiological and ultrasonographical image of knee joints in children with haemophilia.** *Haemophilia : the official journal of the World Federation of Hemophilia* 2001, **7**(3):286-292.
97. Poonnoose PM, Hilliard P, Doria AS, Keshava SN, Gibikote S, Kavitha ML, Feldman BM, Blanchette V, Srivastava A: **Correlating clinical and radiological assessment of joints in haemophilia: results of a cross sectional study.** *Haemophilia : the official journal of the World Federation of Hemophilia* 2016, **22**(6):925-933.
98. Cross S, Vaidya S, Fotiadis N: **Hemophilic arthropathy: a review of imaging and staging.** *Seminars in ultrasound, CT, and MR* 2013, **34**(6):516-524.
99. Kilcoyne RF, Lundin B, Pettersson H: **Evolution of the imaging tests in hemophilia with emphasis on radiography and magnetic resonance imaging.** *Acta Radiol* 2006, **47**(3):287-296.
100. Mauser-Bunschoten EP, Jansen NW, Doria AS, Oldenburg J: **New images in haemophilia.** *Haemophilia : the official journal of the World Federation of Hemophilia* 2008, **14** Suppl 3:147-152.
101. Maclachlan J, Gough-Palmer A, Hargunani R, Farrant J, Holloway B: **Haemophilia imaging: a review.** *Skeletal Radiol* 2009, **38**(10):949-957.
102. Wyseure T, Mosnier LO, von Drygalski A: **Advances and challenges in hemophilic arthropathy.** *Seminars in hematology* 2016, **53**(1):10-19.
103. Pettersson H, Ahlberg A, Nilsson IM: **A radiologic classification of hemophilic arthropathy.** *Clinical orthopaedics and related research* 1980(149):153-159.
104. Funk MB, Schmidt H, Becker S, Escuriola C, Klarmann D, Klingebiel T, Kreuz W: **Modified magnetic resonance imaging score compared with orthopaedic and radiological scores for the evaluation of haemophilic arthropathy.** *Haemophilia : the official journal of the World Federation of Hemophilia* 2002, **8**(2):98-103.
105. Pergantou H, Matsinos G, Papadopoulos A, Platokouki H, Aronis S: **Comparative study of validity of clinical, X-ray and magnetic resonance imaging scores in evaluation and management of haemophilic arthropathy in children.** *Haemophilia : the official journal of the World Federation of Hemophilia* 2006, **12**(3):241-247.
106. Pettersson H, Gillespy T, Kitchens C, Kentro T, Scott KN: **Magnetic resonance imaging in hemophilic arthropathy of the knee.** *Acta Radiol* 1987, **28**(5):621-625.

107. Nuss R, Kilcoyne RF, Geraghty S, Shroyer AL, Rosky JW, Mawhinney S, Wiedel J, Manco-Johnson M: **MRI findings in haemophilic joints treated with radiosynoviorthesis with development of an MRI scale of joint damage.** *Haemophilia : the official journal of the World Federation of Hemophilia* 2000, **6**(3):162-169.
108. Querol F, Rodriguez-Merchan EC: **The role of ultrasonography in the diagnosis of the musculo-skeletal problems of haemophilia.** *Haemophilia : the official journal of the World Federation of Hemophilia* 2012, **18**(3):e215-226.
109. Lundin B, Manco-Johnson ML, Ignas DM, Moineddin R, Blanchette VS, Dunn AL, Gibikote SV, Keshava SN, Ljung R, Manco-Johnson MJ *et al*: **An MRI scale for assessment of haemophilic arthropathy from the International Prophylaxis Study Group.** *Haemophilia : the official journal of the World Federation of Hemophilia* 2012, **18**(6):962-970.
110. Sierra Aisa C, Lucia Cuesta JF, Rubio Martinez A, Fernandez Mosteirín N, Iborra Munoz A, Abio Calvete M, Guillen Gomez M, Moreto Quintana A, Rubio Felix D: **Comparison of ultrasound and magnetic resonance imaging for diagnosis and follow-up of joint lesions in patients with haemophilia.** *Haemophilia : the official journal of the World Federation of Hemophilia* 2014, **20**(1):e51-57.
111. Muca-Perja M, Riva S, Grochowska B, Mangiafico L, Mago D, Gringeri A: **Ultrasonography of haemophilic arthropathy.** *Haemophilia : the official journal of the World Federation of Hemophilia* 2012, **18**(3):364-368.
112. Joshua F: **Ultrasound applications for the practicing rheumatologist.** *Best Pract Res Clin Rheumatol* 2012, **26**(6):853-867.
113. Ceponis A, Wong-Sefidan I, Glass CS, von Drygalski A: **Rapid musculoskeletal ultrasound for painful episodes in adult haemophilia patients.** *Haemophilia : the official journal of the World Federation of Hemophilia* 2013, **19**(5):790-798.
114. Zukotyński K, Jarrin J, Babyn PS, Carcao M, Pazmino-Canizares J, Stain AM, Doria AS: **Sonography for assessment of haemophilic arthropathy in children: a systematic protocol.** *Haemophilia : the official journal of the World Federation of Hemophilia* 2007, **13**(3):293-304.
115. Wilson DJ, McLardy-Smith PD, Woodham CH, MacLarnon JC: **Diagnostic ultrasound in haemophilia.** *The Journal of bone and joint surgery British volume* 1987, **69**(1):103-107.
116. Wyld PJ, Dawson KP, Chisholm RJ: **Ultrasound in the assessment of synovial thickening in the hemophilic knee.** *Australian and New Zealand journal of medicine* 1984, **14**(5):678-680.
117. Chung SS, YJ.; You, CW.; Chun, TJ.; Jung, KJ.; Kim, JH.: **A Combined Ultrasonographic and Conventional Radiographic Assessment of Hemophilic Arthropathy.** *Indian J Hematol Blood Transfus* 2016.
118. Keshava S, Gibikote S, Mohanta A, Doria AS: **Refinement of a sonographic protocol for assessment of haemophilic arthropathy.** *Haemophilia : the official journal of the World Federation of Hemophilia* 2009, **15**(5):1168-1171.
119. Martinoli C, Della Casa Alberighi O, Di Minno G, Graziano E, Molinari AC, Pasta G, Russo G, Santagostino E, Tagliaferri A, Tagliafico A *et al*: **Development and definition of a simplified scanning procedure and scoring method for Haemophilia Early Arthropathy Detection with Ultrasound (HEAD-US).** *Thrombosis and haemostasis* 2013, **109**(6):1170-1179.
120. Melchiorre D, Linari S, Innocenti M, Biscoglio I, Toigo M, Cerinic MM, Morfini M: **Ultrasound detects joint damage and bleeding in haemophilic arthropathy: a proposal of a score.** *Haemophilia : the official journal of the World Federation of Hemophilia* 2011, **17**(1):112-117.
121. Graham JB, Buckwalter JA, *et al.*: **Canine hemophilia; observations on the course, the clotting anomaly, and the effect of blood transfusions.** *J Exp Med* 1949, **90**(2):97-111.
122. Field RA, Rickard CG, Hutt FB: **Hemophilia in a family of dogs.** *Cornell Vet* 1946, **36**(4):285-300.
123. Kitchen H: **Comparative biology: animal models of human hematologic disease. A review.** *Pediatric research* 1968, **2**(3):215-229.
124. Lozier JN, Nichols TC: **Animal models of hemophilia and related bleeding disorders.** *Seminars in hematology* 2013, **50**(2):175-184.
125. Bi L, Lawler AM, Antonarakis SE, High KA, Gearhart JD, Kazazian HH, Jr.: **Targeted disruption of the mouse factor VIII gene produces a model of haemophilia A.** *Nature genetics* 1995, **10**(1):119-121.
126. Nielsen LN, Wiinberg B, Hager M, Holmberg HL, Hansen JJ, Roepstorff K, Tranholm M: **A novel F8 -/- rat as a translational model of human hemophilia A.** *Journal of thrombosis and haemostasis : JTH* 2014, **12**(8):1274-1282.

127. Lozier JN, Dutra A, Pak E, Zhou N, Zheng Z, Nichols TC, Bellinger DA, Read M, Morgan RA: **The Chapel Hill hemophilia A dog colony exhibits a factor VIII gene inversion.** *Proceedings of the National Academy of Sciences of the United States of America* 2002, **99**(20):12991-12996.
128. Bi L, Sarkar R, Naas T, Lawler AM, Pain J, Shumaker SL, Bedian V, Kazarian HH, Jr.: **Further characterization of factor VIII-deficient mice created by gene targeting: RNA and protein studies.** *Blood* 1996, **88**(9):3446-3450.
129. Diehl KH, Hull R, Morton D, Pfister R, Rabemampianina Y, Smith D, Vidal JM, van de Vorstenbosch C, European Federation of Pharmaceutical Industries A, European Centre for the Validation of Alternative M: **A good practice guide to the administration of substances and removal of blood, including routes and volumes.** *Journal of applied toxicology : JAT* 2001, **21**(1):15-23.
130. Monahan PE: **The expanding menagerie: animal models of hemophilia A.** *Journal of thrombosis and haemostasis : JTH* 2010, **8**(11):2469-2471.
131. Booth CJ, Brooks MB, Rockwell S, Murphy JW, Rinder HM, Zelterman D, Paidas MJ, Compton SR, Marks PW: **WAG-F8(m1Ycb) rats harboring a factor VIII gene mutation provide a new animal model for hemophilia A.** *Journal of thrombosis and haemostasis : JTH* 2010, **8**(11):2472-2477.
132. Booth CJ, Brooks MB, Rockwell S: **Spontaneous coagulopathy in inbred WAG/RijYcb rats.** *Comp Med* 2010, **60**(1):25-30.
133. Hakobyan N, Kazarian T, Valentino LA: **Synovitis in a murine model of human factor VIII deficiency.** *Haemophilia : the official journal of the World Federation of Hemophilia* 2005, **11**(3):227-232.
134. Valentino LA, Hakobyan N, Kazarian T, Jabbar KJ, Jabbar AA: **Experimental haemophilic synovitis: rationale and development of a murine model of human factor VIII deficiency.** *Haemophilia : the official journal of the World Federation of Hemophilia* 2004, **10**(3):280-287.
135. Valentino LA, Hakobyan N: **Histological changes in murine haemophilic synovitis: a quantitative grading system to assess blood-induced synovitis.** *Haemophilia : the official journal of the World Federation of Hemophilia* 2006, **12**(6):654-662.
136. Nieuwenhuizen L, Schutgens RE, Coeleveld K, Mastbergen SC, Roosendaal G, Biesma DH, Lafeber FP: **Hemarthrosis in hemophilic mice results in alterations in M1-M2 monocyte/macrophage polarization.** *Thrombosis research* 2014, **133**(3):390-395.
137. Nieuwenhuizen L, Roosendaal G, Coeleveld K, Lubberts E, Biesma DH, Lafeber FP, Schutgens RE: **Haemarthrosis stimulates the synovial fibrinolytic system in haemophilic mice.** *Thrombosis and haemostasis* 2013, **110**(1):173-183.
138. Aigner T, Cook JL, Gerwin N, Glasson SS, Laverty S, Little CB, McIlwraith W, Kraus VB: **Histopathology atlas of animal model systems - overview of guiding principles.** *Osteoarthritis and cartilage / OARS, Osteoarthritis Research Society* 2010, **18 Suppl 3**:S2-6.
139. Manon-Jensen T, Karsdal MA, Nielsen LN, Kjelgaard-Hansen M, Vandahl B, Olsen EH, Enoksson M, Roepstorff K: **Altered collagen turnover in factor VIII-deficient rats with hemophilic arthropathy identifies potential novel serological biomarkers in hemophilia.** *Journal of thrombosis and haemostasis : JTH* 2016.
140. Nieuwenhuizen L, Roosendaal G, Mastbergen SC, Coeleveld K, Biesma DH, Lafeber FP, Schutgens RE: **Deferasirox limits cartilage damage following hemarthrosis in haemophilic mice.** *Thrombosis and haemostasis* 2014, **112**(5):1044-1050.
141. Nieuwenhuizen L, Roosendaal G, Mastbergen SC, Coeleveld K, Biesma DH, Lafeber FP, Schutgens RE: **Antiplasmin, but not amiloride, prevents synovitis and cartilage damage following hemarthrosis in hemophilic mice.** *Journal of thrombosis and haemostasis : JTH* 2014, **12**(2):237-245.
142. Utting JC, Flanagan AM, Brandao-Burch A, Orriss IR, Arnett TR: **Hypoxia stimulates osteoclast formation from human peripheral blood.** *Cell Biochem Funct* 2010, **28**(5):374-380.
143. Modderman WE, Tuinenburg-Bol Raap AC, Nijweide PJ: **Tartrate-resistant acid phosphatase is not an exclusive marker for mouse osteoclasts in cell culture.** *Bone* 1991, **12**(2):81-87.

8. Appendix: Papers and manuscript I-III

Paper I

The F8^{-/-} rat as a model of haemophilic arthropathy

Sørensen, KR.; Roepstorff, K.; Winberg, B.; Hansen, AK.; Tranholm, M.; Nielsen, LN.; Kjelgaard-Hansen, M.
J. Thromb. Haemost. 2016;14:1216-25

ORIGINAL ARTICLE

The F8^{-/-} rat as a model of hemophilic arthropathyK. R. SØRENSEN,*† K. ROEPSTORFF,‡ B. WIINBERG,* A. K. HANSEN,† M. TRANHOLM,§
L. N. NIELSEN*¶¹ and M. KJELGAARD-HANSEN*

*Translational Haemophilia Pharmacology, Novo Nordisk A/S, Maaloev, Denmark; †Veterinary Disease Biology, University of Copenhagen, Copenhagen, Denmark; ‡Histology and Bioimaging; §Haemophilia Pharmacology Novo Nordisk A/S/Maaloev; and ¶Veterinary Clinical and Animal Sciences, University of Copenhagen, Copenhagen, Denmark

To cite this article: Sørensen KR, Roepstorff K, Wiinberg B, Hansen AK, Tranholm M, Nielsen LN, Kjeldgaard-Hansen M. The F8^{-/-} rat as a model of hemophilic arthropathy. *J Thromb Haemost* 2016; **14**: 1216–25.

Essentials

- Validating the F8 rat as a new intermediate-size animal model of hemophilic arthropathy.
- Factor VIII (FVIII) treated F8^{-/-} rats suffered induced hemarthrosis analyzed by histopathology.
- F8^{-/-} animals develop hemophilic arthropathy upon hemarthrosis, preventable by FVIII treatment.
- The F8^{-/-} rat presents as a new pharmacologic model of hemophilic arthropathy.

Summary. *Background:* Translational animal models of hemophilia are valuable for determining the pathobiology of the disease and its co-morbidities (e.g. hemophilic arthropathy, HA). The biologic mechanisms behind the development of HA, a painful and debilitating condition, are not completely understood. We recently characterized a F8^{-/-} rat, which could be a new preclinical model of HA. *Objectives:* To establish the F8^{-/-} rat as a model of HA by determining if the F8^{-/-} rat develops HA resembling human HA after an induced joint bleed and whether a second joint bleed causes further disease progression. *Methods:* Wild-type and F8^{-/-} rats were treated with vehicle or recombinant human factor VIII (rhFVIII) prior to a needle-induced joint bleed. Joint swelling was measured prior to injury, the following 7 days and upon euthanasia. Histologic sections of the joint were stained, and arthropathic changes identified and scored with regard to synovitis, bone remodelling, cartilage degradation and hemosiderin deposition. *Results:* Vehicle-treated F8^{-/-}

rats experienced marked joint swelling and developed chronic degenerative joint changes (i.e. fibrosis of the sub-synovial membrane, chondrocyte loss and excessive bone remodeling). Treatment with rhFVIII reduced or prevented swelling and degenerative joint changes, returning the F8^{-/-} animals to a wild-type phenotype. *Conclusion:* The hemophilic phenotype of the F8^{-/-} rat resulted in a persistent hemarthrosis following an induced joint bleed. This caused development of HA resembling human HA, which was prevented by rhFVIII treatment, confirming the potential of the F8^{-/-} rat as a model of HA.

Keywords: animal model; Factor VIII; hemarthrosis; hemophilia; *rattus*.

Introduction

Hemophilia A is a x-linked recessive disorder, caused by mutations in the F8 gene, codes for coagulation FVIII [1]. These mutations can lead to partial or complete factor deficiency, causing failure in the coagulation cascade and a bleeding phenotype. Untreated patients with severe hemophilia (< 1% FVIII activity) suffer from recurrent spontaneous bleeding episodes, of which 80% occur in the synovial joints, particularly in the knees, ankles and elbows [2]. These bleeds cause progressive joint degeneration, resulting in chronic pain, immobility and reduced quality of life. This debilitating condition, known as hemophilic arthropathy (HA), is the most frequent co-morbidity of hemophilia. The treatment for hemophilia A is factor replacement therapy, either on-demand when bleeding occurs, or preferably as prophylaxis to prevent bleeding. However, despite prophylactic treatment, patients still suffer breakthrough bleeds and it has been shown that more than 90% of patients on prophylaxis have chronic joint changes in at least one joint by the age of 40 [3,4]. Therefore, the discovery of new, more efficient or longer acting therapeutics and optimized treatment regimens are still required in order to prevent

Correspondence: Kristine Rothaus Sørensen, Novo Nordisk A/S, Novo Nordisk Park 1, 2760 Maaloev, Denmark.
Tel.: +45 30798261; fax: +45 44426220.
E-mail: ktsr@novonordisk.com

University of Copenhagen, Copenhagen, Denmark

Received 30 September 2015

Manuscript handled by: P. H. Reitsma

Final decision: D. DiMichele, 6 March 2016

breakthrough bleeds, thereby improving long-term joint outcomes for patients.

Various hemophilic dog and mouse models have been instrumental in determining the pharmacokinetic (PK) and pharmacodynamic (PD) properties of new or existing drugs in order to optimize treatment [5–9]. Mouse models of induced knee-joint bleeds were also developed to study the pathogenesis of HA and as a pharmacologic model for HA [6]. However, these mouse models are limited by the small size of the animals, which allows only smaller volumes and limited frequency of blood sampling. This limits the possibilities of repetitive and multiple sampling when designing studies.

We have recently characterized a F8^{-/-} rat as a new animal model for severe hemophilia A [10]. The rat has the same breeding and housing advantages as the mouse, but with a body and blood volume approximately 10 times larger, permitting considerably larger and more frequent blood sampling [11]. According to guidelines [11] only 135 µL of blood can be sampled over a full week from a 25-g mouse, whereas a 250-g rat would allow weekly sampling of 1200 µL (e.g. > 135 µL on a daily basis, which is likely to enable individual monitoring that is not possible in mice). This facilitates the use of the animals as their own controls during longitudinal disease progression studies, thereby refining study design and probably reducing the required number of animals. Finally, the F8^{-/-} rats develop spontaneous bleeds comparable to human hemophilia patients [10], indicating a high translational potential of this animal model (although in the current study 10% experienced large spontaneous bleeds, causing exclusion of these animals).

The aim of this study was to establish the F8^{-/-} rat as a model for HA in the knee-joint in hemophilia A. We hypothesized that a single induced joint bleed in the knee would lead to pathologic changes in the joint of untreated F8^{-/-} rats, resembling changes seen after hemarthrosis in human hemophilia A, with further disease progression after a second induced joint bleed. Furthermore, we hypothesized that prophylactic treatment with recombinant human FVIII (rhFVIII) would reduce or completely abolish pathologic changes, qualifying the F8^{-/-} rat as a model of HA.

Material and methods

Experimental randomized blinded case control study

This experimental study was performed as a case control study, with animals treated with either vehicle or rhFVIII given as a single injection prior to an induced joint bleed. Animals were grouped according to genotype (into wild-type or F8^{-/-} rats) and randomly assigned to treatment. The study was blinded during dosing, joint measurements and scoring of histologic images.

All animal studies were performed according to guidelines from and approved by the Danish Animal Experiments Council, the Danish Ministry of Justice.

All invasive procedures were performed under inhalation anesthesia using 5% isoflourane/0.7 L min⁻¹ O₂/0.3 L min⁻¹ N₂O for induction and 2% isoflourane/0.7 L min⁻¹ O₂/0.3 L min⁻¹ N₂O for anesthesia maintenance.

All animals were monitored daily and assessed for signs of spontaneous bleeding. Discoloration and macroscopically visible swelling of the injured joint was also noted on a daily basis.

The rats were housed under standard conditions with a 12-h/12-h light/dark cycle, at 20–23 °C and 30–60% relative humidity, with *ad libitum* food and water consumption; food was placed in the bottom of the cage to ensure easy access for hemarthrosis-affected animals.

Study population

Sixty F8^{-/-} and 20 wild-type (WT) rats on a Sprague Dawley background [10], bred at Novo Nordisk A/S (Maaloev, Denmark), between 13 and 15 weeks of age, were used in the study.

To examine the effect of both a single injury and two injuries, the animals were randomly assigned to two injury types, one group receiving a single needle-induced joint bleed of the left knee at day 0 and euthanized at day 14 (10 WT animals and 40 F8^{-/-} animals), and the other group (10 WT animals and 20 F8^{-/-} animals) receiving two separate needle-induced joint bleeds at day 0 and 14, respectively, and euthanized at day 28.

The F8^{-/-} animals were randomized to receive a single intravenous injection prior to each joint bleed of either 300 IU/kg rhFVIII (4.8 mL/kg ReFacto AF[®] 250 IE/a.e.; Pfizer, Paris, France) or vehicle buffer solution (10 mM L-Histidine, 8.8 mM sucrose, 30.8 mM NaCl, 1.7 mM CaCl₂, 0.01% Tween 80) at a volume equivalent to rhFVIII-dosed animals. The rhFVIII dose was based on complete *in vitro* normalization of APTT in F8^{-/-} rat plasma [10], as well as experience in handling spontaneous bleeds in the F8^{-/-} rat population (unpublished data). WT rats received buffer solution.

rhFVIII exposure in treated animals was confirmed by qualitative detection of rhFVIII activity in samples obtained 5 min after injection.

Exclusion criteria

Upon study initiation, animals with preexisting macroscopically evident bleeding in their legs were excluded from the study. Animals developing spontaneous bleeding, after study initiation, unrelated to the induced hemarthrosis were euthanized at any sign of distress. Animals euthanized before the end of the study were excluded.

Hemarthrosis induction

Following the intravenous injection of either rhFVIII or vehicle, a subcutaneous injection of buprenorphine (Temgesic 0.3 mg/mL, Reckitt Benckiser Pharmaceuticals Ltd, Berkshire, Slough, UK) at 0.03 mg/kg was administered to all animals and after a 5-min distribution period, a joint bleed was induced in the left knee. Rats were anesthetized, hair on the left knee clipped and the skin cleaned using an alcohol swap. The animals were placed in dorsal recumbency with the left leg in a slightly flexed position, and hemarthrosis was induced by briefly inserting a 30-gauge (g) needle once through the patella ligament. On subsequent days (minimum 7 days) the animals were supplemented with buprenorphine (Temgesic) in the drinking water at a concentration of 6 mg/L.

Clinical assessment of hemarthrosis as measured by joint swelling

The relative swelling of the left knee-joint was determined prior to injury, on each of the following 7 days and upon euthanasia. Following the second joint bleed the joints were measured on days 15, 16, 20, 21 and 28. At each time-point, the diameters of the injured knee and contralateral knee (control) were measured five times using a digital Vernier calliper gauge (Mitutoyo Corporation, Kawasaki, Kanagawa, Japan), and the mean diameter of each knee calculated, as well as the mean difference between the injured and control knees, designated the delta diameter.

Blood sampling

Carotid arterial blood was collected before euthanasia in fully anesthetized animals, through a 0.8-mm polyethylene catheter (PE90; Becton, Dickinson and Company, Franklin Lakes, NJ, USA), as 3.2% citrated whole blood. The citrated blood was centrifuged immediately at 4000×g for 5 min, and platelet-poor plasma collected and stored at -80°C until analysis.

After blood sampling procedures the animals were euthanized by an injection of pentobarbital (Mebumal, SAD, Amgros I/S, Copenhagen, Denmark) administered through the carotid artery catheter.

Antibody analysis

The rhFVIII treatment could potentially result in development of inhibitory anti-FVIII antibodies. Plasma samples from the day of termination were therefore analyzed for the presence of FVIII neutralizing antibodies (nAbs). In short, plasma samples were tested using a modified chromogenic assay (Coamatic FVIII kit, Chromogenix, Instrumentation Laboratory, Bedford, MA, USA), as previously described [12]. A FVIII-activity calibration curve, as well as antibody-positive and negative control samples

(QCs), was included in each assay. The FVIII activity of the antibody-negative control samples (QC neg) was set to 100%, and the signals of the study samples were compared with this and expressed as FVIII remaining activity (IU/mL). The % remaining activity level was transformed into Bethesda Units (BU) [13] and values above 5 BU defined as high titers, as applied in clinical settings [14].

Histology

Both hind legs were dissected at the femoral head, mildly stripped of muscle and skin and placed in 4% paraformaldehyde for 2 days, then decalcified in a 12.5% EDTA decalcifying solution for 3 weeks, tissue processed and paraffin embedded.

Following trimming, 3- μ m-thick sagittal tissue sections were collected from all injured knees and from six contralateral control knees and mounted on glass slides.

Adjacent sections were stained with hematoxylin (Ampligon, Odense, Denmark; VWR International Ltd, Radnor, PA, USA) and eosin (Sigma-Aldrich, St Louis, MO, USA), Safranin O (VWR International Ltd) or Perls' Prussian Blue (Merck, Kenilworth, NJ, USA, and Sigma-Aldrich). All slides were scanned using the Nanozoomer 2.0 slide scanner (Hamamatsu Photonics K.K., Hamamatsu City, Japan) with a 20 \times magnification whole-slide scan, and scored according to the arthropathy score described below.

Histologic assessment

Hematoxylin and eosin (HE) stained sections were scored semi-quantitatively for the presence of synovitis and bone remodeling; Safranin O stains were scored for cartilage degradation and Perls' Prussian blue stains scored for hemosiderin deposition. The assessments were performed blinded to treatment and genotype according to a scoring system (the arthropathy score) identifying chronic arthropathic changes. The score was based on a modification of the Valentino and Hayakobyan score of hemophilic synovitis, taking more chronic changes into account [15], as seen in Table 1. Interobserver agreement on the arthropathy score was tested (kappa) and assessed to be good to very good (data not shown).

Statistics

A longitudinal (days) delta diameter area-under-the-curve (AUC) score was generated for each animal. Within each type of injury (one or two) the delta diameter AUC and individual and total mean arthropathy scores were tested for significant differences between groups using the sequential Student's *t*-test, in the following order to separately test the relevant hypotheses: untreated vs. WT (positive and negative controls, respectively), hereafter untreated vs. treated, and untreated vs. treated animals without nAbs (positive controls vs. treated), and finally,

Table 1 Overview of the histopathology scoring system (the arthropathy score) assessing severity of synovitis, bone remodeling, cartilage degradation and hemosiderin deposition in the experimental F8^{-/-} rat model of hemophilic arthropathy.

	0	1	2	3
Synovitis (HE)	No changes	Increased number of lining cell layers and/or slight proliferation of subsynovial tissue	Increased number of lining cell layers. Moderate proliferation of subsynovial tissue and/or infiltration of few inflammatory cells	Increased number of lining cell layers. Massive proliferation of subsynovial tissue and/or infiltration of large numbers of inflammatory cells
Bone remodeling (HE)	No bone remodeling	A single area of focal bone remodeling	Moderate bone remodeling covering < 50% of the cortical bone surface, and/or formation of subchondral cysts	Severe bone remodeling covering > 50% of the cortical bone surface, with or without subchondral cysts
Cartilage degradation (Safranin O)	No cartilage degradation	Loss of proteoglycan and/or chondrocytes in the superficial cartilage layer (above the tidemark) without structural changes	Loss of proteoglycan and chondrocytes extending through the calcified layer of cartilage, and/or fibrillations without loss of cartilage	Erosions extending to the calcified cartilage
Hemosiderin (Perls' Prussian Blue)	No hemosiderin deposition	Minor hemosiderin deposition, with on average < 5% of FOV in the three most intensely stained areas	Moderate hemosiderin deposition, with on average between 5 and 25% of FOV in the three most intensely stained areas	Severe hemosiderin deposition, with on average > 25% of FOV in the three most intensely stained areas

HE, hematoxylin and eosin; FOV, field of view, 20× magnification.

treated vs. WT, and treated without nAbs vs. WT (treated vs. negative controls).

To test whether the second injury made HA findings progress, the delta diameter AUC and total arthropathy scores of untreated animals across one or two injuries were compared.

Data were expressed as mean ± standard deviation. A *P*-value < 0.05 was considered significant at each level of the testing sequence. Statistical analysis was performed using the GraphPad Prism (Version 6.05, GraphPad Software, San Diego, CA, USA).

Results

Study population

Out of the 80 rats, 79 were enrolled in the study, as one F8^{-/-} animal had developed spontaneous bleedings in the left leg on the day of study initiation. An additional nine F8^{-/-} animals were excluded during the study period; four because of massive bleeding following the induced joint bleed and the remaining five because of new spontaneous bleeds requiring treatment during the study period. These bleeds were situated in the paw, shoulder, thigh and ankle. A total of 70 rats completed the study, distributed between study groups as shown in Table 2.

FVIII inhibitor formation

Of the 60 rhFVIII-treated animals, eight (four with one injury and four with two injuries) had developed high-titer neutralizing antibodies (> 5 BU) towards rhFVIII during the time-course of the study (range of BU for high-titer

Table 2 Overview of the final animal numbers and group distribution

Rat genotype Treatment	F8 ^{-/-} vehicle	F8 ^{-/-} rhFVIII*	Wild-type vehicle
One joint bleed	16	20	10
Excluded	4 3 because of new bleeds 1 because of the size of the induced bleed	0	0
Two joint bleeds	6	8	10
Excluded	4 1 because of a new bleed 3 because of the size of the induced bleed	2 because of new bleeds	0

The treatment with rhFVIII or vehicle was given as a single injection prior to injury (i.e. one single bolus was injected for the one-joint-bleed group and two boluses before each injury for the two-joint-bleed group). *300 IU/kg.

animals 13.9–601.3 BU). The data from the joint swelling and histologic scoring were therefore presented as 'treated', encompassing all rhFVIII animals, and as 'treated without neutralizing antibodies (treated w/o nAbs)', where only treated animals free of nAbs were included.

Joint swelling following induced hemarthroses

Visually evident swelling and discoloration of the knee were common sequelae of the induced hemarthrosis, as

observed during daily assessment of the animals. All but one (from the one joint-bleed group) of the 22 untreated F8^{-/-} rats presented with both symptoms during the study, seven of the 28 rhFVIII-treated F8^{-/-} rats had signs of swelling or discoloration (three only after the second joint bleed), and WT animals did not develop any visual signs of bleeding.

When swelling was measured objectively as joint diameter using a caliper, untreated F8^{-/-} rats had a dramatic

joint swelling after both the first and second injury. The swelling for untreated rats peaked at day two after the joint bleed and then slowly declined towards the pre-injury delta diameter (see Fig. 1A). Treatment with rhFVIII significantly reduced the overall swelling, and excluding the rhFVIII-treated animals with high-titer nAbs against rhFVIII, completely abolished the apparent increase in swelling after the second joint bleed in this group (Fig. 1A). For the one-joint-bleed group, removing

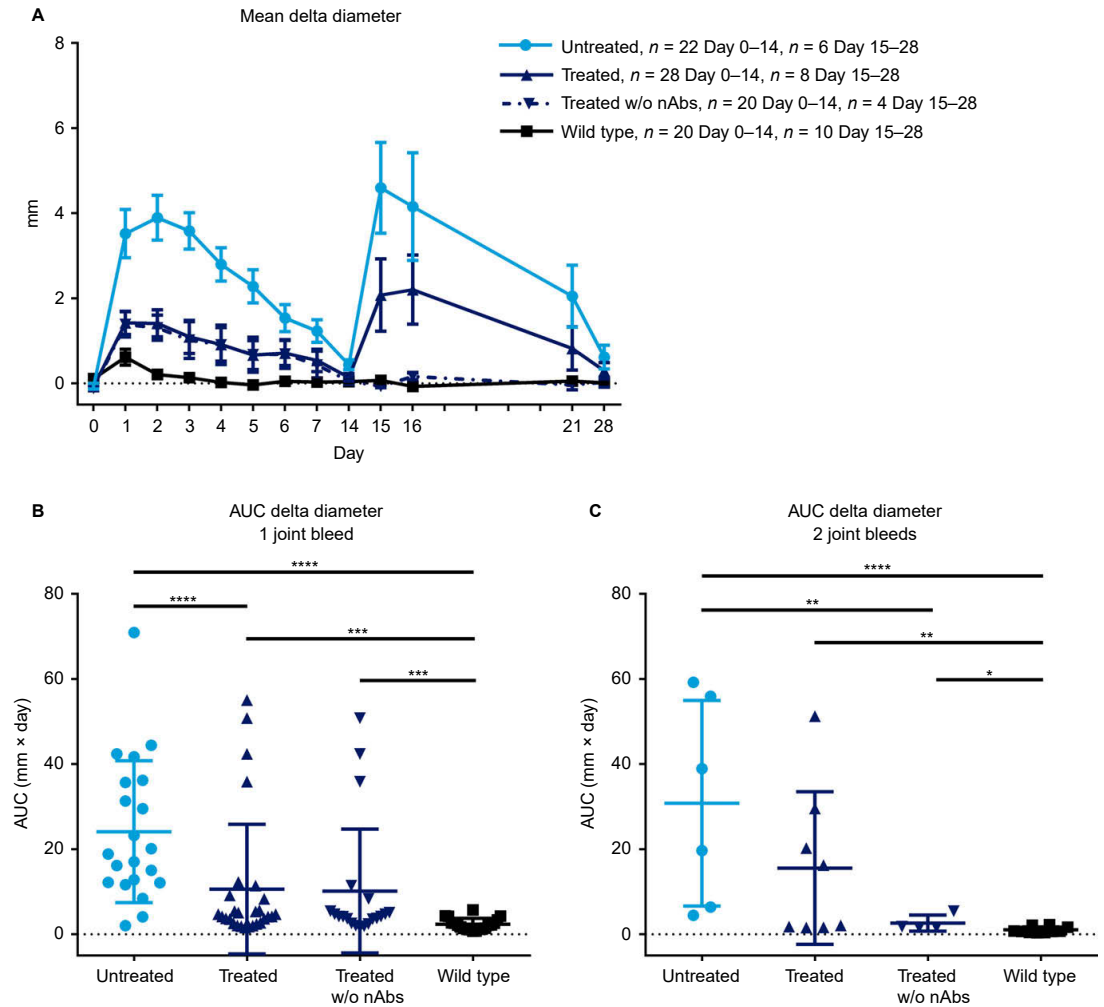


Fig. 1. Joint swelling according to genotype and treatment, shown as mean temporal and AUC delta diameter measurements. (A) Mean delta diameter ± SEM for each group from day 0–7 (encompassing all animals in the study, hence n = 22 for F8^{-/-} untreated, n = 28 for F8^{-/-} rhFVIII-treated and n = 20 for wild-type [WT] rats), day 14–16, day 21 and day 28 (encompassing only two-joint-bleed animals; n = 6 for untreated F8^{-/-} rats, n = 8 for rhFVIII-treated F8^{-/-} rats and n = 10 for WT animals). (B–C) AUC (delta diameter × days) for each individual animal from the one and two-joint-bleed groups, respectively. Line represents mean. *P < 0.05, **P < 0.005, ***P < 0.0005, ****P < 0.0001 (Student's *t*-test). Treated w/o nAbs refers to treated animals that did not develop neutralizing anti-FVIII antibodies during the study. AUC, area under the curve; nAbs, neutralizing antibodies against rhFVIII.

nAbs-free animals only slightly reduced the overall swelling. The WT group only had a minor brief joint swelling after the first joint bleed. The severity of the swelling over time (AUC) was significantly increased for untreated F8^{-/-} compared with WT rats both after a single injury and after two injuries ($P < 0.0001$ for both comparisons, see Fig. 1B). Likewise, treated F8^{-/-} rats had a significantly lower AUC compared with untreated F8^{-/-} rats after a single joint bleed ($P < 0.0001$) and when comparing untreated F8^{-/-} rats with treated F8^{-/-} rats without nAbs after the second injury ($P = 0.0096$).

No difference in swelling was observed when comparing a single injury or two injuries in the untreated animals.

Histologic evaluation of arthopathic changes as a consequence of the induced hemarthrosis

The histopathologic evaluation of sections from all untreated HA animals revealed pathology consistent with hemophilic arthropathy [15–17]. In Fig. 2, pictures representing the F8^{-/-} untreated, treated and WT groups are shown. An increased number of synovial lining cells, in some cases with massive subsynovial proliferation and inflammatory infiltrations, was identified. These findings were seen in 63% (10/16) of the F8^{-/-} untreated animals and 25% (5/20) of the treated animals, of which two had developed nAbs (Fig. 3) following a single joint bleed. After two joint bleeds 100% (6/6) of the untreated F8^{-/-} rats had pathologic findings, whereas this was seen only in 50% (4/8) of treated rats with nAbs and 25% (1/4) of treated F8^{-/-} rats without nAbs. Generally the WT animals had no identified pathology; however, a few presented with minor signs of hemosiderin deposition, chondrocyte loss or bone remodeling. This was true for 50% of the one-joint-bleed group and for 10% (1/10) of the two-joint-bleed group.

Chondrocyte and proteoglycan loss was seen in 31% (5/16) and 33% (2/6) of the untreated animals in the one- and two-joint-bleed groups, respectively. No fibrillations or aberrations of the cartilage were observed. Only 15% (3/20) of treated animals showed signs of cartilage degradation after a single joint bleed, of which one was positive for nAbs. For the F8^{-/-} treated rats subjected to two joint bleeds, 12.5% (1/8) had pathologic cartilage findings and this animal was also positive for nAbs.

Hemosiderin deposition was present in all groups, but more pronounced and frequent in the untreated groups, with an incidence of 75% (12/16) and 100% (6/6), for the one- and two-joint-bleed groups, respectively. Finally, bone remodeling in the form of periosteal bone formation was evident on the femoral shaft (see Fig. 2G). Again, this was primarily seen in untreated animals; 44% (7/16) and 67% (4/6) of the one- and two-joint-bleed groups had bone pathology, with only 10% (2/20) and 0% (0/4) of the corresponding nAbs-free rhFVIII-treated groups identified as having abnormal bone remodeling.

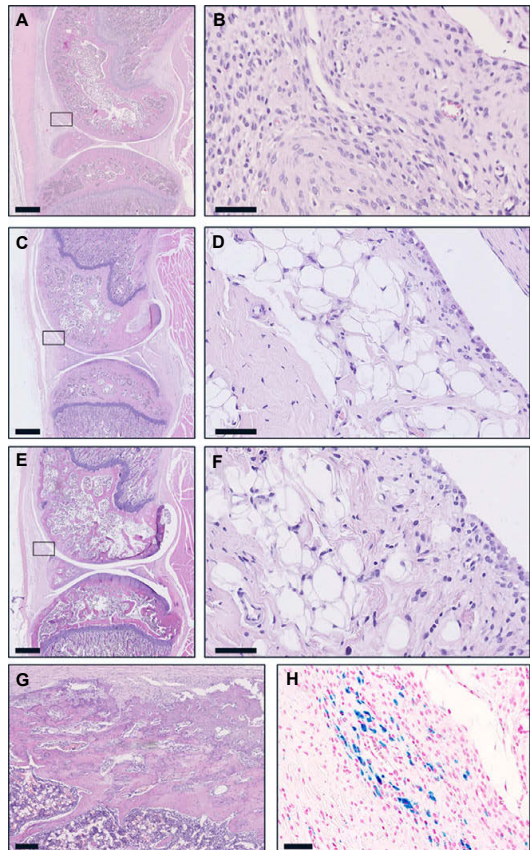


Fig. 2. Histologic findings of the joints according to genotype and treatment. (A) and (B) show the joint from an untreated F8^{-/-} rat from the one-joint-bleed group; (B) is a magnification of (A), showing an enlarged and inflamed synovial membrane; (C) and (D) show the joint of a treated F8^{-/-} rat from the one-joint-bleed group; (D) is a magnification of (C) showing a thin synovial membrane with subsynovial adipose tissue comparable to the wild-type animal; (E) and (F) are from a wild-type animal from the one-joint-bleed group; (F) is a magnification of (E), showing a normal synovial membrane with subsynovial adipose tissue; (G) shows excessive periosteal bone formation on the femoral shaft; (H) shows hemosiderin deposition in the subsynovial area of an untreated F8^{-/-} rat. Bars: 1000 μ m in the left panels (A), (C) and (E). (G) 200 μ m and 50 μ m in the right panels. (A) to (G) are stained with HE and (H) stained with Perls' Prussian Blue.

The arthropathy score was applied to the histologic analysis (see Fig. 3). The majority, 81% (13/16) and 100% (6/6), of the untreated F8^{-/-} animals from the one- and two-joint-bleed groups, respectively, had a positive total score. Only 35% (7/20) of the treated animals from the one-joint-bleed group had a positive score, with three of these being positive for rhFVIII nAbs. Similarly, 50% (4/8) of the treated F8^{-/-} rats from the two-joint-bleed group had positive arthropathy scores, with three out of

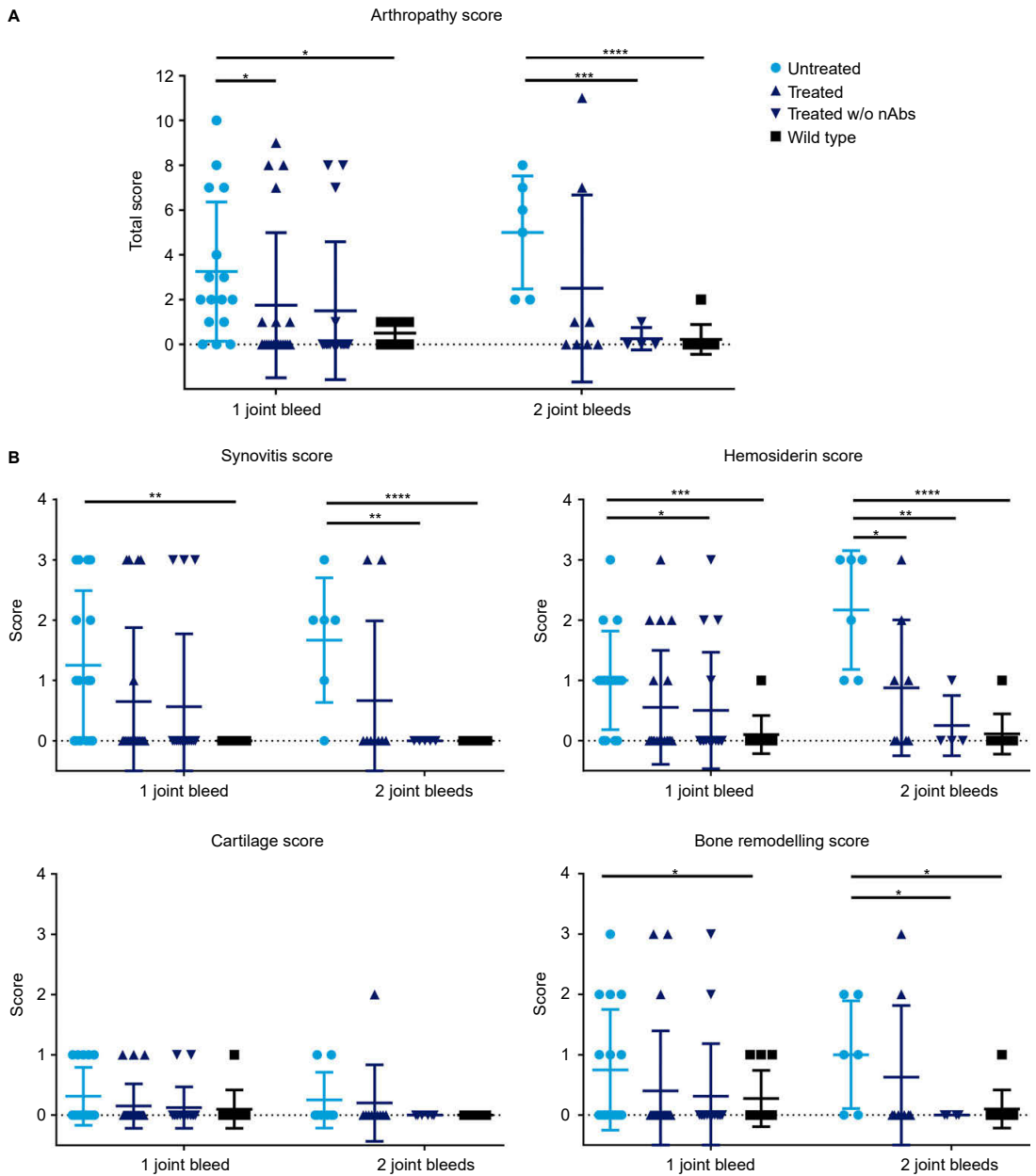


Fig. 3. Histopathologic scoring according to genotype and treatment. Histologic images of injured knee-joints were scored according to the severity of synovitis, hemosiderin deposition, bone remodeling and cartilage degradation. (A) Total arthropathy score for the individual animals presented according to treatment and genotype for both the one- and two-joint-bleed groups. (B) Individual arthropathy scores of the four hemophilic arthropathy (HA) characteristics according to genotype and treatment. Dots represent scores of individual animals. Lines represent mean \pm standard deviation. * $P < 0.05$, ** $P < 0.005$, *** $P < 0.0005$, **** $P < 0.0001$ (Student's *t*-test). nAbs, rhFVIII-neutralizing antibodies.

four animals with a positive score having developed nAbs. A total of six WT animals (from both joint bleed groups) had a positive arthropathy score (five had a score

of one and a single WT animal had a score of two). When compared, the mean score in the single-joint-bleed untreated F8^{-/-} group (3.25 ± 3.11) was significantly

higher than the mean of the WT animals (0.5 ± 0.53 , $P = 0.004$) and the mean of the treated F8^{-/-} group (1.90 ± 3.55 , see Fig. 3A). Importantly, no difference between treated and WT animals was found (Fig. 3A) after a single joint bleed. For the two-joint-bleed group a significant difference ($P < 0.0001$) in mean arthropathy score was found between the untreated F8^{-/-} rats (5 ± 2.53) and the WT animals (0.22 ± 0.67). Here no significant difference was found between untreated and all treated animals (2.5 ± 4.18); however, removing nAbs animals from the treated group led to a significant difference ($P = 0.0007$) between the untreated F8^{-/-} animals and the nAbs-free treated F8^{-/-} animals (0.25 ± 0.5). Again, no difference between WT and treated F8^{-/-} animals was found.

For the individual parameters, a significant difference between untreated and WT animals from both the one- and two-joint-bleed groups was observed for hemosiderin deposition ($P = 0.0009$ and 0.0001), synovitis ($P = 0.002$ and 0.0001) and bone remodeling ($P = 0.0136$ and 0.0103). For the one-joint-bleed group a significant difference between untreated rats and those treated without nAbs was also found ($P = 0.04$) for hemosiderin deposition (Fig. 3B). For the two-joint-bleed group a significant difference between untreated and treated (either with or without nAbs) F8^{-/-} rats was found for hemosiderin deposition ($P = 0.034$), synovitis ($P = 0.0029$) and bone remodeling ($P = 0.0463$). No difference in total arthropathy score was observed when comparing a single injury or two injuries in the untreated animals.

Discussion

The present study showed that the newly characterized F8^{-/-} rat developed chronic degenerative joint changes following an induced joint bleed. HA was present after both a single injury and two injuries, with a higher average score, but with no statistically significant progression induced by the second injury. Prophylactic treatment with rhFVIII significantly reduced the pathology in the joints and demonstrated a reduction in the clinical signs of hemarthrosis, thereby confirming the potential of this F8^{-/-} rat as a relevant model of HA.

Observation of the animals following the induced joint bleed revealed clinical signs of hemarthrosis, especially in untreated animals that developed moderate to large swellings, which normalized towards pre-injury measurements during the time-course of the study. Signs of hemarthrosis were less pronounced for rhFVIII-treated animals and absent in WT animals.

Hyperplasia of the synovial membrane, with concomitant inflammatory infiltration and fibrous tissue formation in the subsynovial area, was identified in the majority of untreated F8^{-/-} animals. This was often seen together with apoptotic or complete loss of chondrocytes in conjunction with proteoglycan reduction and thinning of articular

cartilage, along with abnormal bone remodeling, resulting in both excessive bone formation and degradation. Likewise, hemosiderin deposition was found in the majority of untreated animals. Already 2 weeks after an induced joint bleed, all of the above-mentioned pathology was identified. Therefore, the rat is likely to develop chronic degenerative changes faster than humans, allowing studies of HA with a relatively short timeline. However, unlike the human disorder, the rats only presented with minor cartilage damage within this timespan, when compared with synovitis and bone damage. Combined, the identified pathologies resemble findings in human HA [6,7,16,18], confirming the translational relevance of this F8^{-/-} rat.

Assessment of the histologic images was performed according to a new composite arthropathy score, developed in order to identify and grade animals with chronic degenerative changes, covering the most important characteristics seen in human HA patients [18], assessing severity of synovitis, bone remodeling, cartilage degradation and hemosiderin deposition. Whereas the arthropathy score supported diagnosis of HA in all but three untreated animals, this was only the case for a minor subset of the rhFVIII-treated (primarily nAbs-positive animals) and WT animals. This trend was true both for the total arthropathy score and for the individual parameters. Combined, we found a significantly more severe arthropathy in untreated animals compared with both WT and rhFVIII-treated animals after a single joint bleed and compared with WT and nAbs-free rhFVIII-treated animals after two joint bleeds. Although a higher proportion of untreated F8^{-/-} animals presented with a positive arthropathy score, no significant increase in pathology between the one-joint-bleed and two-joint-bleed untreated F8^{-/-} groups was identified. This could be a result of lack of power, as the two-joint-bleed untreated F8^{-/-} group has a mean arthropathy score almost twice as high as the corresponding one-joint-bleed group (5 vs. 3.25), but is composed of a low number of animals ($n = 4$). Importantly, despite some pathologic findings in the treated F8^{-/-} groups, which could be the result of suboptimal dosing, no significant difference was found between WT and treated animals (with or without nAbs) for both joint bleed groups. The novel scoring system can thus successfully differentiate between animals receiving different treatment regimens (rhFVIII or vehicle solution). Furthermore, the findings resemble previous models of hemarthrosis and synovitis, substantiating the use of the F8^{-/-} rat to evaluate therapeutic intervention [6,7,19–21] as a model of HA.

The F8^{-/-} rat, unlike the F8^{-/-} mouse, develops spontaneous bleeds (though rarely observed in the knee-joint [10]) often requiring treatment. In this study a total of eight of the 19 treated animals (four from each joint bleed group) had suffered spontaneous bleeds prior to study inclusion and had previously been treated with rhFVIII on demand. Six of these are identical to the animals developing nAbs

during the time-course of the study. It is likely that the dosage of 300 IU/kg rhFVIII prior to the induced joint bleed led to a rapid and large antibody response in the previously treated animals, rendering the treatment ineffective in this study. This would explain why a few of the treated animals had both joint swelling and histopathologic findings. This, however, does not explain why three nAbs-free rhFVIII-treated animals developed signs of hemarthrosis and HA. It is possible that these animals simply resemble the clinical situation, where treatment with rhFVIII occasionally fails to restore an adequate hemostatic potential, or the dosed amount of rhFVIII (based on *in vitro* normalization of F8^{-/-} plasma APTT) could be too low or perhaps should have been repeated, following the induced joint bleed, in order to completely prevent bleeding. The dose in this study was chosen to ensure complete coverage; however, in future studies the efficacy of additional doses should be investigated.

Compared with the F8^{-/-} mouse, the F8^{-/-} rat has an advantageous size with a larger blood volume and joints. In future studies, this will allow for more frequent and larger blood sampling, enabling longitudinal studies using the rat as its own baseline control, which is likely to reduce the required number of animals. Moreover, the rat is a gregarious creature with little aggressive behavior, making it possible to house the animals together without the risk of fight-induced bleeding. This is not only more convenient, but also a more natural and ethical housing of the animals. Finally, the larger size of the rat also allows for clinically relevant imaging (e.g. ultrasonography), with greater ease than in the mouse models.

In conclusion, it was possible to establish a new model of HA for hemophilia A using the F8^{-/-} rat model. The bleeding phenotype of the F8^{-/-} rat led to development of clinically evident hemarthrosis following needle-puncture of the knee-joint, causing chronic degenerative changes resembling human HA, as shown by histological analysis. Treatment with rhFVIII prior to the joint bleed ameliorated arthropathic changes in the vast majority of the animals, returning them to a wild-type phenotype. The potential of the F8^{-/-} rat as an *in vivo* model of HA for preclinical PK and PD testing of drug candidates for replacement or bypassing therapy, as well as adjunctive therapy, therefore appears promising.

Addendum

K. R. Sørensen, L. N. Nielsen, K. Roepstorff, A. K. Hansen, and B. Wiinberg designed the study. K. R. Sørensen performed the experiments as well as the scoring with help from K. Roepstorff, who developed the arthropathy score. K. R. Sørensen and M. Kjelgaard-Hansen performed the statistical analysis. K. R. Sørensen prepared the manuscript. M. Tranholm took part in designing the rat. All authors received the manuscript and approved the final version.

Acknowledgements

We acknowledge H. F. Kierkegaard for aiding in the animal experiments, J. Juul, M. N. Nielsen and J. Mandelbaum for sectioning of tissue, J. Juul for staining, K. N. Weldingh and B. Klitgaard for blood sample analyses and S. Skov for scientific input.

Disclosure of Conflict of Interests

M. Tranholm, L. N. Nielsen, B. Wiinberg, M. Kjelgaard-Hansen and K. Roepstorff report fees from Novo Nordisk A/S, outside the submitted work. K. R. Sørensen reports grants from the University of Copenhagen and Novo Nordisk A/S, during the conduct of the study. A. K. Hansen has nothing to disclose.

References

- Bolton-Maggs PH, Pasi KJ. Haemophilias A and B. *Lancet* 2003; **361**: 1801.
- Roosendaal G, Lafeber FP. Blood-induced joint damage in hemophilia. *Semin Thromb Hemost* 2003; **29**: 37.
- Oldenburg J. Optimal treatment strategies for hemophilia: achievements and limitations of current prophylactic regimens. *Blood* 2015; **125**: 2038.
- Aledort LM, Haschmeyer RH, Pettersson H. A longitudinal study of orthopaedic outcomes for severe factor-VIII-deficient haemophiliacs. The Orthopaedic Outcome Study Group. *J Intern Med* 1994; **236**: 391.
- Pastoft AE, Lykkesfeldt J, Ezban M, Tranholm M, Whinna HC, Lauritzen B. A sensitive venous bleeding model in haemophilia A mice: effects of two recombinant FVIII products (N8 and Advate®). *Haemophilia* 2012; **18**: 782.
- Hakobyan N, Enockson C, Cole AA, Sumner DR, Valentino LA. Experimental haemophilic arthropathy in a mouse model of a massive haemarthrosis: gross, radiological and histological changes. *Haemophilia* 2008; **14**: 804.
- Valentino LA, Hakobyan N, Kazarian T, Jabbar KJ, Jabbar AA. Experimental haemophilic synovitis: rationale and development of a murine model of human factor VIII deficiency. *Haemophilia* 2004; **10**: 280.
- Broze GJ Jr, Yin ZF, Lasky N. A tail vein bleeding time model and delayed bleeding in hemophilic mice. *Thromb Haemost* 2001; **85**: 747.
- Elm T, Karpf DM, Ovlisen K, Pelzer H, Ezban M, Kjalke M, Tranholm M. Pharmacokinetics and pharmacodynamics of a new recombinant FVIII (N8) in haemophilia A mice. *Haemophilia* 2012; **18**: 139.
- Nielsen LN, Wiinberg B, Hager M, Holmberg HL, Hansen JJ, Roepstorff K, Tranholm M. A novel F8^{-/-} rat as a translational model of human hemophilia A. *J Thromb Haemost* 2014; **12**: 1274.
- Diehl KH, Hull R, Morton D, Pfister R, Rabemampianina Y, Smith D, Vidal JM, van de Vorstenbosch C, European Federation of Pharmaceutical Industries A, European Centre for the Validation of Alternative M. A good practice guide to the administration of substances and removal of blood, including routes and volumes. *J Appl Toxicol* 2001; **21**: 15.
- Lovgren KM, Sondergaard H, Skov S, Weldingh KN, Tranholm M, Wiinberg B. Antibody response to recombinant human coagulation factor VIII in a new rat model of severe hemophilia A. *J Thromb Haemost* 2016; **14**: 747–56.

- 13 Duncan E, Collecutt M, Street A. Nijmegen-Bethesda assay to measure factor VIII inhibitors. *Methods Mol Biol* 2013; **992**: 321.
- 14 Srivastava A, Brewer AK, Mauser-Bunschoten EP, Key NS, Kitchen S, Llinas A, Ludlam CA, Mahlangu JN, Mulder K, Poon MC. Guidelines for the management of hemophilia. *Haemophilia* 2013; **19**: e1–47.
- 15 Valentino LA, Hakobyan N. Histological changes in murine haemophilic synovitis: a quantitative grading system to assess blood-induced synovitis. *Haemophilia* 2006; **12**: 654.
- 16 Roosendaal G, Vianen ME, Wenting MJ, van Rinsum AC, van den Berg HM, Lafeber FP, Bijlsma JW. Iron deposits and catabolic properties of synovial tissue from patients with haemophilia. *J Bone Joint Surg Br* 1998; **80**: 540.
- 17 Speer DP. Early pathogenesis of hemophilic arthropathy. Evolution of the subchondral cyst. *Clin Orthop Relat Res* 1984; **185**: 250–65.
- 18 Stein H, Duthie RB. The pathogenesis of chronic haemophilic arthropathy. *J Bone Joint Surg Br* 1981; **63B**: 601.
- 19 Jin DY, Zhang TP, Gui T, Stafford DW, Monahan PE. Creation of a mouse expressing defective human factor IX. *Blood* 2004; **104**: 1733.
- 20 Lin HF, Maeda N, Smithies O, Straight DL, Stafford DW. A coagulation factor IX-deficient mouse model for human hemophilia B. *Blood* 1997; **90**: 3962.
- 21 Valentino LA, Hakobyan N, Kazarian T, Sorensen BB, Tranholm M. Prevention of haemarthrosis in a murine model of acute joint bleeding. *Haemophilia* 2009; **15**: 314.

Paper II

Visualization of haemophilic arthropathy in F8^{-/-} rats by ultrasonography and micro-computed tomography

Christensen, KR.; Roepstorff, K.; Petersen, M.; Wiinberg, B.; Hansen, AK.; Kjelgaard-Hansen, M.; Nielsen, LN.
Haemophilia. 2017 Jan;23(1):152-162



ORIGINAL ARTICLE

Visualization of haemophilic arthropathy in F8^{-/-} rats by ultrasonography and micro-computed tomographyK. R. CHRISTENSEN,*† K. ROEPSTORFF,‡ M. PETERSEN,‡ B. WIINBERG,* A. K. HANSEN,† M. KJELGAARD-HANSEN* and L. N. NIELSEN*¹

*Translational Haemophilia Pharmacology, Novo Nordisk A/S, Maaloev; †Veterinary Disease Biology, University of Copenhagen, Frederiksberg, and ‡Histology & Bioimaging, Novo Nordisk A/S, Maaloev, Denmark

Introduction: A major complication of haemophilia is haemophilic arthropathy (HA), a debilitating disorder with an incompletely defined pathobiology. High-resolution imaging may provide new knowledge about onset and progression of HA, and thereby support identification of new treatment opportunities. Recently, a F8^{-/-} rat model of HA was developed. The size of the rat allows for convenient and high resolution imaging of the joints, which could enable *in vivo* studies of HA development. **Aim:** To determine whether HA in the F8^{-/-} rat can be visualized using ultrasonography (US) and micro-computed tomography (μ CT). **Methods:** Sixty F8^{-/-} and 20 wild-type rats were subjected to a single or two induced knee bleeds. F8^{-/-} rats were treated with either recombinant human FVIII (rhFVIII) or vehicle before the induction of knee bleeds. Haemophilic arthropathy was visualized using *in vivo* US and *ex vivo* μ CT, and the observations correlated with histological evaluation. **Results:** US and μ CT detected pathologies in the knee related to HA. There was a strong correlation between disease severity determined by μ CT and histopathology. rhFVIII treatment reduced the pathology identified with both imaging techniques. **Conclusion:** US and μ CT are suitable imaging techniques for detection of blood-induced joint disease in F8^{-/-} rats and may be used for longitudinal studies of disease progression.

Keywords: animal model, arthropathy, haemarthrosis, *rattus*, ultrasonography, X-ray microcomputed tomography

Introduction

Patients with haemophilia A have an inherited or spontaneous mutation in the gene coding for coagulation factor VIII (FVIII), causing partial or complete deficiency in factor activity resulting in attenuation of the coagulation cascade and incomplete coagulation [1]. If untreated, patients with severe haemophilia suffer from spontaneous bleeds, most often in the large synovial joints such as the knees, ankles and elbows [2]. Treatment of choice is FVIII replacement therapies, given either on demand when bleeding occurs, or as a prophylactic treatment. However, even patients

receiving intensive prophylaxis may endure breakthrough bleeds. The repeated joint bleeds cause progressive joint deterioration, eventually leading to haemophilic arthropathy (HA), a severely debilitating condition. Consequently, 90% of severe haemophilia A patients on intensive prophylaxis present with joint disease by the age of 30–40 years [2,3].

Recently, a F8^{-/-} rat model for haemophilia A was developed, which is phenotypically comparable to human patients, with impaired haemostasis and suffering from spontaneous musculoskeletal bleeding [4]. We have previously reported that after a single induced joint bleed, F8^{-/-} rats develop histopathological changes in the knee resembling human HA, attenuable by recombinant human FVIII (rhFVIII) treatment [5]. This model provides a valuable tool for investigating progression of HA. Histopathological evaluation is the gold standard for assessing HA in small animal models. However, it does not allow for repeated disease assessment in longitudinal studies. Therefore, non-invasive imaging modalities may be useful for mapping temporal progression of disease from joint bleeds to established HA in the F8^{-/-} rat. This may support identification of new and better therapeutic

Correspondence: Kristine Rothaus Christensen, Novo Nordisk A/S, Novo Nordisk Park 1, 2760 Maaloev, Denmark.
Tel.: +45 30798261; fax: +45 44426220;
e-mail: ktsr@novonordisk.com

¹Present address: Veterinary Clinical and Animal Sciences, University of Copenhagen, Copenhagen, Denmark

The work was conducted at Novo Nordisk A/S, Novo Nordisk Park 1, 2760 Maaloev, Denmark.

Accepted after revision 23 July 2016

strategies to prevent development of HA and reduce the number of animals needed for longitudinal studies.

In patients, radiological evaluation of the joint, along with clinical assessment of joint mobility, are the standard clinical tools for diagnosis of HA [6]. However, standard radiography has poor resolution and primarily detects radiodense, late stage disease complications, such as significant bone related abnormalities including subchondral cysts. It is therefore primarily used for evaluation of established disease [7]. In contrast, computed tomography (CT) provides high resolution and detailed images of bone tissue, allowing identification of even minor pathological changes [8,9]. CT is not frequently applied in human haemophilia patients, due to radiation exposure. However, it could be a powerful tool for detailed visualization of bone pathology in the F8^{-/-} rat model.

For visualization of the early, soft tissue pathologies that precede bone disease, magnetic resonance imaging (MRI) has been the imaging modality of choice. However, its use is limited by both access to scanners and the need for sedation in young children [10].

Ultrasonography (US) is increasingly recognized as a low-cost alternative to MRI [11]. US provides a non-invasive, fast examination without radiation and no requirements for sedation in younger patients. It allows sensitive visualization of soft tissue changes, some of the earliest indicators of HA. US however, lacks the ability to clearly show bone structure [7].

The objectives of this study were to investigate whether US and micro-CT (μ CT) can visualize development of HA in the F8^{-/-} rat model, and assess how the pathological observations identified using the two imaging tools correlate with the histopathological characterization of affected joints.

Materials and methods

Animal studies

Animal studies were performed according to guidelines from, and approved by the Danish Animal Experiments Council, the Danish Ministry of Environment and Food.

Invasive procedures were performed under anaesthesia, as previously described [5].

The rats were housed under standard conditions with a 12-h/12-h light/dark cycle, 20–23°C, 30–60% relative humidity with *ad libitum* food and water consumption and monitored daily for signs of bleeding.

Data from these animals have previously been reported in a study validating the F8^{-/-} rat as a translational model of HA [5].

Exclusion criteria

Upon study initiation, animals with evident bleeding in their legs were excluded. Animals developing

spontaneous bleeds unrelated to the induced haemarthrosis after study initiation were euthanized at any sign of distress and excluded from the study.

Study population and groups

Twenty wild-type and 60 F8^{-/-} rats (SD-F8^{tm1sage}) [4], 13–15 weeks of age bred at Novo Nordisk A/S (Maaloev, Denmark) were included in the study. Ten wild-type and 40 F8^{-/-} rats were subjected to a single induced haemarthrosis (day 0 and euthanized on day 14) and the remaining 10 wild-type and 20 F8^{-/-} rats had two haemarthroses induced (day 0 and 14 and euthanized on day 28). The F8^{-/-} animals were randomized 1:1 to prophylactic treatment with either 300 IU kg⁻¹ rhFVIII (4.8 mL kg⁻¹ ReFacto AF[®] 250 IE/a.e., Pfizer, Paris, France) or vehicle buffer solution (10 mM L-Histidine, 8.8 mM sucrose, 30.8 mM NaCl, 1.7 mM CaCl₂, 0.01% Tween 80) in an equivalent volume to rhFVIII-dosed animals. All wild-type animals were dosed with vehicle. Treatment was given blinded as a bolus injection 5 min before injury.

Needle-induced haemarthrosis

Haemarthrosis was induced as previously described [5]. Briefly, the animals were anaesthetized and a subcutaneous injection of 0.03 mg kg⁻¹ buprenorphine (Temgesic 0.3 mg mL⁻¹, Reckitt Benckiser Pharmaceuticals Ltd, Berkshire, UK) administered. Hereafter, the animals were dosed intravenously with vehicle or rhFVIII. The left leg was mildly flexed, and haemarthrosis induced by inserting a 30 g needle into the joint through the patella ligament.

The animals received analgesia in the drinking water (0.06 mg L⁻¹ Temgesic) for a minimum of seven days after the induced joint bleed.

Blood sampling and euthanasia

A polyethylene 0.8 mm catheter (PE90, Becton, Dickinson and Company, Franklin Lakes, NJ, USA) was placed in the carotid artery, blood collected, and the animals euthanized by an injection of pentobarbital (Mebumal 50 mg mL⁻¹, SAD, Amgros I/S, Copenhagen, Denmark) through the catheter.

Citrated whole blood (3.2%) was collected and platelet-poor plasma obtained by centrifugation at 4000 g for 5 min and stored at -80°C.

Antibody analysis

Plasma samples from the day of termination were analysed for the presence of rhFVIII neutralizing antibodies (nAbs), using a modified chromogenic assay from Chromogenix (Coamatic FVIII kit), as previously

described [12,13]. Animals with BU \geq 5 were considered high-titre animals equivalent to the clinical setting [14].

Ultrasonography

US was performed at baseline and on day 14 (before euthanasia or the second induced knee bleed) and on day 28 before euthanasia. For the US procedure the rat was anaesthetized, placed on the back with the left leg mildly flexed, hair removed and the skin cleaned with an ethanol swap, before applying scanning gel (EKO GEL, Ekkomarine Medico A/S, Holstebro, Denmark).

The US exam was performed using a VEVO2100 (Visualsonics, Toronto, ON, Canada) and a MS-700 transducer with a 30–70 MHz range, by a single observer blinded according to genotype and treatment.

The knee was investigated in the sagittal and transverse plane in B mode (with the transducer positioned as displayed in Fig. 1 [15]), and assessed for intra-articular fluid, fat pad deviation, haematoma formation as well as bone and cartilage degeneration (see Fig. 1).

Postmortem collection of knees and μ CT

Left hind-legs were dissected at the femoral head, mildly stripped of muscle and skin and placed in 4% paraformaldehyde. Injured formalin-fixed knees were scanned *ex vivo*, using a Perkin Elmer Quantum FX μ CT scanner (Perkin Elmer, Waltham, MA, USA). Optimized scan settings were 90 kV, 160 μ A with a field of view of 20 mm.

Histology and histopathological evaluation

Histological evaluation of the knees from this population of rats has been reported previously [5]. In brief, histological sections from the sagittal plane were scored from 0 to 3 for four different disease characteristics (synovitis, haemosiderin deposition, cartilage degradation and bone remodelling) and the sum score calculated (maximum score of 12).

Assessment of US and μ CT images

A US scoring system was developed using a visual analogue scale (VAS), assessing four parameters; oedema, patella ligament changes, fat pad displacement and bone/cartilage ruffling (see Fig. 1b). Briefly, a 10 cm line is drawn and a mark set for each of the four parameters between zero and ten according to the observer's perception of severity of pathological changes. The assessments were made based on recorded US images. A sum score was calculated, with a maximum score of 40 (see Figures 1 and S1 for atlas of US scoring). The inter-observer integrity of the score was tested by analysis of agreement between two independent observers assessing a selected sample set ($n = 13$) representing full range of observed scores. Criteria for acceptable agreement was met (linear analysis, data not shown) with a narrow interval of observed differences (95% CI [-1.0; 1.9]). The US was performed in an optimized position where the clearest and most reproducible images were obtained with clear landmarks for the performer (in the sagittal view; the ligament (corresponding to the infrapatellar ligament in human), fat pad (corresponding to Hoffa's

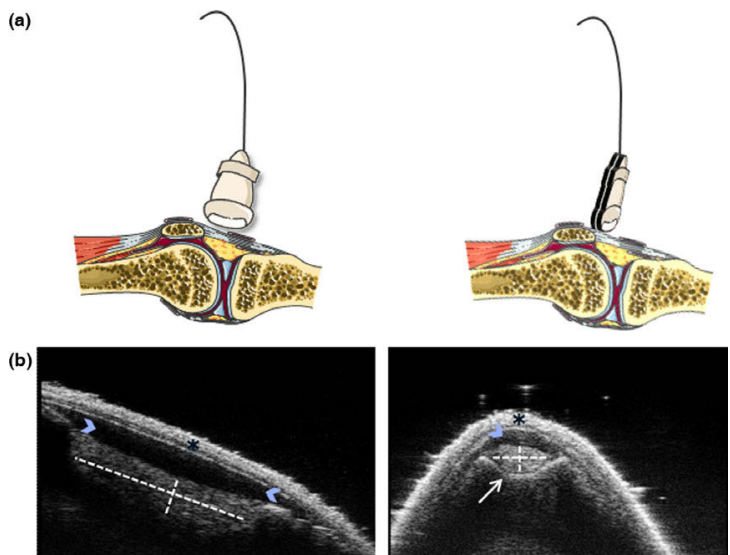


Fig. 1. Position of the transducer and ultrasonography images showing the anatomical structures assessed (a) Schematic view of the transducer position. Left; sagittal scan. Right; transverse scan. Figures modified from <http://servier.com/Powerpoint-image-bank>. (b) Left image is a sagittal B-mode scan of a normal joint showing the skin (*), the hypoechoic patella ligament (arrowheads) above the fat pad (dashed lines) stretching from the femoral condyle down across the tibial plateau. The hyperechoic cortex of the tibial plateau and the femoral condyles are visible below and extending from the fat pad. To the right an image of a transverse B-mode scan of a normal joint showing the skin (*), the hypoechoic patella ligament (arrowhead) above the fat pad (dashed lines) lying in the patellofemoral groove (intercondylar notch), and the hyperechoic cortex of the femoral condyles (white arrow).

fat pad in human), the femoral and tibial bone surfaces and for the transverse view; the femoral condyles just distal to the patella).

μ CT scans were assessed in sagittal, coronal and transverse planes by evaluating 2D images. Scans were scored 0 or 1 (0 = normal, 1 = pathologic) according to the presence of periosteal bone formation on femur, tibia and patella, osteophytosis of femoral epicondyles, tibial epicondyles and patella as well as a score for the presence of subchondral cysts (maximum sum score of 7, see Figures S2 and S3 for atlas of μ CT scoring).

All assessments were performed blinded towards genotype, treatment and time point, by the same observer.

Statistics

To test whether US or μ CT could reliably discriminate between the different groups, statistical analysis was performed on sum scores for each assessment tool (US and μ CT) using Mann–Whitney tests. Single and two joint-bleed groups were tested separately using hierarchical hypothesis testing; first, the untreated $F8^{-/-}$ rats were compared to WT animals. In presence of the expected discrimination (i.e. a significant difference between untreated $F8^{-/-}$ and WT animals in both injury groups), the $F8^{-/-}$ untreated animals were compared to rhFVIII treated animals. This was followed by a comparison of untreated and nAbs-free treated animals (animals without neutralising anti-FVIII antibodies). Finally, the treated group (followed by the nAbs-free treated group) was compared to the WT group.

Additionally, the correlation between the histopathology score reported in [5] and the US sum score and the μ CT sum score was analysed (two-tailed Spearman's correlation test).

P -values < 0.05 were considered significant. Statistical analysis was performed using GraphPad Prism (Version 6.05, GraphPad Software, Inc. San Diego, CA, USA).

Results

HA development in $F8^{-/-}$ rats

Characterization of HA development following induced knee bleeds in this population of rats has previously been reported [5]. In summary, histopathological evaluation showed synovitis, haemosiderin deposition, chondrocyte- and proteoglycan loss, as well as bone resorption and remodelling in untreated $F8^{-/-}$ rats, whereas WT rats did not develop HA. Prophylactic treatment with rhFVIII prevented HA development in the majority of treated rats. A few rhFVIII treated animals showed pathology of the joint,

however, these were primarily animals that had developed FVIII neutralizing antibodies (nAbs). When HA was scored using a semiquantitative scoring system, a significant difference in the histopathological score between untreated and treated animals was demonstrated. In the present study we investigated whether US and μ CT can be used for assessment of HA and determined the correlation between disease severity assessed by imaging and the gold standard histopathology reported in Sørensen *et al.* [5].

In vivo ultrasonography detected HA in untreated $F8^{-/-}$ rats

The US examination prior to injury showed normal joints with a clearly delineated patella ligament and fat pad, no oedema and well defined tibial and femoral heads (see Fig. 2a). Induced haemarthrosis in untreated $F8^{-/-}$ rats lead to detectable subcutaneous oedema, patella ligament deformation, as well as displacement, and in some instances a severe disruption, of the fat pad (see Fig. 2a). In a few transverse ultrasonography scans, ruffling of the bone were evident.

When applying the US scoring system, there was a significant difference between WT and untreated $F8^{-/-}$ rats both after a single and two haemarthroses ($P < 0.0005$ for both comparisons, see Fig. 3a, with one WT rat from each group having a score above 3). The total US score was significantly higher after a single joint bleed in untreated $F8^{-/-}$ animals compared to treated $F8^{-/-}$ animals ($P = 0.0004$, 6/20 treated animals had a score above 3 after a single joint bleed) or both after a single and two joint bleeds in $F8^{-/-}$ animals when compared to treated animals without nAbs ($P = 0.0006$ and $P = 0.0095$ after a single or two haemarthroses, respectively, with no animals having a score above 3). Similarly, the WT animals were only significantly different from the rhFVIII treated animals when including animals that had developed nAbs, and only after two induced haemarthroses ($P = 0.022$, see Fig. 3a).

Bone degeneration was clearly visualized by *ex vivo* μ CT

μ CT detected HA-related pathology in untreated $F8^{-/-}$ animals (see Figs 3b and 4). Osteophytes and periosteal bone formation were present in 50% (8/16) and 83% (5/6) of $F8^{-/-}$ rats following a single or two haemarthroses, respectively. For rhFVIII treated animals (including nAbs positive animals), the percentages were 20% (4/20) and 25% (2/8) for one and two haemarthroses, respectively. No bone abnormalities were detected in WT rats (see Fig. 4).

To quantify the degree of bone pathology, the images were assessed for osteophytosis and periosteal bone formation on patella, femur and tibia and given

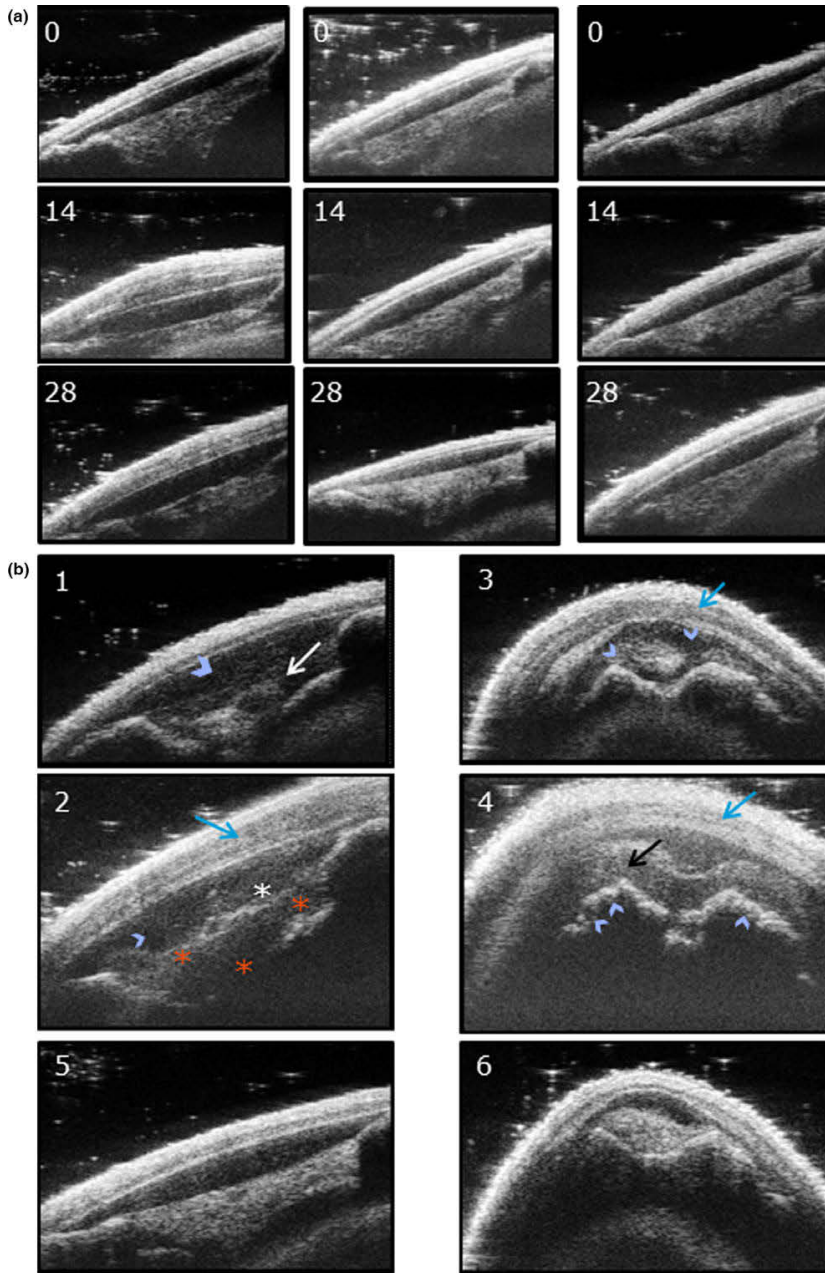


Fig. 2. US scans show joint pathology in untreated F8^{-/-} animals. (a) Example of a sagittal US scan from day 0 (before injury), 14 and 28 after haemarthrosis, from an untreated F8^{-/-} rat (left), a rhFVIII treated F8^{-/-} rat (middle) and a wild-type rat (right). After injury, the untreated animal presents with a heterogeneous echogenicity in the subcutaneous area (soft tissue swelling/oedema) and enlarged patella ligament with loss of hypoechoogenicity indicating intra-articular fluid. rhFVIII treated and WT animals show no sign of pathology. (b) Examples of US images of F8^{-/-} rat knees with pathology (1–4) and WT rat knees with no signs of pathology (5–6) following two joint bleeds. (b1) sagittal scan showing a swollen patella ligament (arrowhead) and disruption of the fat pad (white arrow). (b2) sagittal scan showing subcutaneous oedema (blue arrow), swollen patella ligament (arrowhead) with loss of hypoechoogenicity (white asterisk), and disruption of the fat pad with heterogeneous echogenicity (red asterisks). (b3) transverse scan showing slight subcutaneous oedema (blue arrow) and signs of intra-articular effusion (arrowheads). (b4) transverse scan with slight subcutaneous oedema (blue arrow) and heterogeneous intra-articular echogenicity indicating effusion (black arrow) along with marked ruffling of the femoral condyles (arrowheads). (b5 and b6) sagittal and transverse scans from two different WT animals at day 28 with no signs of pathology.

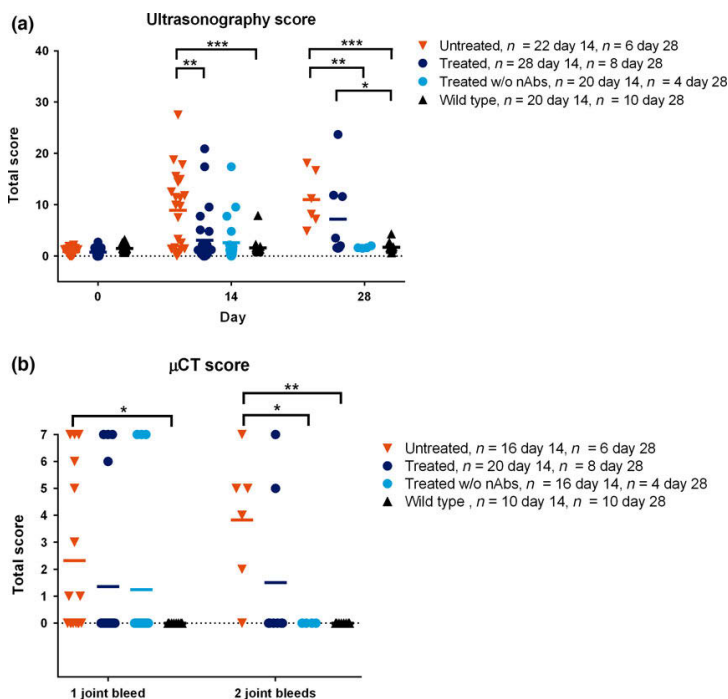


Fig. 3. *In vivo* US and *ex vivo* μ CT can discriminate between wild-type rats, rhFVIII treated $F8^{-/-}$ rats and untreated $F8^{-/-}$ rats following induced joint bleeds. (a) US sum score combining the four assessment parameters (subcutaneous oedema, ligament changes, fat pad displacement and bone ruffling). (b) μ CT sum score combining the seven assessment parameters (periosteal bone formation on femur, patella and tibia, osteophytes on patella, femur and tibia and the presence of subchondral cysts). Lines represent mean * $P < 0.05$, ** $P < 0.005$, *** $P < 0.0005$, **** $P < 0.0001$. P -values were calculated using sequential Mann-Whitney tests comparing groups. Treated w/o nAbs refers to treated animals that did not develop neutralizing antibodies during the study. nAbs: neutralizing antibodies against rhFVIII.

a score of 0 (normal) or 1 (pathologic) for each compartment and pathology as well as a score for the presence of subchondral cysts on either femur or tibia. A significant difference in μ CT sum score was present between untreated $F8^{-/-}$ and WT animals after both one ($P = 0.014$) and two joint bleeds ($P < 0.0014$, see Fig. 3b). Effect of rhFVIII treatment could be demonstrated by μ CT after two injuries (difference between untreated and treated $F8^{-/-}$ animals without nAbs, $P = 0.033$, see Fig. 3b). No significant difference between WT and treated $F8^{-/-}$ animals was found.

Interestingly, pathology resembling subchondral cysts was identified in six animals (see Fig. 5). To verify the μ CT based detection of subchondral cysts, two knees with each two μ CT-visualized cysts were selected for full histological sectioning. All four cysts were identified by histology (see Fig. 5) and importantly, no additional subchondral cysts were found.

Strong correlation between μ CT and the histological arthropathy score

To test the feasibility of using US or μ CT for studying HA severity, a correlation analysis between the disease severity determined by imaging (the sum US score or the sum μ CT score) and histology (the arthropathy sum score) was performed. The analysis revealed significant and good correlation between the US- and histological arthropathy score after two joint bleeds (see Fig. 6a, $r = 0.79$, $P < 0.0001$).

There was a significant and strong correlation between the μ CT- and histological arthropathy score (see Fig. 6b) both following one ($r = 0.80$, $P < 0.0001$) and two ($r = 0.84$, $P < 0.0001$) joint bleeds.

Discussion

In this study, we establish US and μ CT as imaging modalities for visualization of soft tissue and bone deformation, respectively, following induced knee bleeds in $F8^{-/-}$ rats.

Application of *in vivo* US in animal models of HA is a new area of investigation, with only few publications [15–17]. In the present study, US revealed joint pathology 14 days after induction of one or two joint bleeds, including oedema (soft tissue swelling), ligament swelling and disruption of the fat pad. As expected, bone changes were difficult to clearly visualize with US. The pathology identified in the present study mimics that found by US in human HA, i.e. loss of joint architecture with swelling of the ligaments [18], effusions and bone erosions [10,19,20], albeit the level of detail is considerably higher in humans compared to rats due to the size of the joints. Hence, US can be used to study soft tissue pathology, as well as to monitor effect of treatment *in vivo*, in the $F8^{-/-}$ rat.

μ CT detected extensive bone pathology (osteophytosis and periosteal bone formation) in untreated $F8^{-/-}$ rats following induced haemarthrosis, consistent with

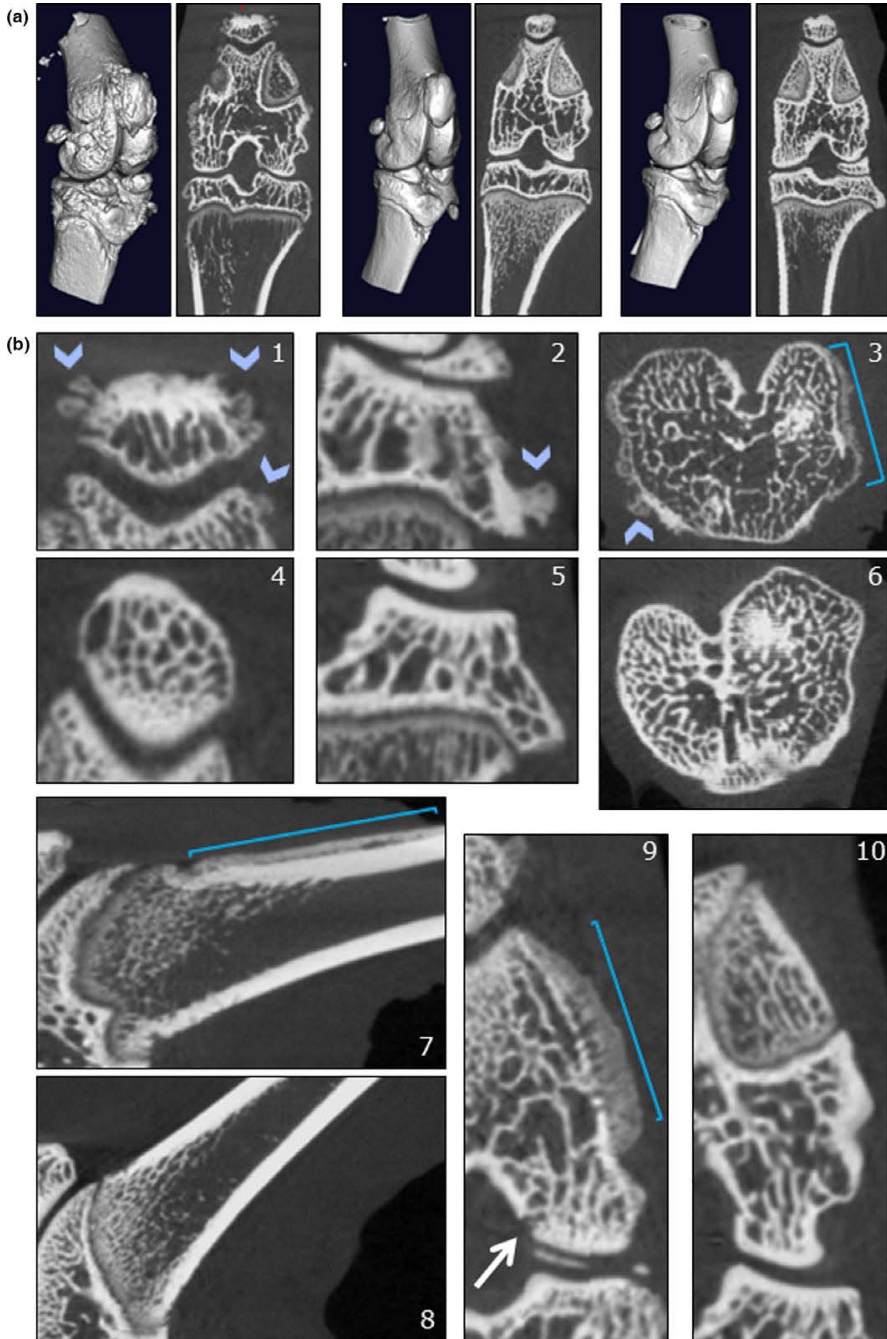


Fig. 4. μ CT scans show bone pathology in untreated F8^{-/-} animals. (a) Example of 3D surface rendering and coronal 2D images from *ex vivo* μ CT scans on day 28, from an untreated F8^{-/-} rat (left), rhFVIII treated F8^{-/-} rat (middle) and a wild-type rat (right), showing extensive pathological bone remodelling in the untreated F8^{-/-} animal with osteophytes on both patella, femur and tibia and no pathological findings on the rhFVIII treated F8^{-/-} rat and the WT rat. (b) Examples of pathological findings on μ CT scans from untreated F8^{-/-} animals (1–3, 7 and 9) compared to scans of WT animals without pathology (4–6, 8, 10). Arrowheads show the presence of osteophytes (1–3) on femur, patella and tibia, brackets and lines indicate areas of periosteal bone formation (3, 7 and 9) and the white arrow in image 9 indicates the presence of a subchondral cyst.

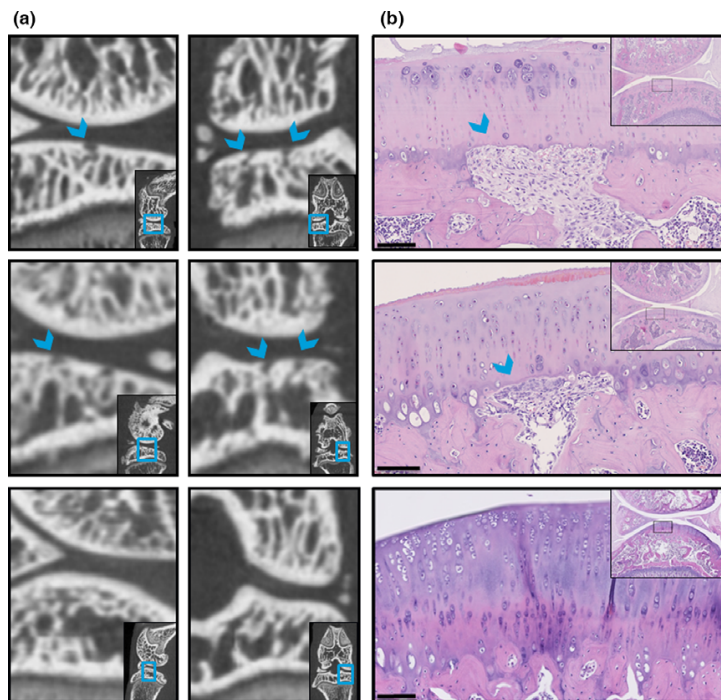


Fig. 5. *Ex vivo* μ CT can detect subchondral cysts as confirmed by histology. (a) 2D μ CT images in the coronal and sagittal plane from three different joints subjected to a single joint bleed. Top and middle rows show $F8^{-/-}$ joints with extensive bone pathology including the presence of two subchondral cysts in each joint. The bottom row shows a WT control rat subjected to a single joint bleed with no subchondral cysts or bone pathology. (b) Histological section of the corresponding joint from (a) confirming subchondral cyst formation in the $F8^{-/-}$ rats (top and middle rows) with no pathological changes in the WT control rat (bottom row). Blue arrowheads indicate cysts. Bars in (b) are 100 μ m in size.

previous mouse studies [21] and observations in patients, where excessive bone formation and degradation as well as cyst formation are evident [22,23]. Interestingly, unlike the mouse models, but comparable to human haemophilia A [6], we also identified subchondral cysts in six $F8^{-/-}$ rats confirmed by histological evaluation. If applied *in vivo*, μ CT can be used to visualize temporal progression of bone deformation. Furthermore, μ CT scans provide quantitative measures of bone density, volume and thickness, which may be used as endpoints in future studies [24].

Currently, the gold standard assessment tool for blood-induced joint disease in rodent knee bleeding models is histology. We therefore investigated how well disease severity measured by US or μ CT correlated to disease severity assessed by histology. The μ CT score and the histological arthropathy score correlated strongly after both a single and two joint bleeds. The US score showed a significant though somewhat weaker correlation to the histological arthropathy score. It should be noted that these three tools measure different disease characteristics and focus on different anatomical structures within the knee: US visualizes primarily soft tissues in the infrapatellar region, μ CT captures bone pathology of the entire knee, whereas histology assess both soft tissues, cartilage and bone, but is limited to a single anatomical plane of the knee. In addition, the US score

measures not only the pathology of the intra-articular space but also the skin and subcutaneous tissues. However, the moderate-to-strong correlation of US and μ CT scores to the gold standard histopathological evaluation confirms the feasibility of using these two imaging modalities as reliable tools for quantification of HA, enabling *in vivo* assessment of disease severity.

Conclusion

In the present study, both *in vivo* US and *ex vivo* μ CT consistently detected HA in $F8^{-/-}$ rats following induced knee bleeds. When disease severity was assessed using semiquantitative scoring systems, in particular the μ CT score correlated strongly with the histopathology score. Both imaging modalities could differentiate between treated and untreated $F8^{-/-}$ rats, making them suitable endpoints for therapeutic studies in this animal model. Future longitudinal studies where both modalities are applied *in vivo* may further establish the sensitivity of these techniques for detecting early and subtle pathological changes following joint bleeds.

In conclusion, combining US and μ CT imaging allows for visualization of both soft tissue and bone pathology following induced knee-joint bleeds in this model, enabling future longitudinal *in vivo* studies of the development and progression of HA.

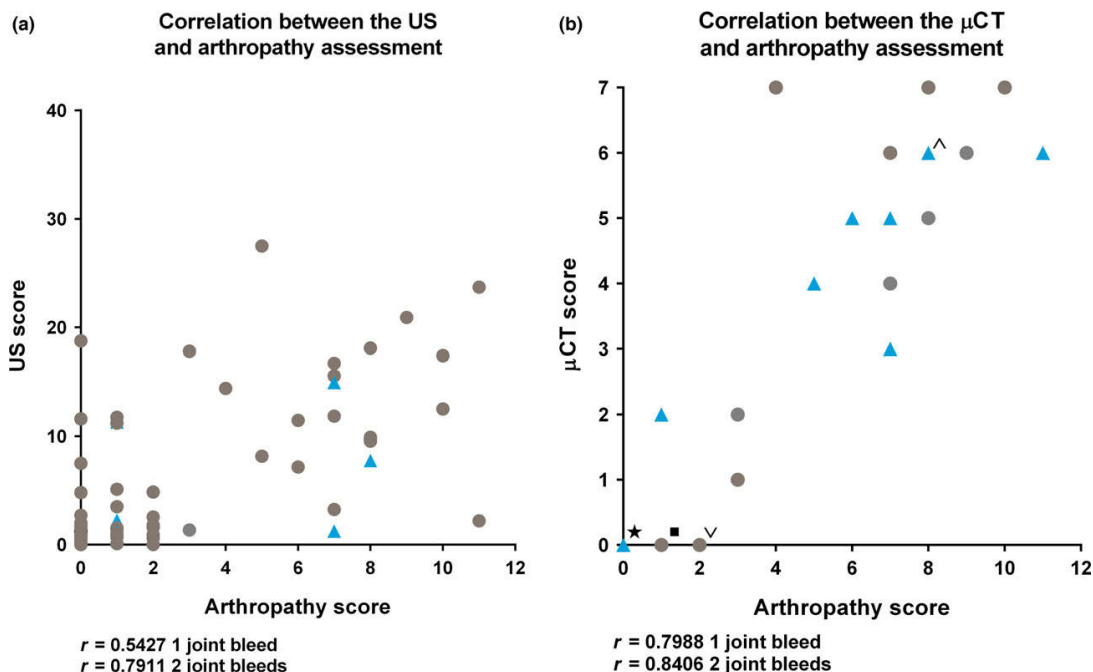


Fig. 6. Correlation between histological assessment and US or μ CT. Correlation between *in vivo* US (a) or *ex vivo* μ CT (b) sum scores and the corresponding arthropathy score for all animals is shown. The grey dots represent animals subjected to a single joint bleed, while the blue dots represent animals subjected to two joint bleeds. The asterisk marks a total of 34 overlaying scores, the square marks an overlay of 9 scores, the downward facing arrowhead an overlay of 6 points and the upward facing arrowhead an overlay of 2 points. R is shown for animals of the single and double joint bleed groups. The correlation coefficient r was calculated using a two-tailed Spearman's correlation test. $N = 46$ for the 1 joint bleed analyses and $n = 24$ for the 2 joint bleeds analyses.

Addendum

K. R. Christensen, L. N. Nielsen, K. Roepstorff, A. K. Hansen and B. Wiinberg designed the study. K. R. Christensen performed the experimental part and all scoring with help from L. N. Nielsen, K. Roepstorff and M. Petersen, who developed the US VAS, arthropathy and μ CT, score, respectively. M. Kjelgaard-Hansen and K. R. Christensen performed the statistical analyses. K. R. Christensen prepared the manuscript. All authors reviewed the manuscript and approved the final version.

Acknowledgements

The study was sponsored by Novo Nordisk A/S and the University of Copenhagen. H. F. Kierkegaard is acknowledged for her assistance

References

- Bolton-Maggs PH, Pasi KJ. Haemophilias A and B. *Lancet* 2003; **361**: 1801–9.
- Aledort LM, Haschmeyer RH, Pettersson H. A longitudinal study of orthopaedic outcomes for severe factor-VIII-deficient haemophiliacs. The Orthopaedic Outcome Study Group. *J Intern Med* 1994; **236**: 391–9.
- Oldenburg J. Optimal treatment strategies for hemophilia: achievements and limitations of current prophylactic regimens. *Blood* 2015; **125**: 2038–44.
- Nielsen LN, Wiinberg B, Hager M *et al.* A novel F8^{-/-} rat as a translational model of human hemophilia A. *J Thromb Haemost* 2014; **12**: 1274–82.
- Sorensen KR, Roepstorff K, Wiinberg B *et al.* The F8 rat as a model of hemophilic arthropathy. *J Thromb Haemost* 2016; **14**: 1216–25.
- Dunn AL. Pathophysiology, diagnosis and prevention of arthropathy in patients with

regarding the animal experiments. J. Juul, M. N. Nielsen and J. Mandelbaum for sectioning of the tissue, and J. Juul for staining. K. N. Weldingh and B. Klitgaard for blood sample analyses. S. Skov, P. H. Kvist and H. E. Jensen for scientific input. K. R. Christensen, A. K. Hansen, L. N. Nielsen is employed by the University of Copenhagen. M. Kjelgaard-Hansen, B. Wiinberg, K. Roepstorff and M. Petersen are minor shareholders of and employed by Novo Nordisk A/S. During the time of the study L. N. Nielsen was employed by Novo Nordisk A/S.

Disclosures

K. R. Christensen, A. K. Hansen and L. N. Nielsen are employed by the University of Copenhagen and K. Roepstorff, M. Petersen, B. Wiinberg and M. Kjelgaard-Hansen are employed by Novo Nordisk A/S. The authors stated that they had no interests which might be perceived as posing a conflict or bias.

- haemophilia. *Haemophilia* 2011; 17: 571–8.
- 7 Doria AS. State-of-the-art imaging techniques for the evaluation of haemophilic arthropathy: present and future. *Haemophilia* 2010; 16(Suppl 5): 107–14.
 - 8 Lau AG, Sun J, Hannah WB *et al.* Joint bleeding in factor VIII deficient mice causes an acute loss of trabecular bone and calcification of joint soft tissues which is prevented with aggressive factor replacement. *Haemophilia* 2014; 20: 716–22.
 - 9 Yu W, Lin Q, Guermazi A *et al.* Comparison of radiography, CT and MR imaging in detection of arthropathies in patients with haemophilia. *Haemophilia* 2009; 15: 1090–6.
 - 10 Sierra Aisa C, Lucia Cuesta JF, Rubio Martinez A *et al.* Comparison of ultrasound and magnetic resonance imaging for diagnosis and follow-up of joint lesions in patients with haemophilia. *Haemophilia* 2014; 20: e51–7.
 - 11 Monahan PE, Doria AS, Ljung R, Jimenez-Yuste V. Optimizing joint function: new knowledge and novel tools and treatments. *Haemophilia* 2012; 18(Suppl 5): 17–26.
 - 12 Lovgren KM, Sondergaard H, Skov S, Weldingh KN, Tranholm M, Wiinberg B. Antibody response to recombinant human coagulation factor VIII in a new rat model of severe hemophilia A. *J Thromb Haemost* 2016; 14: 747–56.
 - 13 Duncan E, Collett M, Street A. Nijmegen-Bethesda assay to measure factor VIII inhibitors. *Methods Mol Biol* 2013; 992: 321–33.
 - 14 Srivastava A, Brewer AK, Mauser-Bunschooten EP *et al.* Guidelines for the management of hemophilia. *Haemophilia* 2013; 19: e1–47.
 - 15 Clavel G, Marchiol-Fournigault C, Renault G, Boissier MC, Fradelizi D, Bessis N. Ultrasound and Doppler micro-imaging in a model of rheumatoid arthritis in mice. *Ann Rheum Dis* 2008; 67: 1765–72.
 - 16 Bhat V, Olmer M, Joshi S *et al.* Vascular remodeling underlies rebleeding in hemophilic arthropathy. *Am J Hematol* 2015; 90: 1027–35.
 - 17 Wang KC, Amirabadi A, Wang KC *et al.* Longitudinal assessment of bone loss using quantitative ultrasound in a blood-induced arthritis rabbit model. *Haemophilia* 2015; 21: e402–10.
 - 18 Kidder W, Nguyen S, Larios J, Bergstrom J, Ceponis A, von Drygalski A. Point-of-care musculoskeletal ultrasound is critical for the diagnosis of hemarthroses, inflammation and soft tissue abnormalities in adult patients with painful haemophilic arthropathy. *Haemophilia* 2015; 21: 530–37.
 - 19 Ceponis A, Wong-Sefidan I, Glass CS, von Drygalski A. Rapid musculoskeletal ultrasound for painful episodes in adult haemophilia patients. *Haemophilia* 2013; 19: 790–8.
 - 20 Muca-Perja M, Riva S, Grochowska B, Mangiafico L, Mago D, Gringeri A. Ultrasonography of haemophilic arthropathy. *Haemophilia* 2012; 18: 364–8.
 - 21 Hakobyan N, Enockson C, Cole AA, Sumner DR, Valentino LA. Experimental haemophilic arthropathy in a mouse model of a massive haemarthrosis: gross, radiological and histological changes. *Haemophilia* 2008; 14: 804–9.
 - 22 Cross S, Vaidya S, Fotiadis N. Hemophilic arthropathy: a review of imaging and staging. *Semin Ultrasound CT MR* 2013; 34: 516–24.
 - 23 Solimeno L, Luck J, Fondanesche C *et al.* Knee arthropathy: when things go wrong. *Haemophilia* 2012; 18(Suppl 4): 105–11.
 - 24 Lee A, Boyd SK, Kline G, Poon MC. Premature changes in trabecular and cortical microarchitecture result in decreased bone strength in hemophilia. *Blood* 2015; 125: 2160–3.

Supporting Information

Additional Supporting Information may be found in the online version of this article:

Figure S1. US atlas showing transverse (left column) and sagittal (right column) scans from nine individual animals with their corresponding VAS score. (a–a') B-mode scan of a normal joint day 0 before induction of a joint bleed. (a) Transverse scan showing the skin (asterisk), the hypochoic patella ligament (arrowhead) above the fat pad (dashed lines) lying within the intercondylar notch (white arrow). Total VAS score: 0. (a') Sagittal scan showing the skin, the hypochoic patella ligament above the fat pad stretching from the femoral condyle down across the tibial plateau. The hyperechoic cortex of the tibial plateau and the femoral condyles are visible below and extending from the fat pad. Total VAS score: 0. (b–b') B-mode scan of a joint day 14 after an induced joint bleed. (b) Transverse scan indicating displacement of the fat pad (white arrow). (b') Sagittal scan showing a swollen patella ligament (arrowhead) and displacement of the fat pad (white arrow). No signs of oedema or bone pathology. Total VAS score: 17.80. Oedema: 2.8, ligament: 7, fat pad: 7.8, ruffling of the bone: 0.2. (c–c') B-mode scan of a joint day 14 after an induced joint bleed. (c) Transverse scan showing slight subcutaneous oedema (white arrow) along with intra-articular effusion (arrowhead). No signs of bone pathology. (c') Sagittal scan showing loss of echogenicity of the fat pad (red asterisks). Total VAS score: 9.55. Oedema: 4.7, ligament: 1.8, fat pad: 2.35, bone ruffling: 0.7. (d–d') B-mode scan day 28 after two induced joint bleeds. (d) Transverse scan showing slight subcutaneous oedema (white arrow) and signs of intra-articular effusions around the patella ligament and the fat pad (arrowheads). (d') Sagittal scan showing subcutaneous oedema across the joint (white arrow), loss of hypogenicity of the patella ligament (arrowhead) as well as disruption of the fat pad (red asterisks). Total VAS score: 8.2. Oedema: 4, ligament: 0.4, fat pad: 3.7, ruffling of the bone: 0.1. (e–e') B-mode scan

on day 28 after two induced joint bleeds. (e) Transverse scan showing slight irregularity (ruffling, arrowheads) of the femoral condyles as well as extensive subcutaneous oedema (blue arrow) and intra-articular effusion (white arrows). (e') Sagittal scan showing subcutaneous oedema (blue arrow), enlargement/swollen patella ligament (arrowhead) with loss of hypogenicity (white asterisk), disruption and loss of echogenicity of the fat pad (red asterisks). Total VAS score: 23.7. Oedema: 7.75, ligament: 6.3, fat pad: 8, bone ruffling: 1.65. (f–f') B-mode scan on day 14 after a single induced joint bleed. (f) Transverse scan showing slight subcutaneous oedema (blue arrow) effusions (white arrow) along with clear/rufling of the femoral condyles (arrowheads). (f') Sagittal scan showing slight swelling of the patella ligament (arrowhead), as well as a heterogeneously echoic fat pad (white asterisk). Total VAS score: 20.9. Oedema: 5.5, Ligament: 5.2, fat pad: 5.75, ruffling of the bone: 4.45. (g–g') B-mode scan on day 28 after two induced joint bleeds. (g) Transverse scan showing loss of echogenicity of the fat pad (white arrow). (g') Sagittal scan showing swelling of the patella ligament with slight loss of echogenicity (arrowhead), as well as a heterogeneously echoic fat pad (red asterisk) with displacement (white asterisks). Total VAS score: 8.15. Oedema: 0.9, ligament: 2.5, fat pad: 3.75, ruffling of the bone: 1. (h–h') B-mode scan at day 14 after a single induced joint bleed. (h) Transverse scan showing loss of echogenicity of the fat pad (red asterisk). (h') Sagittal scan showing swelling of the patella ligament (arrowhead) with displacement of the fat pad (red asterisks). No signs of subcutaneous oedema. Total VAS score: 11.75. Oedema: 0.15, ligament: 4.6, fat pad: 4.85, ruffling of the bone: 2.15. (i–i') B-mode scan day 28 after two induced joint bleeds. (i) Transverse scan with signs of effusion in the joint (white arrow) and slight irregularity of the bone (white arrowheads). (i') Sagittal scan showing swelling of the patella ligament with slight loss of hypogenicity (arrowhead), displacement of the fat pad (red asterisks) and loss of echogenicity (white asterisks). No signs of subcutaneous oedema. Total VAS score: 11.85. Oedema: 2.95, ligament: 3.1, fat pad: 3.95, Ruffling of the bone: 1.85.

Figure S2. Atlas of the μ CT scoring system. Examples of the individual parameters scored in the μ CT scoring system. (a–g) show images of F8/- rat knees with examples of the individual parameters scored in the μ CT scoring system. (a–g') show images in the same anatomical planes obtained from wild-type rats without pathology. (a) Periosteal bone formation on tibia shown in the axial and coronal plane, respectively. (b) Periosteal bone formation on patella shown in the coronal and sagittal plane, respectively. (c) Periosteal bone formation on femur seen in the axial and sagittal view, respectively. (d) Osteophytosis on femur seen in the coronal and axial

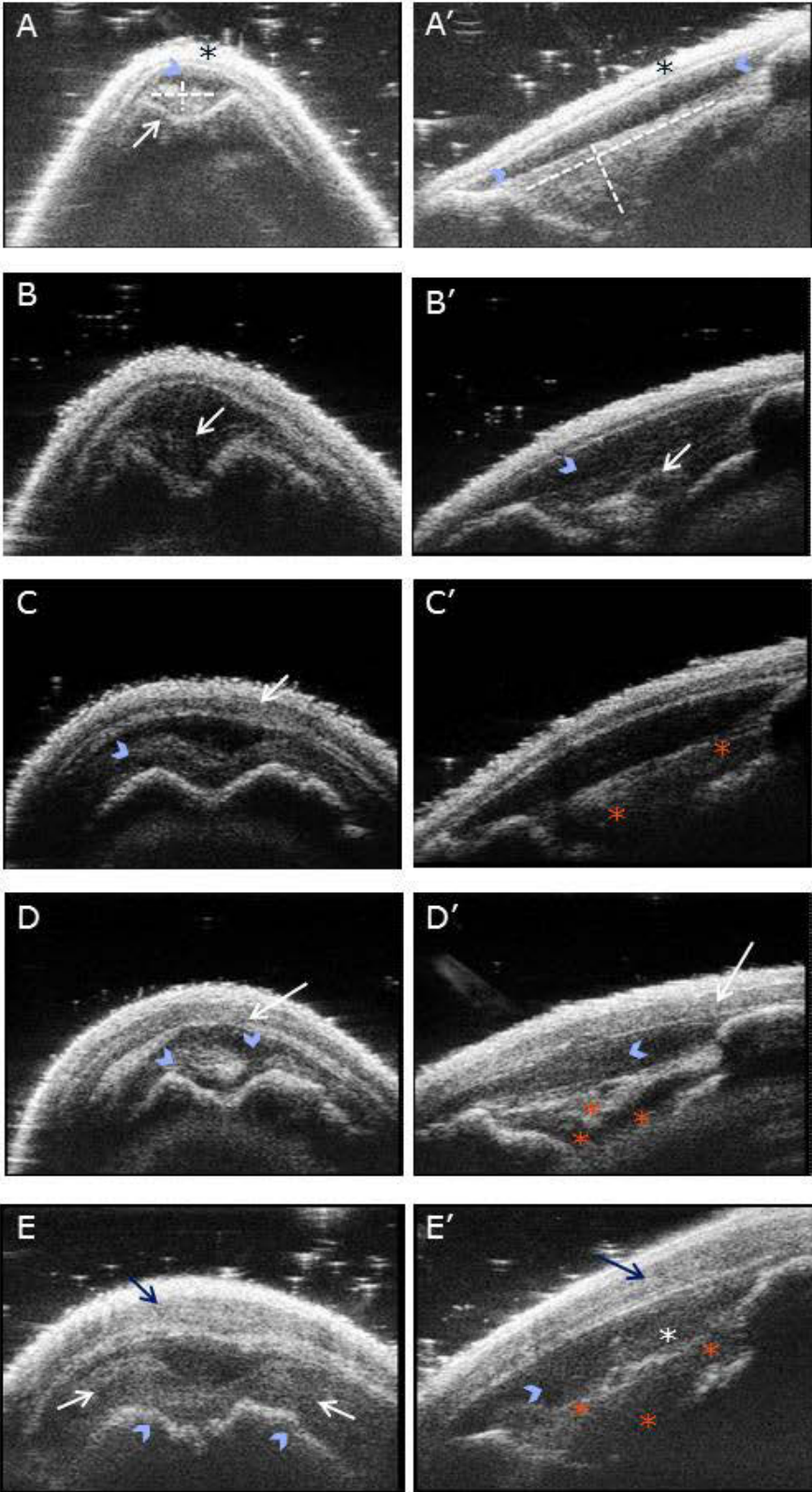
view, respectively. (e) Osteophytosis on tibia as seen in the axial and coronal view, respectively. (f) Osteophytosis on patella as seen in the coronal and sagittal view, respectively. (g) Subchondral cysts as seen in the sagittal and coronal view. White arrowheads point to areas of periosteal bone formation, blue arrowheads point towards areas of osteophytosis, while red arrowheads point towards subchondral cysts.

Figure S3. μ CT images of rat knees showing examples of different degrees of arthropathy and the corresponding μ CT coronal, sagittal and axial 2D images, as well as a 3D rendering of the joint from 3 untreated F8^{-/-} rats and a single wild-type rat. (a) Knee from an untreated F8^{-/-} rat following a single joint bleed. Osteophytosis on femur and tibia is visible in the coronal view, while periosteal

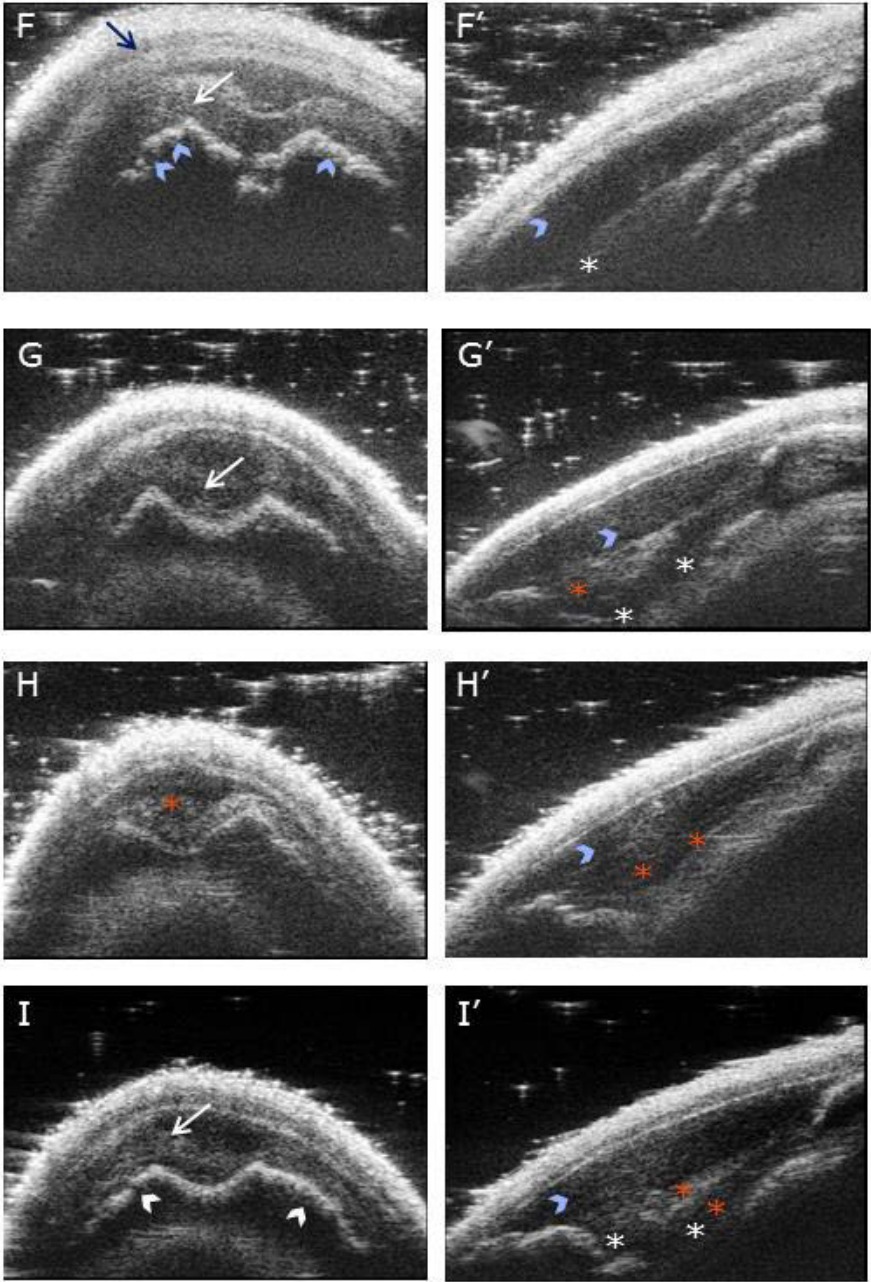
bone formation and osteophytosis of patella is visible on the sagittal and axial view respectively. Likewise, periosteal bone formation on femur is visible in the axial view. The 3D rendering shows irregular bone surfaces caused by extensive bone remodelling. Total score for this animal was 7 (positive score for periosteal bone formation on tibia, femur and patella as well as osteophytosis on femur, tibia and patella and the presence of a subchondral cyst, not visible at this magnification). (b) Knee from an untreated F8^{-/-} rat following two joint bleeds. Osteophytosis on femur and tibia as well as patella is visible in the coronal and axial plane, respectively, while periosteal bone formation on femur is visible in the sagittal and axial view. The 3D rendering shows uneven surfaces and outgrowths on patella. Total score for this animal was 4 (scored

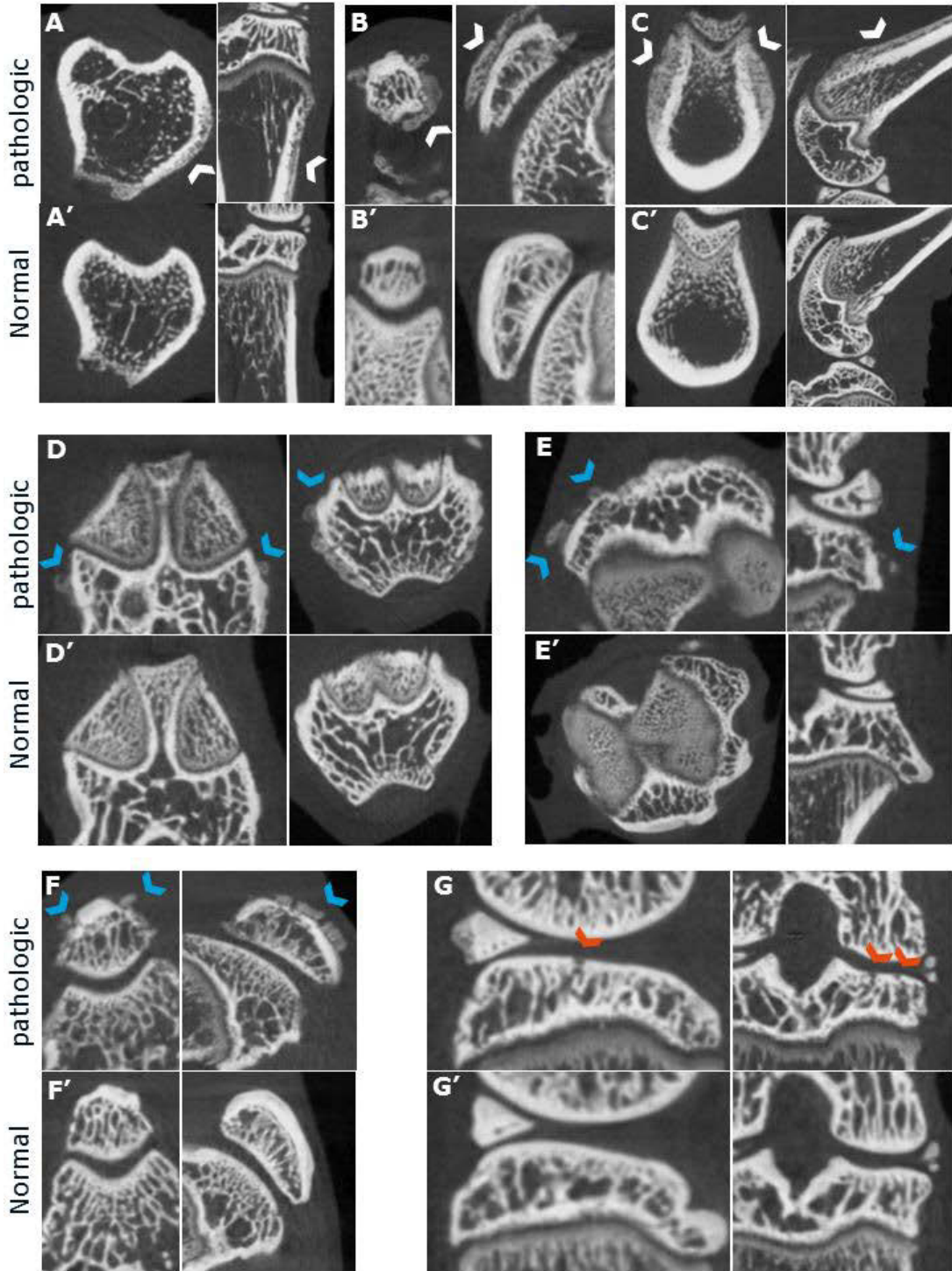
positive for periosteal bone formation on femur and osteophytosis on femur, tibia and patella). (c) Knee from an untreated F8^{-/-} rat after two joint bleeds with minor bone changes. Osteophytosis on femur and patella is visible in the coronal and axial view respectively. The 3D rendering shows minor ruffling of the bone surface of the tibial plateau, femoral condyles and on patella. Total score for this animal was 3 (scored positive for osteophytosis on femur, tibia and patella). (d) Knee from a wild-type rat after a single joint bleed. No signs of periosteal bone formation or osteophytosis. The 3D rendering shows smooth bone surfaces. The total score for this animal was 0. White arrowheads point to areas of periosteal bone formation, while blue arrowheads point towards areas of osteophytosis.

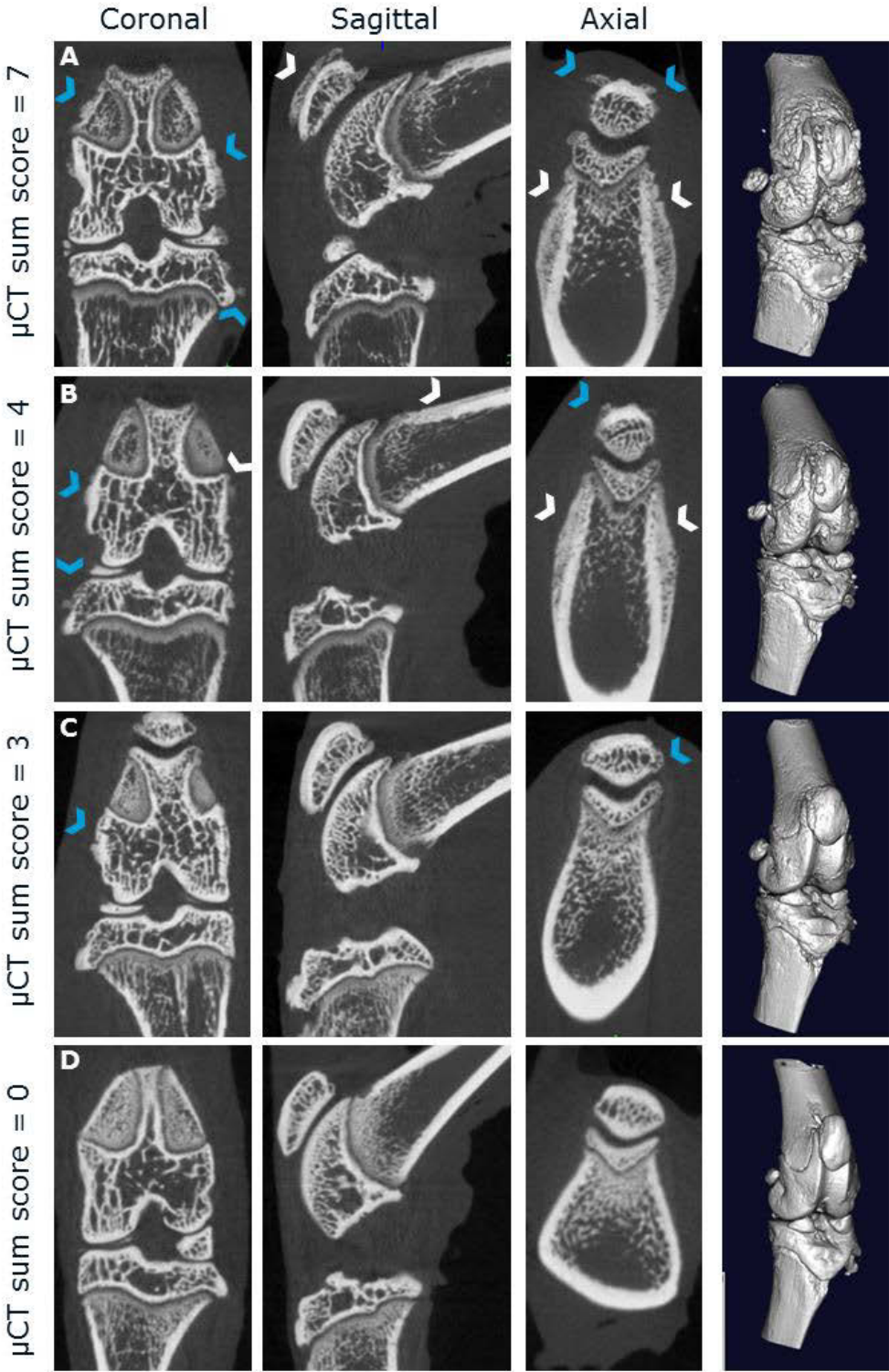
Hae13080-sup-0001. Figure S1:



Hae13080-sup-0002. Figure S1 continued







Paper III

Rapid inflammation and early degeneration of bone and cartilage revealed in a time-course study of induced hemarthrosis in hemophilic rats

Christensen, KR.; Kjelgaard-Hansen, M.; Nielsen, LN.; Wiinberg, B.; Althoehn, FA.; Poulsen, NB.; Vøls, KK.; Thyme, A.; Lövgren, KM.; Hansen, AK.; Roepstorff; K.

Manuscript

Rapid inflammation and early degeneration of bone and cartilage revealed in a time-course study of induced hemarthrosis in hemophilic rats

K. R. Christensen^{1,2,*}, M. Kjelgaard-Hansen^{1,#}, L. N. Nielsen^{3,#}, B. Wiinberg^{4,#}, F. A. Althoehn^{5,§}, N. B. Poulsen^{5,§}, K. K. Vøls^{5,2}, A. P. Thyme¹, K. M. Lövgren^{1,#}, A. K. Hansen^{2,‡}, and K. Roepstorff^{5,¶}

¹Translational Haemophilia Pharmacology, ⁵Histology & Bioimaging, ⁴Haemophilia Translational Biology, Global Research, Novo Nordisk A/S, Maaloev. ²Veterinary Disease Biology, ³Veterinary Clinical and Animal Sciences, University of Copenhagen, Denmark.

*Cand. Scient; [#]Dr. Med. Vet., PhD; [§]Veterinary student; [‡]Professor, Dr. Med. Vet., PhD; [¶]PhD.

Corresponding author: Kristine Rothaus Christensen, Novo Nordisk A/S, Novo Nordisk Park 1, 2760 Maaloev, Denmark.

Tel.: +45 30798261

Fax: +45 44426220

Mail: ktsr@novonordisk.com

Keywords: Hemophilia, immunohistochemistry, inflammation, *rattus*, X-ray computed tomography

Running title: Hemophilic arthropathy onset and progression

Word count summary: 250

Word count text: 4038

Number of figures: 8

Number of tables: 1

Summary:

Background: Detailed knowledge of the sequential cell and tissue responses following hemarthrosis is important for a deep understanding of the pathological process initiated upon extensive bleeding into the joint causing hemophilic arthropathy (HA). The underlying pathobiology driving hemarthrosis towards HA has been difficult to establish in detail, although animal models have shed light on some processes of HA. Previous studies have focused on a single or few distant time points and often only characterising one tissue type of the joint.

Objectives: The objective of this study was to carefully map early onset of synovitis and HA following induced hemarthrosis. *Methods:* One hundred and thirty hemophilia A rats were subjected to induced hemarthrosis or a sham procedure in full anesthesia and euthanized from 30 min to seven days after the procedure. Pathological changes of the joints were visualized using micro-computed tomography, histology and immunohistochemistry. *Results:* Synovitis developed within 24 h and was dominated by myeloid cell infiltrations, identified as early as 2 h after hemarthrosis. Cartilage and bone pathology were evident as early as 48-96 h after hemarthrosis, and the pathology rapidly progressed with extensive periosteal bone formation and formation of subchondral cysts. *Conclusion:* Fast, extensive and simultaneous cartilage and bone degeneration developed shortly after hemarthrosis, as shown by the detailed mapping of the early pathogenesis of HA. The almost immediate loss of cartilage and the pathological bone turnover suggest a direct influence of blood on these processes and are unlikely to be attributed simply to an indirect effect of inflammation.

Introduction:

Hemophilia A is caused by a lack of coagulation factor VIII (FVIII) resulting in impaired coagulation¹. Severity of the disease is inversely related to the activity of FVIII in plasma, with severe hemophilia A patients having less than one percent FVIII activity and a severe bleeding phenotype resulting in multiple spontaneous bleeds throughout their lifetime¹⁻⁴.

Hemophilic arthropathy (HA) develops as a result of spontaneous or trauma-induced hemarthroses which cause progressive joint deterioration, and is recognised as a major complication of hemophilia⁵⁻⁸. The overall development of blood-induced arthropathy is characterised by changes in the synovial membrane in the form of hyperplasia, inflammation and fibrosis^{9,10}. Synovial membrane deposition of the iron breakdown product hemosiderin is also a characteristic of HA, as is cartilage damage with chondrocyte apoptosis and proteoglycan loss^{9,11,12}. Finally, pathological bone remodelling such as bone erosions and subchondral cysts are often identified as a result of HA^{5,6,13,14}. Combined, these changes in the joint cause pain, reduced mobility and loss in quality of life for affected patients, many of whom eventually require surgical intervention^{1,15}.

Studies on the pathobiology of HA have been complicated by the inability to study the early development of HA as hemophilia patients are vulnerable to tissue sampling. Therefore, human tissue samples of HA are often late-stage joint disease biopsies obtained during surgery¹⁴.

Studies using animal models of hemophilia have clarified some of the early processes responsible for the blood-induced breakdown of the joint, but several aspects remain unclear. Human explant and hemophilic mouse studies have successfully shown that synovial cells respond to blood in the joint by producing pro-inflammatory signals and proliferate in order to remove the blood^{5,12,16-18}. Furthermore, lysis and erythrophagocytosis release heme-incorporated iron, which is degraded by macrophages thereby releasing reactive oxygen species^{10,11,19,20}. The process of iron-degradation together with the released pro-apoptotic inflammatory cytokines, have been shown to cause apoptosis of the chondrocytes^{12,16}. Loss of chondrocytes causes disruption of cartilage extracellular matrix homeostasis and an overall loss of cartilage in the joint^{11,19,21}. The

combination of cartilage damage, inflammation and reactive oxygen species also cause damage to the bone, well-known from hemophilia patients and from HA animal studies²²⁻²⁹.

These detailed studies in specific mechanisms of HA development often concentrate on a single tissue type of the joint and single or few distant time points following hemarthrosis. Although synovitis and cartilage damage are generally believed to occur before pathological changes to the bone^{7,10,30}, the exact sequence of events remains unknown.

With this study, our objectives were to carefully map the early progression from hemarthrosis to HA in a hemophilia A (F8 KO) rat model of induced hemarthrosis and HA.

One hundred F8 KO rats were subjected to an induced hemarthrosis or sham procedure in full anesthesia and euthanized day one to seven after the induction. Hereafter, micro-computed tomography (μ CT) was performed to study bone pathology and the joints examined by histology for general pathology and by immunohistochemistry to study the cellular inflammatory response. A second *post hoc* study was performed, investigating the cellular infiltration of the synovial membrane in the initial hours (h) after hemarthrosis using immunohistochemistry. Results showed a sequential pathobiology initiated by synovitis, closely followed by progressive cartilage and bone degeneration, indicating a direct pathological effect of blood on these tissues.

Methods:

Animal studies

Animal studies were performed according to guidelines from, and approved by the Danish Animal Experiments Council, the Danish Ministry of Environment and Food as well as the Novo Nordisk Ethical Research Committee.

The animals were 11-24 weeks (with the majority being 11-16 weeks, n=84) at study initiation and housed under standard conditions^{31,32}. Invasive procedures were performed under inhalation anesthesia (Isoflourane 2-5 vol%, N₂O 0.7L/min, O₂ 0.3L/min), as previously described^{31,32}.

Study design

In study one, a total of 100 F8 KO rats (Sage: SD-F8^{tm1sage})³³ were included in the study, with rats blocked for age and randomly assigned to either induced hemarthrosis or sham procedure (shaving of the joint area). Four sham rats and nine rats subjected to hemarthrosis were euthanized each day from day one to seven after the procedure (group 1-7) with nine sham rats acting as baseline controls (group 0).

In study two, 30 F8 KO rats were subjected to an induced hemarthrosis, and euthanized in equal numbered groups (n=5) at 0 h (sham controls) and 0.5 h, 2 h, 4 h, 6 h, 24 h after induction. Group sizes were based on power calculations and previous studies.

Rats showing signs of distress due to the induced hemarthrosis or as a result of new spontaneous bleeds were euthanized and excluded from the study.

Induction of hemarthrosis

Rats were anesthetized and 5 min prior to the procedure received a subcutaneous injection of buprenorphine (0.3 mg/mL, Reckitt Benckiser Pharmaceuticals Ltd, Berkshire, UK) of 0.03 mg/kg to ensure analgesia, whereafter hemarthrosis was induced in the left knee, as previously described^{31,32}. After the sham or hemarthrosis procedure the rats were supplemented with buprenorphine in the drinking water (6 mg/L)³¹.

Ultrasonography (US)

To confirm the presence or absence of hemarthrosis, an ultrasonography scan was performed 24 hours after the sham or joint bleed procedure. Briefly, the animals were anesthetized, placed in dorsal recumbence, the left leg mildly flexed and scanned in the sagittal and transverse view, as previously described³².

μCT

Following euthanasia the left hind-leg was dissected at the femoral head and *ex vivo* micro-computed tomography (μCT) scans were performed immediately after, using a Perkin Elmer

Quantum FX μ CT scanner (Perkin Elmer, Waltham, MA, USA). The scans were performed at 90 kV, 160 μ A with a field of view (FOV) of 20 mm, as previously described³².

Histology and immunohistochemistry

Immediately after the μ CT procedure (within 10 min), skin and muscle were carefully dissected from the left hind-leg and the legs fixated and decalcified as previously described³¹. The legs were then tissue processed, paraffin embedded and 3 μ m sections in the coronal plane were collected and mounted on glass slides. Adjacent sections were stained with hematoxylin and eosin (HE, for bone and synovitis), Perl's Prussian Blue (hemosiderin), and Safranin O (proteoglycan and chondrocyte loss), as previously described³¹ or Tartrate-Resistant Acid Phosphatase (TRAP).

For immunohistochemistry, heat induced antigen retrieval was performed at 59°C overnight, followed by washing, avidin-biotin incubation and blocking with 0.5% skimmed milk, 3% bovine serum albumin (Sigma-Aldrich, St. Louis, Missouri, USA), and 7% rat/donkey serum (Jackson Immuno Research Labs). Hereafter, the sections were incubated for 1 h at room temperature with primary antibodies followed by 1 h with secondary antibodies at room temperature before development using 3,3'-Diaminobenzidine (DAB, Sigma-Aldrich). Stained slides were scanned using the Nanozoomer 2.0 slide scanner (Hamamatsu Photonics K.K., Hamamatsu City, Japan) using a 20x magnification whole-slide scan.

Antibodies

Primary antibodies were mouse-anti-rat CD68 (0.5 μ g/mL, Ab31630, Abcam, Cambridge, Great Britain), Rabbit-anti-rat CD3 (1.3 μ g/mL, Ab5690, Abcam), Goat-anti-Mouse myeloperoxidase (MPO, 0.25 μ g/mL, AF3667, RnD Systems, Minneapolis, Minnesota, USA), Rabbit-anti-mouse Pax5 (0.5 μ g/mL, Ab109443, Abcam), rabbit-anti-human Ki67 (Ab16667, Abcam). Secondary antibodies were obtained from Jackson Immuno Research Labs, or Immunologic (Duiven, the Netherlands).

Assessment of ultrasonography, μ CT and histological images

Ultrasonography images were assessed according to the presence of patella ligament swelling, fat pad deviation, hematoma formation as well as bone and cartilage degeneration and scored according to a visual analogue scale (VAS), as previously described³².

μ CT images were assessed for osteophytosis, periosteal bone formation and subchondral cysts according to the μ CT score described previously³².

Histological sections were scored according to an arthropathy score, including scoring for the presence and degree of synovitis, hemosiderin deposition, bone remodelling and cartilage or chondrocyte loss as previously described^{31,32}. All scorings were performed randomized and blinded by the same observer.

Digital image analysis of histological sections was performed using Visiopharm Integrator System software (Visiopharm, Hoersholm, Denmark): An unsupervised K-means clustering algorithm was run generating a region of interest (ROI) corresponding to total tissue section, followed by manual blinded exclusion of the spongy bone and bone marrow. Within the obtained ROI, the stained area was quantified using threshold analysis in the DAB, hematoxylin or contrast red-green channel, with the threshold set to 100 (CD3, MPO, Pax5), 120 (CD68), 130 (Ki67) 80-120 (TRAP) and 80 (hemosiderin). Data are reported as percentage of positively stained tissue area (except TRAP where total TRAP stain is shown).

Statistics

For all parameters investigated, an ordinary one-way ANOVA between sham animals (including group 0) was performed to test for differences between groups, with no group of sham animals of any tested parameter being significant different from baseline. Likewise, the groups of animals subjected to hemarthrosis were tested for significant difference from baseline using an ordinary one-way ANOVA, followed by sequential Students' *t*-tests between baseline and individual hemarthrosis groups to determine the first day with significant difference to baseline (data from study two covering the first 24 h after hemarthrosis was log₁₀ transformed to obtain Gaussian distribution).

Finally, a regression analysis was performed on the total arthropathy score, to test for disease progression across all time points.

P-values<0.05 were considered significant. Statistical analyses were performed using GraphPad Prism (Version 6.05, GraphPad Software, Inc. San Diego, CA, USA).

Results:

Group distribution

Of the 100 F8 KO rats included in study one, 90 completed the study. Six were euthanized due to anemia as a result of the size of the hemarthrosis, and four due to new spontaneous bleeds. The final group sizes are shown in Table I.

Ultrasonography confirmed hemarthrosis following knee puncture

Hemarthrosis was assessed using US examination 24 h after the hemarthrosis or sham procedure. Of the 54 rats subjected to hemarthrosis, 41 showed varying degree of intra-articular and subcutaneous bleeding (see example in Fig.1B). Overall, the rats subjected to hemarthrosis had moderate to large subcutaneous edema, swelling of the patella ligament with loss of hypogenicity as well as a heterogeneous signal of the fat pad. No sham rats (n = 36) showed signs of intra-articular bleeding or pathology when examined by US (see example in Fig.1A).

When VAS scoring the US images³², there was an overall significant difference between sham rats and rats subjected to an induced hemarthrosis (P<0.0001, ordinary one-way ANOVA), whereas no difference was found between sham groups or between groups of rats subjected to hemarthrosis (see Fig.1C). This indicates the success of the induced hemarthrosis, and an even distribution of damage between the hemarthrosis groups.

Histological assessment shows progression from synovitis to HA

Histological assessment revealed that animals subjected to an induced hemarthrosis had hyperplasia and immune cell infiltration of the synovial tissue (synovitis) alongside proteoglycan loss in cartilage primarily in the lateral tibial plateau as well as excessive bone remodelling in

particularly at the surface of the cortical bone covering the femoral growth plate. Examples of HE and Safranin O stains from an induced hemarthrosis and sham animal (with no pathology) are shown in Fig.2A and B.

When applying the histological arthropathy score³¹ no pathology was detected in sham rats across all time points (see Fig.2C. No difference from 0 in a linear regression analysis and no difference between groups). In the rats subjected to hemarthrosis, a significant increase in the total arthropathy score was evident already on day one ($P=0.0006$) with a subsequent increase in the total score of approximately one per day (linear regression analysis with a slope of 1.175 ± 0.1196 , $P<0.0001$).

The first affected structure was the synovial membrane as shown by studying the individual parameters of the arthropathy score (see Fig.2D). A fast and progressive pattern of synovitis and hyperplasia/hypertrophy was evident already 24 h after hemarthrosis with a significant difference to baseline ($P<0.0001$, see Fig.2A and 2D). Significant hemosiderin deposition was apparent four days after hemarthrosis and increased over time. As early as two days after hemarthrosis, signs of chondrocyte and proteoglycan loss were seen (see Fig.2D). This was exacerbated over time with the first significant difference from baseline on day three ($P<0.05$). Interestingly, bone remodelling, in the form of excessive periosteal bone formation, was clearly evident within the timeframe of the study. As early as day two to three, the first minor signs of pathological bone remodelling were identified. As for the cartilage score, there was a significant difference between the baseline group and the hemarthrosis group on day four ($P<0.05$, see Fig.2D), with a continued increase in pathological bone remodelling throughout the study. On day five, all rats subjected to hemarthrosis had a positive score for pathological bone remodelling.

Inflammation of the synovial membrane follows a sequential pattern of cellular infiltration

Immunohistochemical stains for neutrophils (MPO), macrophages (CD68), T- (CD3) and B-lymphocytes (Pax5) as well as proliferation (Ki67) were performed.

Overall, the stains showed a massive infiltration of inflammatory cells present within the joint shortly after induction of hemarthrosis (see Fig.3) with a clear sequential infiltration by specific immune cells. Few to no inflammatory cells were observed in the knees of the sham rats.

The inflammatory response was dominated by myeloid cells (i.e. neutrophils and macrophages), with an early significant synovial infiltration of neutrophils 24 h after induction ($P=0.001$, see Fig. 3A), followed by a slow decline towards day seven.

The macrophages were the most abundant infiltrating cell type, infiltrating all areas of the joints, in particular in the subsynovial area, around ligament attachments on the bone surfaces (femur and tibia) and in the intercondylar notch. Quantification of the CD68 stain by digital image analysis confirmed the histological assessment and showed a large significant macrophage infiltration from 24 h after induction ($P<0.0001$) with elevated amounts of CD68 positive cells persisting throughout the study (see Fig.3B).

Staining of T- and B-lymphocytes revealed a markedly smaller degree of infiltration by these cell types compared to neutrophils and macrophages. However, a significant increase in the presence of these cells was found for T- and B-lymphocytes after 24 h ($P=0.002$) and 48 h ($P=0.006$), respectively. Furthermore, the observed increase in T- and B- lymphocytes for rats subjected to induced hemarthrosis remained until the final day of the study (see Fig.3C-D).

The extent of proliferation of the synovial membrane was assessed by staining for the proliferation marker Ki67. Proliferating cells were observed throughout the subsynovial tissue of the joint and within 24 h a strong significant signal appeared ($P<0.0001$) which remained elevated until day five and then dropped towards day seven (see Fig.3E).

Myeloid cell infiltration is evident within hours after hemarthrosis

Since the two dominating infiltrating cell types, neutrophils and macrophages were identified 24 h after the induced hemarthrosis at the first time point of observation, a second study with an additional 30 F8 KO rats was performed to determine the time of infiltration for these cells more accurately.

A significant increase was found after 2 h for neutrophils ($P=0.016$, see Fig.4A), however most of these were found in the blood vessels of the joint. The peak infiltration was at 24 h, at which time point the neutrophils had clearly extravasated into the joint tissue (see Fig.4B). The earliest significant increase of macrophage infiltration was at 6 h ($P=0.011$) with a continuous increase throughout the 24 h (see Fig.4B).

Hemarthrosis induces proteoglycan loss and chondrocyte apoptosis within days and before appearance of hemosiderin deposition

Loss of intensity in the Safranin O stain indicating proteoglycan loss in the uncalcified articular cartilage was evident in several rats with hemarthrosis; along with chondrocyte apoptosis (see Fig.5A-C). No cartilage fissures were identified.

The semi-quantitative arthropathy score revealed indications of apoptotic chondrocytes along with a slight loss of proteoglycans two days after the induced joint bleed (see Fig.2C). Pronounced proteoglycan loss was evident from day three with significance reached on day four ($P<0.05$, see Fig.2C) and a continuous increase in the loss of proteoglycans with a concurrent increase in apoptotic chondrocytes throughout the study.

Hemosiderin deposits first appeared as discrete spots, but gradually increased their presence and at later time points were readily identified intracellularly in areas with CD68 positive cells (see Fig.5D-F').

The semi-quantitative arthropathy score for hemosiderin deposition of rats with an induced hemarthrosis, showed a significant increase compared to baseline on day five ($P<0.01$, see Fig.2C), with the earliest detection of hemosiderin on day four. Additionally, quantification of the hemosiderin stain by digital image analysis showed a significant increase in the level of hemosiderin on day six, (see Fig.5G, $P<0.05$), slightly later than when applying the semi-quantitative hemosiderin score (see Fig.1D).

Early and extensive pathological bone formation and degradation were identified

In addition to the evaluation by histology, bone remodelling was assessed by *ex vivo* μ CT imaging of the entire joint. Surprisingly, rats subjected to hemarthrosis presented with bone pathology appearing shortly after the induced hemarthrosis. Hemarthrosis-affected rats developed extensive bone pathology during the time-course of the study, with no sham rats having signs of bone pathology (see Fig.2C and 6A-C' and F).

Grading pathological changes using the μ CT score revealed subtle changes in the form of periosteal bone formation evident already three days after induction although significance was not reached until day five (μ CT score $P<0.0001$, see Fig.6F, day four when applying the HA score

P<0.05, see Fig.2C). For a few rats the bone pathology was so extensive that even within this short time period they received the maximum score of seven (see Fig.6A-D and Fig.7A-C).

Subchondral cysts were identified in eight rats subjected to hemarthrosis and euthanized days four to seven (with one rat day four, two day five, one day six and four day seven). Figure seven shows μ CT images and histological sections of one of these subchondral cysts. Beneath the proteoglycan-deficient articular cartilage, fibrovascular tissue is seen on the Safranin O stained section (see Fig.7B) and when inspecting the identical area on a TRAP stain, a very intense positive signal of bright red osteoclasts is seen in the bone-cartilage interface (see Fig.7C).

The TRAP stain also showed an increase in osteoclast activity on the cortical bone surface starting early after the hemarthrosis reaching significance on day five (see Fig.6D, E and G, P<0.01) with a continuous increase in osteoclast activity throughout the study.

TRAP positive cells were not only identified along the bone surface, but also in the inflamed synovial membrane where they co-localized with CD68 positive cells (see Fig.7D-D"). Additionally, the TRAP positive cells of the synovial membrane appeared exclusively within areas either heavily loaded with erythrocytes or areas positive for hemosiderin (see Fig.7D-D").

Discussion

In this study we present a detailed characterisation of the pathological events following induced hemarthrosis until onset of HA in the F8 KO rat using histology, immunohistochemistry and μ CT.

The study confirms previous findings of the early consequences of hemarthrosis^{29,34,35} as rats subjected to induced hemarthroses had hyperplastic and inflamed synovial membranes already from day one. Hyperplasia was confirmed by Ki67 staining showing a transient increase in proliferating cells starting 24 h after hemarthrosis and gradually declining towards day seven. This stain captures the overall proliferative signal as it includes both resident and infiltrating cells. The early proliferative response is thus in line with the infiltration of immune cells and expansion of the synovial membrane in response to blood, as previously reported in synovial tissue exposed to ferric citrate^{36,37}.

Despite only a very early temporary proliferative response, the inflammation of the synovial membrane exacerbated over time and was dominated by myeloid cells. The initial infiltrating cells were neutrophils which were significantly increased in number 2 h after hemarthrosis, but were only present temporarily. The dominating cell type, CD68 positive cells (representing both A-type macrophage-like cells of the synovial membrane and infiltrating monocytes/macrophages) were significantly increased as early as 6 h after hemarthrosis induction and persisted over the time-span of the study, consistent with findings of macrophages in synovia of hemophilia patients with HA^{9,38}.

Although a significant and continued presence of T- and B-lymphocytes was demonstrated, the infiltration of these cells following hemarthrosis was subtle compared to that of the myeloid cells indicating only a minor role of lymphocytes in the acute immune response following hemarthrosis.

Cartilage was the second structure to be affected by hemarthrosis, with the earliest observations of pathology registered one to two days after hemarthrosis induction. The initial events causing cartilage damage remain uncertain, but both direct (blood) and indirect (inflammatory) damage of cartilage following hemarthrosis have been identified as potential causes^{7,39,40}. Iron and monocytes alone have thus been shown to cause cartilage damage as a result of iron degradation by the monocytes leading to formation of damaging reactive oxygen species as well as hemosiderin deposition¹⁹. Interestingly, cartilage damage in this study appeared early and days before the first signs of hemosiderin in the joint. This strongly suggests that the direct effect of blood on cartilage is an important driver of cartilage degradation.

Concurrently and with a similar progression as the cartilage damage, we found early and extensive pathological bone remodelling already on day three to four, primarily in the form of periosteal bone formation, confirmed by both μ CT and histological evaluation. Only few imaging studies have been conducted in human hemophilia patients and none focusing on bone changes following the first experiences of hemarthrosis or with such high resolution of bone as in the present study. This is likely due to the general belief that bone pathology develops secondary to synovitis and severe cartilage damage as well as the difficulty in obtaining images of such early bone pathology⁴¹⁻⁴³. Bone deformation is, however, a well-known consequence of HA with

erosions, subchondral cysts, and osteoporosis being some of the complications identified by imaging in human HA patients^{24,44,45}. Likewise, studies of F8 KO mice and rats subjected to induced hemarthrosis have shown extensive bone pathology two weeks after induction^{25,29,31,32} including both excessive formation of bone and increased bone resorption, as seen by osteophytosis and subchondral cyst formation.

The early pathological bone degeneration identified in this study has to our knowledge never been described. The striking findings of very early bone pathology could be due to a direct effect of blood on bone homeostasis. Further studies are needed to identify the molecular mechanisms causing the early cartilage and bone pathology.

As expected, a great amount of TRAP activity was identified in areas where considerable bone remodelling had occurred, e.g. in areas where excessive cortical bone had developed and in areas with subchondral cysts (from day four/five and onwards). These findings confirm the great extent of pathological bone conversion occurring within the first days after hemarthrosis in this model.

Finally, we also identified TRAP positive cells in the subsynovial area and these co-localised with CD68 positive cells, which are known to be capable of expressing TRAP⁴⁶. Interestingly, however, in this study the co-localization of TRAP-activity with CD68-positive cells was only identified in areas heavily loaded with erythrocytes or hemosiderin. Whether the degradation of iron into hemosiderin influences macrophages, converting them into an osteoclastic phenotype has to our knowledge not been described previously. Such a mechanism could play a role in the development of bone pathology in hemophilia and HA.

On the basis of our findings we propose a model of onset and progression of pathology in the individual tissue types following hemarthrosis as depicted in Figure 8.

In conclusion, we successfully mapped the development from hemarthrosis to synovitis and HA. The results reveal a proliferative synovitis dominated by neutrophil and macrophage infiltration that develops within hours after hemarthrosis, in line with previous animal studies of synovitis.

Strikingly, both bone and cartilage degradation were early parallel events, suggesting that these processes are caused by a direct effect of blood exposure, and not simply as a secondary consequence of inflammation. Thus, even a very short exposure to blood may be sufficient to cause damage to tissues not easily regenerated such as cartilage and bone. This is in agreement

with HA disease observations in patients treated with on-demand therapy, which does not completely protect against joint deterioration.

Addendum

K. R. Christensen, L. N. Nielsen, M. Kjelgaard-Hansen, B. Wiinberg and A. K. Hansen planned the study. K. R. Christensen performed the *in vivo* and *in vitro* study. K. K. Vøls and A. P. Thyme assisted in micro-computed tomography scanning. F. A. Althoehn and N. B. Poulsen performed the immunohistochemic *post hoc* study. K. M. Lövgren assisted in animal welfare surveillance and blood sampling. All authors received the manuscript and approved the final version. Conflict-of-interest disclosure: The authors state that they have no interests which might be perceived as posing a conflict or bias.

Acknowledgements

We acknowledge H.F. Kierkegaard for aiding in the animal experiments and J. Juul and M. N. Nielsen for advice and help with the immunohistochemical analyses.

Figures

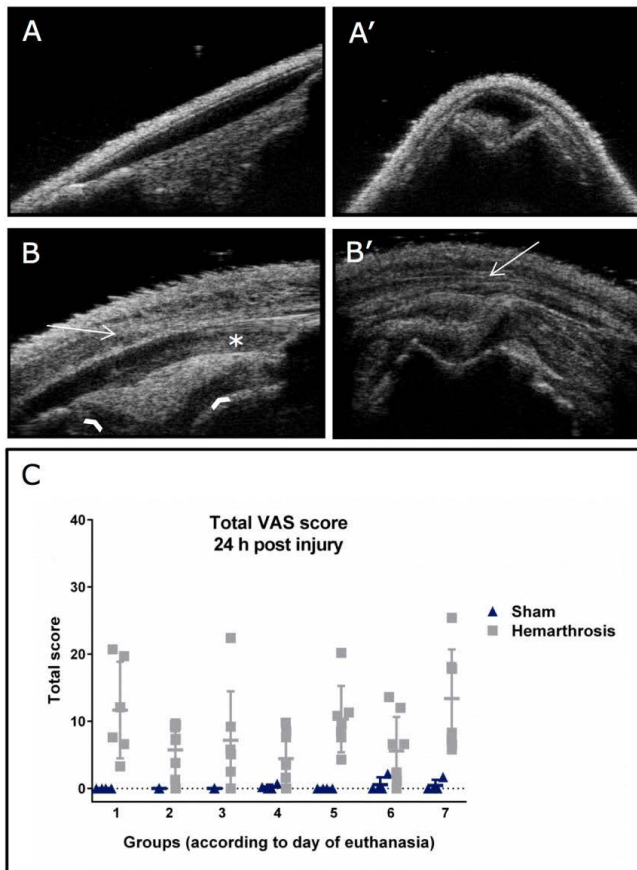
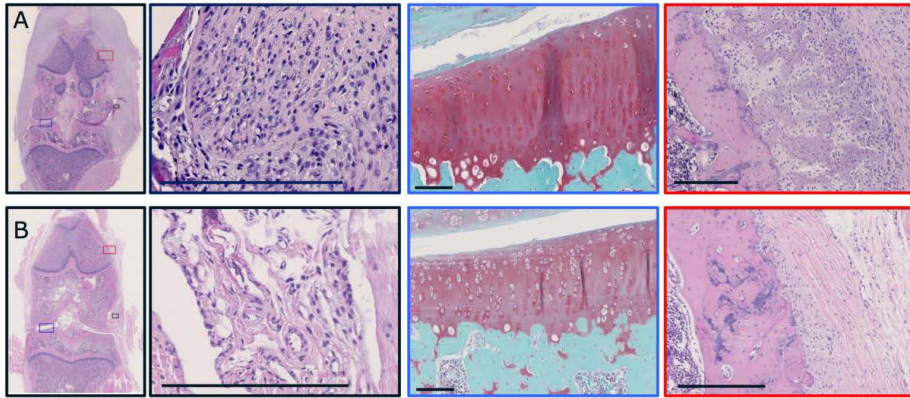
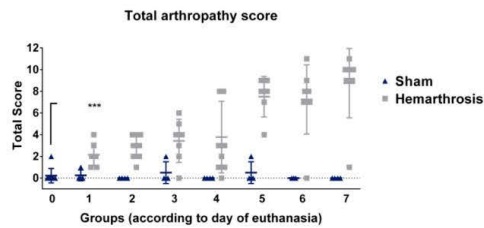


Figure 1: Examples of ultrasonography observations and VAS scoring

Ultrasonography was performed 24 h after the sham or hemarthrosis procedure and used to assess hemarthrosis in *SD-F8^{tm1sage}* rats. Ultrasonography images were also VAS scored for severity of joint changes, scoring zero to ten for severity of edema, patella ligament or fat pad changes and bone ruffling with a maximum sum score of 40. **A-A'**) Sagittal and transverse images of a sham rat with no detectable pathology. **B-B'**) Sagittal and transverse images of a rat subjected to hemarthrosis. Arrows point to hematoma/subcutaneous edema. Asterisk marks disturbance in the hypoechoic signal of the ligament indicating intra-articular cellular-rich fluid. Arrowheads point to dislocation of the fat pad. **C)** Graphic representation of the total VAS score, with no sham rats having a positive score for pathology, whereas almost all animals subjected to hemarthrosis have a positive score.



C



D

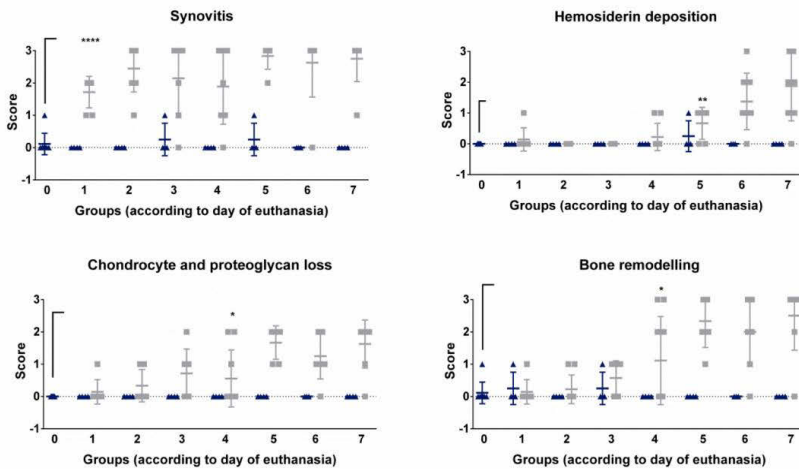


Figure 2: Verification of disease development following induced hemarthrosis

Histological sections were stained to assess the degree of synovitis and HA and scored according to the arthropathy score, assessing for synovitis (0-3), chondrocyte and cartilage loss (0-3), bone pathology (0-3) and hemosiderin deposition (0-3) with a maximum sum score of 12. **A-B)** HE and Safranin O stained sections from the joint of a rat subjected to hemarthrosis and sham procedure, respectively. Magnifications show signs of synovitis, proteoglycan loss and

pathological bone formation in the rat subjected to hemarthrosis. **C)** Total arthropathy score, shows an overall increase in pathology in the hemarthrosis affected rats starting on day one and exacerbating over time. **D)** The individual parameters scored for in the total arthropathy score. Synovitis appears first and reaches a plateau at the maximum score within the first days after hemarthrosis. Hemosiderin does not appear until day four, but then increases in amount. Cartilage damage in the form of chondrocyte and proteoglycan loss appears 24-48 h after hemarthrosis and the pathology progresses over time. Pathological bone remodelling is evident around 48 h after hemarthrosis and also progresses over time. Bars are 250 μm in the left and right panel and 100 μm in the central panel. The first time of significant difference to baseline was established using sequential Students *t*-test and the first significant difference is thus the only significance reported for all scores. * $P < 0.05$ ** $P < 0.01$ *** $P < 0.001$ **** $P < 0.0001$.

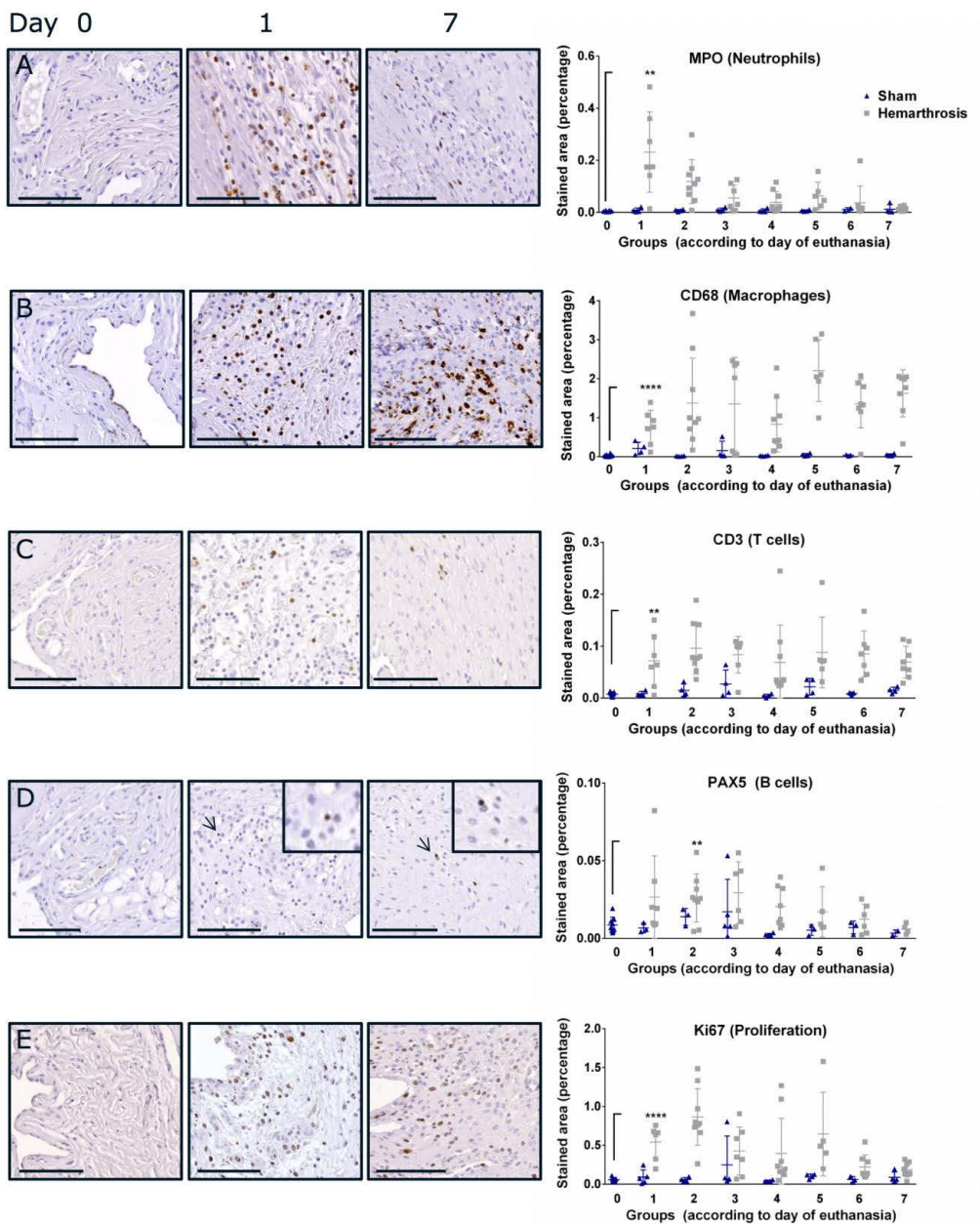


Figure 3: Infiltration of inflammatory cells and proliferation of the synovia

The three left panels are immunohistochemical stains showing the presence of inflammatory cells i.e. **A**) neutrophils (MPO), **B**) macrophages (CD68), **C**) T-lymphocytes (CD3), **D**) B-lymphocytes (Pax5) in the joint as well as **E**) the synovial membranes proliferative response after hemarthrosis (Ki67). To the right are graphs showing quantification of the immunohistochemical stains by digital image analysis. **A**) Neutrophils, which were present in large amounts 24 h after hemarthrosis, quickly declining towards baseline. **B**) Macrophages, which appeared 24 h after

induction and remained elevated throughout the seven days. **C)** T-lymphocytes, which were only sparsely identified. Quantification, however, confirms their presence from 24 h after induction of hemarthrosis until day seven. **D)** B-lymphocytes with magnifications from day one and seven. The quantification also confirms their significant presence from 48 h after hemarthrosis until day seven. **E)** Proliferating cells in the synovial membrane, with a significant increased signal at 24 h, which remains until day six. Bars are 100 μm . The first time of significant difference to baseline was established using sequential Students *t*-test and the first significant difference is thus the only significance reported for all scores. ** $P < 0.01$ **** $P < 0.0001$.

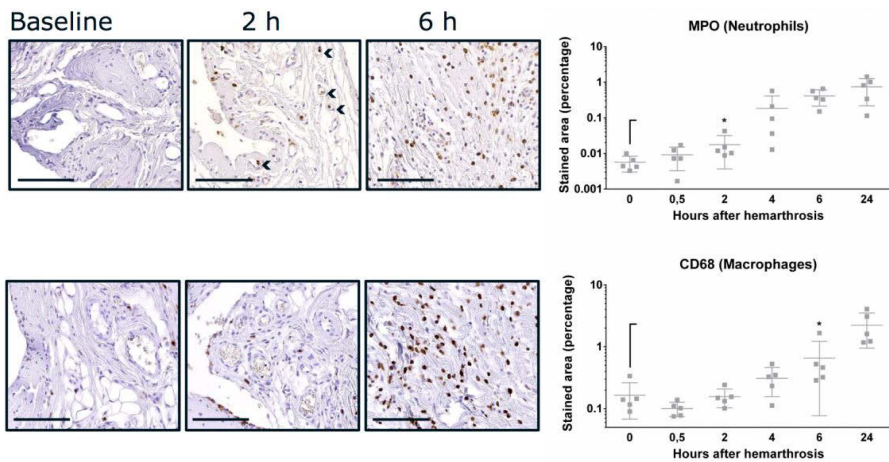


Figure 4: Earliest infiltration of neutrophils and macrophages

The earliest infiltration of the two major infiltrating cell types, neutrophils (MPO) and macrophages (CD68), were identified in an additional 30 SD-*F8^{tm1sage}* rats euthanized 0.5-24 h after an induced hemarthrosis.

Top row shows the presence of neutrophils, as well as the graphic presentation of the digital image analysis quantification of neutrophils in the joint. The quantification shows a significant increase of neutrophils in the joint at 2 h. At this time point, however, most neutrophils were still in the blood vessels, as indicated by arrowheads in the image of the stain. The peak infiltration in this study was at 24 h after hemarthrosis. The bottom row shows the presence of macrophages, as well as the quantification of the stain. The quantification shows a significant increase at 6 h with a continuously elevated percentage of stained area of macrophages in the joint throughout the 24 h. Bars are 100 μ m, arrowheads point to vessels containing neutrophils. Y-axis log₁₀ scale, to obtain gaussianity. The first time of significant difference to baseline was established using sequential Students *t*-test and the first significant difference is thus the only significance reported for both scores. * $P < 0.05$.

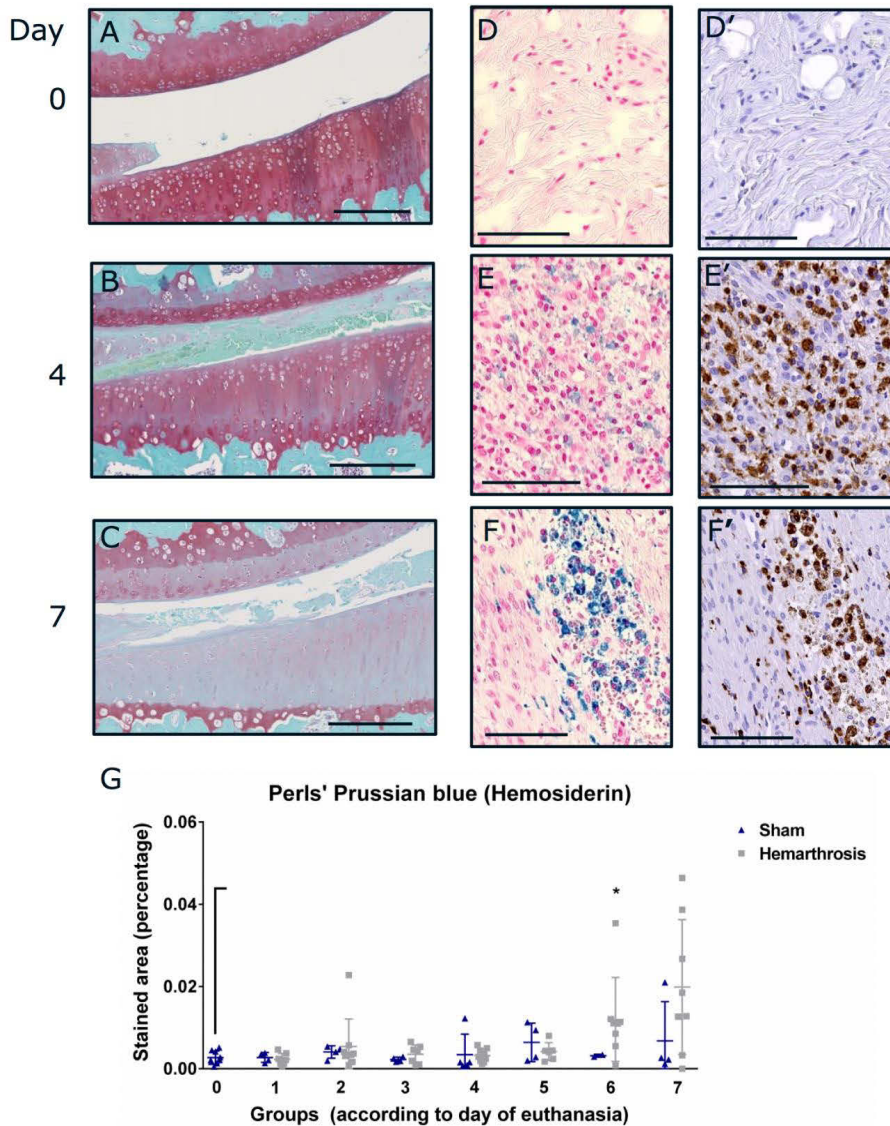


Figure 5: Cartilage damage and hemosiderin deposition

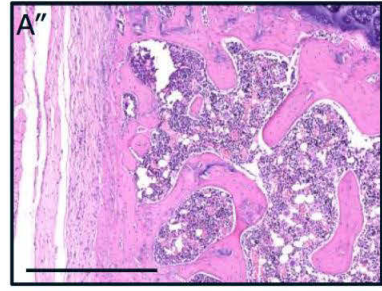
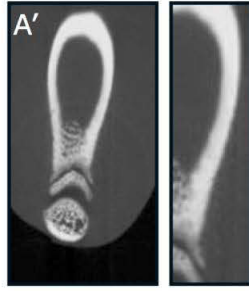
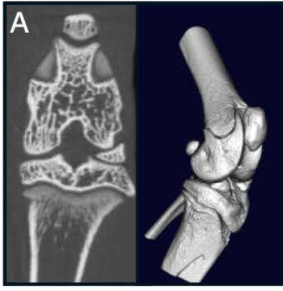
Safranin O staining was performed to show proteoglycan loss and chondrocyte apoptosis.

Perls' Prussian Blue was used to verify the presence of hemosiderin in the joint.

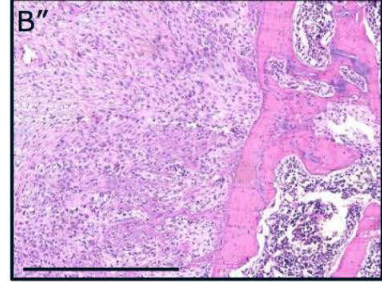
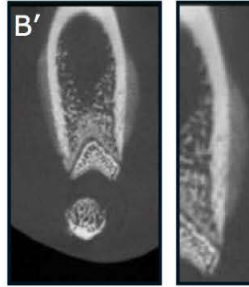
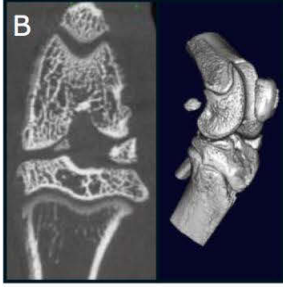
A-C Safranin O stained sections from day 0, 4 and 7 following hemarthrosis. On day four (B) the proteoglycan loss is evident in the tibial plateau, and on day seven (C) the cartilage is almost completely deprived of proteoglycans and the chondrocytes appear pycnotic. **D-F** Hemosiderin

staining of rats subjected to hemarthrosis. On day four hemosiderin depositions are identified and on day seven intense hemosiderin staining is evident. **D'-F')** CD68 stained sections from the same rat and in the corresponding area as D-F, respectively. Particularly in F' the hemosiderin co-localizes with the CD68 positive cells. **G)** Quantification of hemosiderin in the joint using digital image analysis. The quantification shows the first appearing hemosiderin on day five, with significant difference to baseline on day six. Bars are 250 μm (A-C) and 100 μm (D-F'). The first time of significant difference to baseline was established using sequential Students *t*-test and the first significant difference is thus the only significance reported for all scores. * $P < 0.05$.

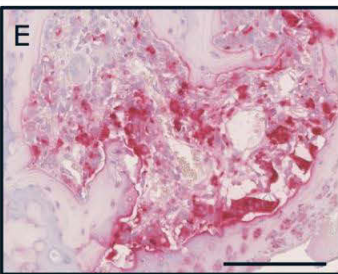
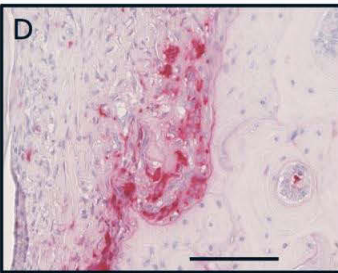
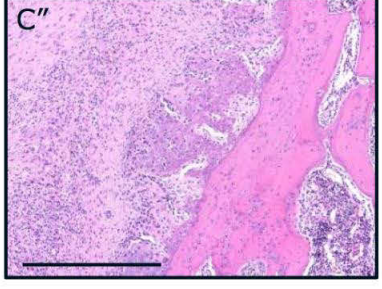
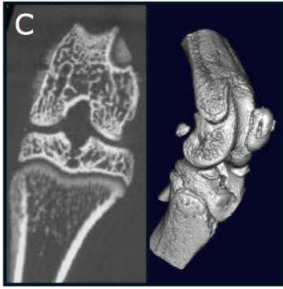
Day 0



Day 4

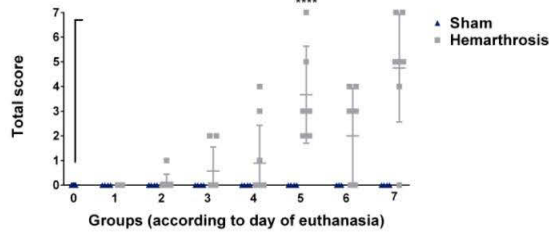


Day 7



F

Total μ CT score



G

TRAP (osteoclasts)

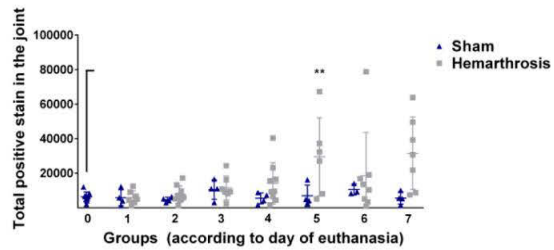


Figure 6: Pathological bone changes verified by μ CT and histology

μ CT, HE and TRAP stains were performed to assess bone changes following hemarthrosis.

A-C') 2D images and a 3D rendering of μ CT scans in the coronal (A-C) and axial (A'-C') plane. On day four minor outgrowths appear on the surface of the bone, and in particular in the axial plane large amounts of periosteal bone are visible. This is exacerbated on day seven, where the periosteal bone stretches far along the tibial (coronal plane) and femoral (axial plane) shaft. **A''-C'')** Corresponding HE stains of the joints in A-C. Here the periosteal bone formation is evident on the surface of the cortical bone. **D-E)** Positive TRAP stains showing the TRAP activity on the cortical bone of the femoral head (D) and an increased TRAP activity in the trabecular-cortical bone interface of the femoral condyle (E). **F)** Total μ CT score, assessing for osteophytosis and periosteal bone formation on femur, tibia and patella, respectively as well as subchondral cysts, giving a maximum sum score of seven. A positive score from day three for rats subjected to hemarthrosis are seen and progresses over time. **G)** Quantification of the TRAP stain in the joint by digital image analysis, showing an increase in TRAP staining starting on day four and persisting throughout the study, with a significant difference to baseline from day five. Bars are 500 μ m (A''-C'') and 100, and 150 μ m in D-E, respectively. The first time of significant difference to baseline was established using sequential Students *t*-test and the first significant difference is thus the only significance reported for all scores. ** $P < 0.01$ **** $P < 0.0001$.

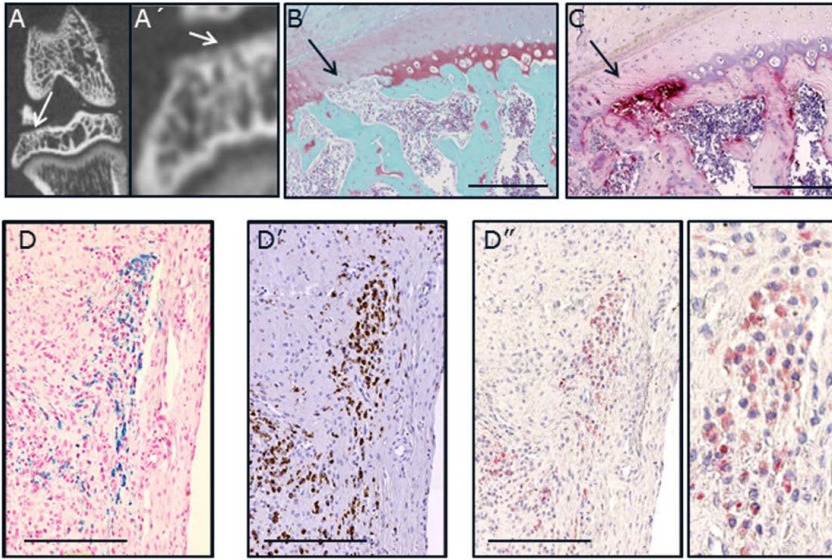


Figure 7: Early subchondral cyst formation and synovial TRAP activity

A-A') Identification of a subchondral cyst using μ CT in a rat subjected to hemarthrosis. **B-C)** Safranin O and TRAP stains of the corresponding area in A-A', showing the fibrovascular tissue of the cyst, and an intense TRAP activity, respectively. **D-D''')** Co-localization of hemosiderin, CD68 and TRAP positive cells in the synovial membrane, respectively. Bars are 250 μ m (B and C) and 200 μ m (D-D''').

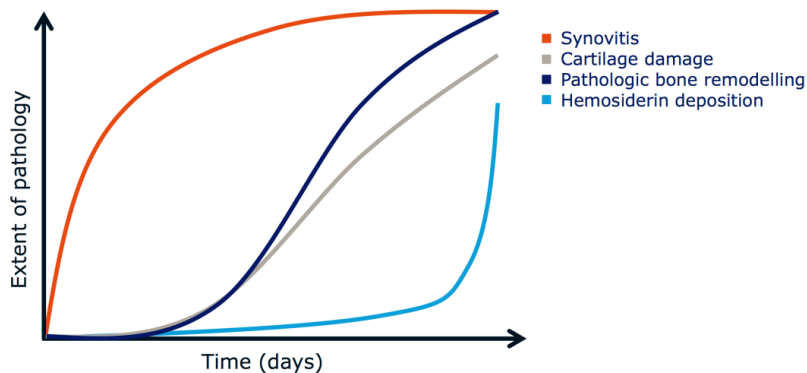


Figure 8: Suggested model of development of synovitis and early stages of hemophilic arthropathy

Based on the observations in this study, we suggest a model of disease onset and progression as shown schematically in this figure. Initially, the hemarthrosis leads to a proliferative and inflammatory synovitis that quickly reaches a plateau of continuous severe synovitis. Eventually, a thickened and fibrous synovial membrane embedded with macrophages will develop as a result of this inflammatory condition.

Shortly after development of synovitis, damage to the cartilage develops in the form of chondrocyte apoptosis and proteoglycan loss. This exacerbates and continues to progress over time, resulting in an almost complete disappearance of proteoglycans and chondrocytes in the outer layer of the intra-articular cartilage. Almost simultaneously to the onset of cartilage damage, pathological bone turnover is initiated. This is first apparent as increased periosteal bone formation resulting in large calcifications on the bone surface followed by subchondral cyst formation, possibly as a result of a gradual increase in osteoclast activity.

Finally, after the onset of synovitis, cartilage damage and pathological bone turnover, hemosiderin depositions appear in the joint.

References:

1. Srivastava, A., *et al.* Guidelines for the management of hemophilia. *Haemophilia : the official journal of the World Federation of Hemophilia* 2013;19:e1-47.
2. Evatt, B.L. The natural evolution of haemophilia care: developing and sustaining comprehensive care globally. *Haemophilia : the official journal of the World Federation of Hemophilia* 2006;12 Suppl 3:13-21.
3. Fischer, K., *et al.* Changes in treatment strategies for severe haemophilia over the last 3 decades: effects on clotting factor consumption and arthropathy. *Haemophilia : the official journal of the World Federation of Hemophilia* 2001;7:446-452.
4. Mannucci, P.M. & Tuddenham, E.G. The hemophilias--from royal genes to gene therapy. *The New England journal of medicine* 2001;344:1773-1779.
5. Valentino, L.A., *et al.* Exploring the biological basis of haemophilic joint disease: experimental studies. *Haemophilia : the official journal of the World Federation of Hemophilia* 2012;18:310-318.
6. Caviglia, H., *et al.* Treatment of subchondral cysts in patients with haemophilia. *Haemophilia : the official journal of the World Federation of Hemophilia* 2015.
7. Roosendaal, G. & Lafeber, F.P. Blood-induced joint damage in hemophilia. *Seminars in thrombosis and hemostasis* 2002;29:37-42.
8. Manco-Johnson, M.J., *et al.* Prophylaxis versus episodic treatment to prevent joint disease in boys with severe hemophilia. *The New England journal of medicine* 2007;357:535-544.
9. Stein, H. & Duthie, R.B. The pathogenesis of chronic haemophilic arthropathy. *The Journal of bone and joint surgery. British volume* 1981;63B:601-609.
10. Lafeber, F.P., Miossec, P. & Valentino, L.A. Physiopathology of haemophilic arthropathy. *Haemophilia : the official journal of the World Federation of Hemophilia* 2008;14 Suppl 4:3-9.
11. Roosendaal, G., Vianen, M.E., van den Berg, H.M., Lafeber, F.P. & Bijlsma, J.W. Cartilage damage as a result of hemarthrosis in a human in vitro model. *J Rheumatol* 1997;24:1350-1354.
12. Roosendaal, G., *et al.* Iron deposits and catabolic properties of synovial tissue from patients with haemophilia. *The Journal of bone and joint surgery. British volume* 1998;80:540-545.
13. Van Meegeren, M.E., *et al.* Joint distraction results in clinical and structural improvement of haemophilic ankle arthropathy: a series of three cases. *Haemophilia : the official journal of the World Federation of Hemophilia* 2012;18:810-817.
14. Speer, D.P. Early pathogenesis of hemophilic arthropathy. Evolution of the subchondral cyst. *Clinical orthopaedics and related research* 1984; 250-265.
15. Hilberg, T., Czepa, D., Freialdenhoven, D. & Boettger, M.K. Joint pain in people with hemophilia depends on joint status. *Pain* 2011;152:2029-2035.
16. Ovlisen, K., Kristensen, A.T., Jensen, A.L. & Tranholm, M. IL-1 beta, IL-6, KC and MCP-1 are elevated in synovial fluid from haemophilic mice with experimentally induced hemarthrosis. *Haemophilia : the official journal of the World Federation of Hemophilia* 2008;15:802-810.
17. Niibayashi, H., *et al.* Proteoglycan degradation in hemarthrosis. Intraarticular, autologous blood injection in rat knees. *Acta Orthop Scand* 1995;66:73-79.
18. Nieuwenhuizen, L., *et al.* Identification and expression of iron regulators in human synovium: evidence for upregulation in haemophilic arthropathy compared to rheumatoid arthritis, osteoarthritis, and healthy controls. *Haemophilia : the official journal of the World Federation of Hemophilia* 2013;19:e218-227.
19. Roosendaal, G., *et al.* Blood-induced joint damage: a human in vitro study. *Arthritis Rheum* 1999;42:1025-1032.
20. Nieuwenhuizen, L., *et al.* Hemarthrosis in hemophilic mice results in alterations in M1-M2 monocyte/macrophage polarization. *Thrombosis research* 2014;133:390-395.

21. Dunn, A.L. Pathophysiology, diagnosis and prevention of arthropathy in patients with haemophilia. *Haemophilia : the official journal of the World Federation of Hemophilia* 2011;17:571-578.
22. Zhang, S., et al. Inflammatory focal bone destruction in femoral heads with end-stage haemophilic arthropathy: a study on clinic samples with micro-CT and histological analyses. *Haemophilia : the official journal of the World Federation of Hemophilia* 2015;21:e472-478.
23. Klukowska, A., et al. Correlation between clinical, radiological and ultrasonographical image of knee joints in children with haemophilia. *Haemophilia : the official journal of the World Federation of Hemophilia* 2001;7:286-292.
24. Cross, S., Vaidya, S. & Fotiadis, N. Hemophilic arthropathy: a review of imaging and staging. *Seminars in ultrasound, CT, and MR* 2013;34:516-524.
25. Lau, A.G., et al. Joint bleeding in factor VIII deficient mice causes an acute loss of trabecular bone and calcification of joint soft tissues which is prevented with aggressive factor replacement. *Haemophilia : the official journal of the World Federation of Hemophilia* 2014;20:716-722.
26. Graham, J.B., Buckwalter, J.A. & et al. Canine hemophilia; observations on the course, the clotting anomaly, and the effect of blood transfusions. *J Exp Med* 1949;90:97-111.
27. Swanton, M.C. Hemophilic arthropathy in dogs. *Lab Invest* 1959;8: 1269-1277.
28. Wang, K.C., et al. Longitudinal assessment of bone loss using quantitative ultrasound in a blood-induced arthritis rabbit model. *Haemophilia : the official journal of the World Federation of Hemophilia* 2015;21:e402-410.
29. Hakobyan, N., Enockson, C., Cole, A.A., Sumner, D.R. & Valentino, L.A. Experimental haemophilic arthropathy in a mouse model of a massive haemarthrosis: gross, radiological and histological changes. *Haemophilia : the official journal of the World Federation of Hemophilia* 2008;14:804-809.
30. Valentino, L.A. Blood-induced joint disease: the pathophysiology of hemophilic arthropathy. *Journal of thrombosis and haemostasis : JTH* 2010;8:1895-1902.
31. Sorensen, K.R., et al. The F8 rat as a model of hemophilic arthropathy. *Journal of thrombosis and haemostasis* 2016;14:1216-25.
32. Christensen, K.R., et al. Visualization of haemophilic arthropathy in F8-/- rats by ultrasonography and micro-computed tomography. *Haemophilia : the official journal of the World Federation of Hemophilia* 2016.
33. Nielsen, L.N., et al. A novel F8 -/- rat as a translational model of human hemophilia A. *Journal of thrombosis and haemostasis : JTH* 2014;12:1274-1282.
34. Sen, D., et al. Nuclear factor (NF)-kappaB and its associated pathways are major molecular regulators of blood-induced joint damage in a murine model of hemophilia. *Journal of thrombosis and haemostasis : JTH* 2013;11:293-306.
35. Valentino, L.A., Hakobyan, N., Kazarian, T., Jabbar, K.J. & Jabbar, A.A. Experimental haemophilic synovitis: rationale and development of a murine model of human factor VIII deficiency. *Haemophilia : the official journal of the World Federation of Hemophilia* 2014;10:280-287.
36. Nishiya, K. Stimulation of human synovial cell DNA synthesis by iron. *J Rheumatol* 1994;21:1802-1807.
37. de Sousa, M., Dynesius-Trentham, R., Mota-Garcia, F., da Silva, M.T. & Trentham, D.E. Activation of rat synovium by iron. *Arthritis Rheum* 1988;31:653-661.
38. Madhok, R., Bennett, D., Sturrock, R.D. & Forbes, C.D. Mechanisms of joint damage in an experimental model of hemophilic arthritis. *Arthritis Rheum* 1988;31:1148-1155.
39. Jansen, N.W., et al. Interleukin-10 protects against blood-induced joint damage. *British journal of haematology* 2008;142:953-961.
40. Gringeri, A., Ewenstein, B. & Reininger, A. The burden of bleeding in haemophilia: is one bleed too many? *Haemophilia : the official journal of the World Federation of Hemophilia* 2014;20:459-463.
41. Roosendaal, G., et al. Synovium in haemophilic arthropathy. *Haemophilia : the official journal of the World Federation of Hemophilia* 1998;4:502-505.
42. Madhok, R., York, J. & Sturrock, R.D. Haemophilic arthritis. *Annals of the rheumatic diseases* 1991;50:588-591.

43. van Vulpen, L.F., *et al.* The detrimental effects of iron on the joint: a comparison between haemochromatosis and haemophilia. *Journal of clinical pathology* 2015;68:592-600.
44. Martinoli, C., *et al.* Development and definition of a simplified scanning procedure and scoring method for Haemophilia Early Arthropathy Detection with Ultrasound (HEAD-US). *Thrombosis and haemostasis* 2013;109:1170-1179.
45. Maclachlan, J., Gough-Palmer, A., Hargunani, R., Farrant, J. & Holloway, B. Haemophilia imaging: a review. *Skeletal Radiol* 2009;38:949-957.
46. Modderman, W.E., Tuinenburg-Bol Raap, A.C. & Nijweide, P.J. Tartrate-resistant acid phosphatase is not an exclusive marker for mouse osteoclasts in cell culture. *Bone* 1991;12:81-87.